Université de Montréal

Modular Construction of New Porous Hydrogen-Bonded Molecular Materials

par Tinasadat Khadivjam

Département de Chimie

Faculté des arts et des sciences

Mémoire présenté

à la Faculté des Études Supérieures

en vue de l'obtention du grade de maître ès sciences (M. Sc.)

en chimie

December 2019

Université de Montréal

Unité académique : département de Chimie, Faculté des Arts et des Sciences

Ce mémoire intitulé

Modular Construction of New Porous Hydrogen-Bonded Molecular Materials

Présenté par

Tinasadat Khadivjam

A été évalué par un jury composé des personnes suivantes

Andreea-Ruxandra Schmitzer

Président-rapporteur

James D. Wuest

Directeur de recherche

Nikolay Kornienko

Membre du jury

Résumé

Au cours des dernières décennies, la conception de complexes moléculaires ayant une organisation et des propriétés prévisibles n'était pas possible. Bien qu'il soit possible de calculer efficacement les propriétés de molécules individuelles, leur comportement collectif demeure imprévisible. Récemment, nous avons assisté au développement d'une nouvelle stratégie intitulée « construction modulaire » permettant de produire des matériaux bien définis et ordonnés dotés de nouvelles propriétés. Cette stratégie utilise des sous-unités moléculaires aptes à réaliser des interactions non-covalentes telles que des ponts hydrogène afin de maintenir des modules voisins à des positions programmables. Puisque les ponts hydrogène sont très forts et directionnels, un objectif important consiste à concevoir des sous-unités moléculaires aptes à réaliser un grand nombre de ponts hydrogène. Les molécules incorporant multiples groupements 4,6-diamino-1,3,5-triazinyles (DAT) sont un exemple de ce type de composés. Nos travaux sont focalisés sur l'introduction d'unités $N(DAT)_2$, qui offrent la possibilité de faire des réseaux ordonnés maintenus ensemble par un nombre encore plus grand de ponts hydrogène par molécule. Nous décrivons les structures et les propriétés de matériaux cristallins de ce type, dans lesquels un nombre croissant de ponts hydrogène donne lieu à la formation de réseaux robustes et hautement poreux.

Mots-clés : Chimie supramoléculaire, Génie cristallin, Ponts hydrogène, Construction modulaire, Matériaux poreux

Abstract

During the past few decades, designing molecular complexes with predetermined properties and predictable architectures was not possible. Although, it is possible to calculate the properties of individual molecules with confidence, the behavior of molecular assemblies remains unpredictable. Recently there has been a development of a strategy called "modular construction," which can lead to producing well-defined and ordered materials with novel properties. This strategy uses molecular subunits that engage in non-covalent interactions such as hydrogen bonds to hold the neighboring modules in programmable positions. Since hydrogen bonds show high strength and directionality, an important objective is to devise molecular subunits that can take part in a large number of hydrogen bonds. Examples are compounds that incorporate multiple 4.6-diamino-1,3,5-triazinyl (DAT) groups. Our work has focused on introducing $N(DAT)_2$ units, which offer the possibility of making ordered networks held together by even larger number of hydrogen bonds per molecule. We describe the structures and properties of crystalline materials of this type, in which increasing the number of hydrogen bonds gives rise to the formation of robust networks with high levels of porosity.

Keywords : Supramolecular Chemistry, Crystal engineering, Hydrogen bond, Modular construction, Porous materials

Table des matières

Liste des tableaux

Chapter 2. Modular Construction of Porous Hydrogen-Bonded Molecular Materials from Melams

Liste des figures

Chapter 1. Introduction

Chapter 2. Modular Construction of Porous Hydrogen-Bonded Molecular Materials of Melams

Annex. Supporting Information

Liste des abréviations

Å	Ångström
BET	Brunauer-Emmett-Teller
°C	Degree Celsius
Calcd	Calculated
DAT	4.6-Diamino-1,3,5-triazinyl
DMSO	Dimethyl sulfoxide
Eq.	Equivalent
ESI	Electrospray ionization
FTIR	Fourier-transform infrared spectroscopy
g	Gram
h	Hours
HRMS	High resolution mass spectrum
IR	Infrared
J	Coupling constant
K	Kelvin
Kcal	Kilocalorie
m	Multiplet
m/e	Mass per unit charge
m/z	Mass/charge ratio
mg	Milligram
MHz	Megahertz

mL	Millilitre
mmol	Millimole
Mol	Mole
m.p.	Melting point
NMR	Nuclear magnetic resonance
obs	Observed
ORTEP	Oak Ridge Thermal Ellipsoid Program
Ph	Phenyl
ppm	Parts per million
R_1	Residual factor
S	Singlet
TFA	Trifluoroacetic acid
THF	Tetrahydrofuran
TOF	Time of flight
δ	Chemical shift

Remerciements

First, I would like to thank my supervisor Dr. James D. Wuest, without whom I wouldn't stand where I am standing today. He is the best boss that anyone could ask for. Chemistry is not the only thing that I learned from him. I learned how to be patient, how to be optimistic in every situation, how to pay attention to all the details, and never give up just because I initially failed. He gave me the chance to be here, be in his research group, and grow in the field of organic chemistry. When I started my master's, I didn't think I was as good as the others in our group and I was scared, but he was supportive and believed in me. He helped me reach my goals. One of his many good qualities is that he is not easily satisfied, which makes me work harder to get the best results that meet his standards. I was so lucky that I had the chance to be under his supervision.

The second person that my gratitude goes is Dr. Thierry Maris. He is the most patient and warm-hearted person that I know. All the amazing results presented in my work wouldn't be done without him. He is the best crystallographer of all times. Sometimes he talked to me about certain crystallographic details, and I didn't have any idea what those things mean. However, since he is super professional, I am pretty sure they are great results. I am so happy that I had the opportunity to work with this amazing crystallographer and learn a lot of things from him.

The other people that I would like to thank are my colleagues in this group, Alexandre Lévesque, Alice Heskia, Johann Sosoe, Nino Petrov, Norbert Villeneuve, Patrick Chartier,

Sébastien Néron, and Sophie Langis-Barsetti, as well as Natasha Zoghi in the Martel Group. These people my friends, especially Alex, Seb, and Johann who supported me a lot and forced me to learn French. Dr. Sophie is the one that I would like to thank specially. During my master she helped a lot and taught me how to run a project and I also learned from her how to control my stress when the project was not working. I had so much fun with my colleagues during these three years and because of them, my workplace was a very motivating space. There was no competition in our work area, and everyone was helping each other to grow, which is the best thing that anyone would want in their workspace.

In the end, I would like to thank my parents who gave me a chance to be here today, and my sister Bita, my best friend Hila, and my brother Mathieu. All these people supported me during these three years. My sister, is the one who pushed me to grow here, see the opportunities, and try to be the best at work. All I have now it is because of her and I will be thankful for that forever. Also, I would like to thank my boyfriend Soroush, who encourage me a lot during my master's, never lost hope for me, and made an amazing cover illustration that he designed for my paper. He believed in me, which helped me to get through all the difficulties during my work.

Chapter 1. Introduction

Chapter 1 : Introduction

1.1 Supramolecular Chemistry

Supramolecular chemistry is defined as "chemistry beyond the molecule," which includes the study of multi-molecular complexes that can be assembled and held together by various weak non-covalent intermolecular forces, such as hydrogen bonding, metal coordination, π-π stacking, hydrophobic interactions, and van der Waals forces.[1] Supramolecular chemistry was pioneered by Nobel laureates Jean-Marie Lehn, Charles J. Pedersen, and Donald J. Cram, who synthesized cryptands, crown ethers,[2] and cavitands, respectively (Figure 1),[3] and revealed concepts related to molecular assembly that are now used throughout the field of chemistry and in many neighboring disciplines. The field has grown explosively during the last decades and has led to many breakthroughs of practical importance, including the development of bulk materials such as metal-organic frameworks (MOFs) and peptide-based materials for use in medicine.[4,5]

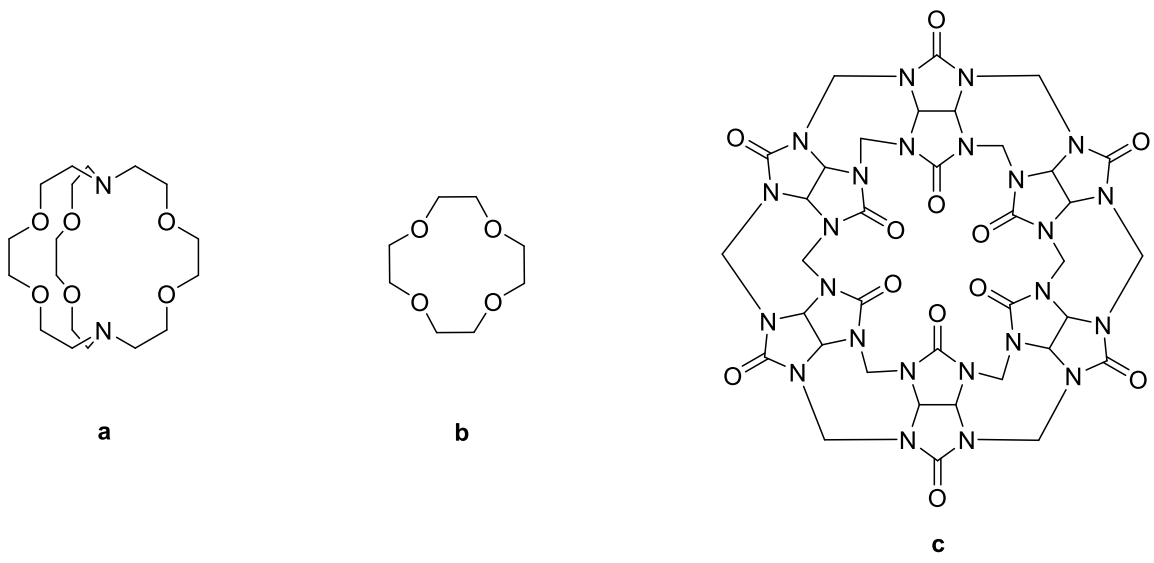

Figure 1. Examples of early cage-type structures used to reveal principles of supramolecular chemistry. (a) [2,2,2]-Cryptand, an illustrative member of the cryptand family. (b) 12-Crown-4, a representative example of crown ethers. (c) Representative of the cucurbiturils, an example of cavitands, with internal cavities that provide space for accepting guests.

Supramolecular chemistry started with an initial focus on host-guest chemistry, involving interactions between compounds of the type shown in Figure 1 (hosts) and smaller molecules (guests) that can be accommodated within the host. The field expanded to include systems of greater size and complexity, such as the self-association of multiple molecular subunits that interact with one another to create ordered supramolecular complexes. Although the study of these subjects represented a new frontier in academic research, it is important to note that there are many impressive examples of controlled assembly in nature. Most notable is the double helical structure of DNA, in which two separate strands are held together by hydrogen bonds between complementary base pairs (Figure 2a). Molecular self-assembly has a crucially important role in nature, and advances made by studying the subject systematically as part of the field of supramolecular chemistry have now made it possible to build complex unnatural

supramolecular architectures. These systems result spontaneously from suitably engineered molecules that have the potential to engage in interactions with their neighbors, leading to the predictable assembly of aggregates held together by multiple non-covalent bonds. Supramolecular chemistry is growing rapidly as a source of complex new structures, and self-assembly is an essential element of this field because it allows the reversible construction of robust, ordered structures with various useful properties as we will describe in further discussions such as formation of crystals that will be analyzed by crystal engineering methods.[5]

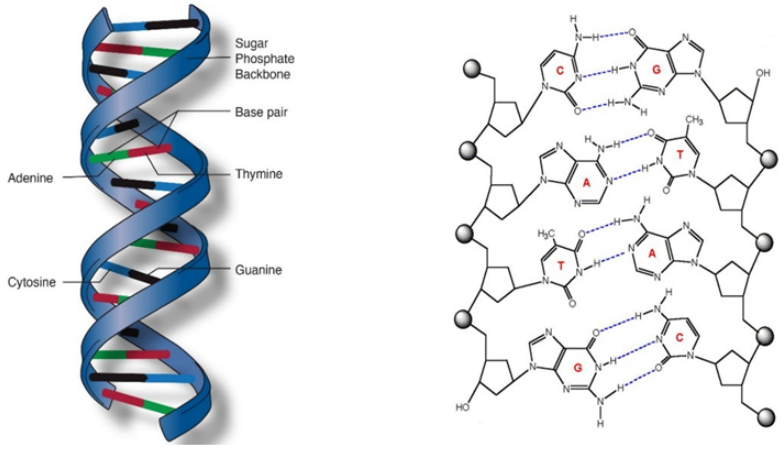

Figure 2. (a) Double helical structure of DNA molecule with sugar and phosphate backbone in each strand. The structure is obtained by forming hydrogen bonds between two complementary bases (Adenine(A)-Thymine(T) or Cytosine(C)-Guanine(G)), which are attached to the backbone of DNA. (b) View showing the hydrogen bonds between two complementary base pairs that are assembling.[6]

1.2 Hydrogen Bonding

The hydrogen bond was first defined as a bond where hydrogen acts as a bridge formed between two strongly electronegative atoms under specific conditions.[7] This classical definition applies chiefly to strong hydrogen bonds such as N-H···O and O-H···O. More recently, the field of hydrogen bonding has been extended to include related interactions involving less electronegative atoms such as N-H···π and C-H···O interactions. This has led to the following new definition for the hydrogen bond: "*The hydrogen bond is an attractive interaction between a hydrogen atom from a molecule or a molecular fragment X–H in which X is more electronegative than H, and an atom or a group of atoms in the same or a different molecule, in which there is evidence of bond formation.*"[8] The geometry and robustness of non-covalent intermolecular interaction such as hydrogen bonds are important factors that determine their utility in controlling molecular association. These interactions are suitable for tailoring new supramolecular structures and for engineering crystals only if they are sufficiently strong and directional to ensure that they can be used predictably and lead to structures in which interacting molecules are properly bonded and oriented. In recent years, chemists have frequently taken advantage of the special strength and directionality of hydrogen bonds to design and assemble novel materials with new properties.[9]

The strength of hydrogen bonds in terms of energy can vary in the range 1-40 kcal/mol. At one end of the scale are relatively weak hydrogen bonds such as N−H···:N (about 3.1 kcal/mol), and at the other are F−H···:F hydrogen bonds (about 38.6 kcal/mol).[10,11] Different types of hydrogen bonds have shown different utility depending on their strength. Even relatively weak hydrogen bonds can be suitable for engineering supramolecular complexes,

particularly when many hydrogen bonds are involved. In supramolecular chemistry, hydrogen bonds involving N and O are often used, due to their high electronegativity and to the fact that many common functional groups incorporate these atoms. As a result, hydrogen bonds involving N and O have proven to be reliable for controlling crystal packing predictably. Functional groups such as amido, carboxyl, amino, and hydroxyl participate in various reliable hydrogen bond patterns These functional groups are widely used in supramolecular chemistry to generate open and well-ordered hydrogen-bonded networks. As an example, triptycene(triscatechol) (Figure **3a**) can be crystallized from methyltetrahydrofuran (Me-THF) to generate a highly open network held together by multiple O−H···O hydrogen bonds (Figure **3b-c**).[12] Moreover, increasing the number of directional hydrogen bonds per molecule typically results in increasing the strength and stability of molecular complexes. Each molecule of triptycene(triscatechol) (Figure **3a**), takes part in a total of six intermolecular O−H···O hydrogen bonds, which leads to the formation of an open network with 63% of its volume accessible to guests.

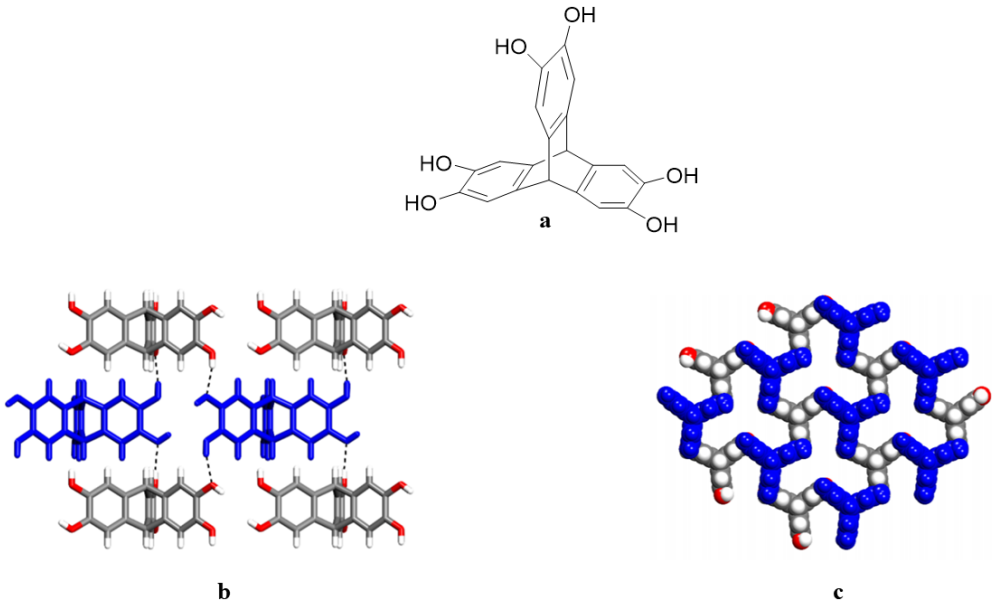

Figure 3. Examples of open networks that are held together by OH functional groups. (a) Structure of triptycene(triscatechol). (b) View showing how molecules are held together in adjacent sheets via O–H···O hydrogen bonds. (c) An open network that is obtained by crystallization from Me-THF, which generates a structure that is held together by O–H···O interactions.

Many disciplines, including chemistry and biology rely on the functionality of hydrogen bonds, since they are frequently used to control the association of molecules. Hydrogen bonds have proven to be among the most reliable non-covalent interactions. Directionality, flexibility, and reversibility are the factors that give hydrogen bonds a preeminent role in directing molecular assembly.

1.3 Molecular Crystal Engineering

An important challenge in science is to develop a detailed understanding of molecular crystallization and an ability to predict the structure that will result. Crystallization is part of supramolecular chemistry because it involves the creation of complex molecular assemblies held together by non-covalent interactions. Crystallization is a kinetic phenomenon where multiple molecules are held together in an ordered manner by non-covalent intermolecular interactions. This phenomenon has many important roles in science, including purifying chemical compounds and providing matter in a form that can be subjected to detailed structural characterization by X-ray diffraction and other techniques.[13] During crystallization, functional groups in a molecule can interact differently to determine how neighboring molecules are positioned. Crystal engineering involves the effort to understand the behavior of these intermolecular interactions and how they can be used to control the organization and properties of crystalline materials.[14]

The term "crystal engineering" is board in scope, but it includes controlling how molecules pack in the crystalline state by making use of non-covalent interactions as a fundamental force that determines how molecular components are positioned relative to their neighbors.[9] Crystal engineering is an interdisciplinary field that includes many aspects of solid-state supramolecular chemistry. The goal is to understand all aspects of crystallization well enough to make it possible to select suitable molecular components for various purposes and ensure that their organization in the solid state provides materials with targeted properties. Crystal engineering was initially introduced by Pepinsky,[17] but the field was more fully developed by Schmidt and coworkers in their research on photodimerization reactions in the

solid state, which revealed that the stereochemistry of the photodimers can be predicted by topochemical theory, based on how neighboring molecules are oriented.[15] Through the years, many other scientists have tried to correlate the structure of individual molecules with the way they are organized in crystals. In particular, Kitaigorodskii demonstrated that size and shape have a crucial role in controlling molecular packing.[11] This theory was augmented to take into account the special role of specific intermolecular interactions, and Etter showed that hydrogen bonds are directional and strong enough to allow the design of crystal architectures.[12] A more general concept related to weak interactions was introduced by Desiraju, called "supramolecular synthons".[20] Synthons are reliable associative motifs that involve the formation of weak non-covalent interactions such as hydrogen bonds and appear within supermolecules as the source of their cohesion (Figure 4).[20] Supramolecular synthons play an important role in understanding and designing crystalline networks. This results from the fact that they involve strong and directional interactions that are robust enough to ensure that they can be transported from one framework to another. Synthons are a practical concept that helps simplify the prediction of crystal structures by identifying information that can be expected to pass from the level of molecular structures to the resulting crystal structures. Through all these various efforts, crystal engineering is paving the way to a deeper understanding of how molecular structure and the potential to engage in intermolecular interactions of varied nature, strength, and directionality can be used to predict and control the structure and properties of crystalline materials.

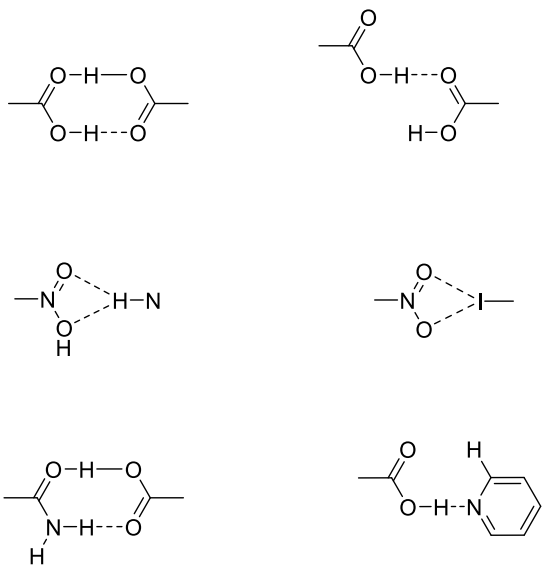

Figure 4. Examples of supramolecular synthons based on hydrogen bonds.[21]

An indispensable tool in the field is X-ray crystallography, which makes it possible to determine molecular structures in atomic detail. The history of X-ray diffraction began with the discovery of X-rays in 1895 by Wilhelm Röntgen, which was a breakthrough that led to the first Nobel Prize in Physics in 1901.[15] Following this discovery, von Laue found that exposing crystals to X-rays led to characteristic patterns of diffraction.[23] The discoveries laid the foundation for the development of X-ray crystallography in 1912-1913 by the Braggs, father, and son, who designed an instrument to observe diffraction patterns and proposed the diffraction law.[17,18] These developments, for the first time, allowed the three dimensional structures of crystalline materials to be determined at the atomic level. Modern X-ray crystallography now allows the structure of molecules to be examined in detail, as well as how molecules are arranged in crystals relative to their neighbors. Convenient determination of detailed structures requires the availability of single crystals of sufficient size; however, powder X-ray diffraction can provide useful information about crystalline materials when adequate single crystals are not

available and is widely used to test for crystallinity in samples, look for mixture of phases, and identify the components in complex materials.[26]

These advances in X-ray diffraction make it possible for crystal engineers to quickly solve structures, to compare the results with predictions and to plan future experiments. Along with important advances in molecular synthesis and increasing needs in science and technology for ordered materials, crystal engineering has evolved to become an increasingly powerful and useful field. Many other areas have come to rely on crystal engineering for new developments related to pharmaceuticals, materials, electronic devices and other important products.

1.4 Modular Construction

The properties of individual molecules can often be predicted with a high degree of confidence, but the collective behaviour of molecules, including their association to give complex assemblies, is far more difficult to foresee. To circumvent this obstacle, substantial effort has been made by Wuest and co-workers, as well as other groups to develop and exploit a powerful strategy that can be called “modular construction”. This strategy provides a tool for designing molecules that can associate strongly by specific interactions in a way that yields materials in which neighboring molecules are held in predetermined positions.[24,25]

The historical roots of modular construction can be found in Etter’s studies of hydrogen bonds, which led to the identification of many assembly motifs characteristic of hydrogen bonds.[12] In her work, Etter showed that hydrogen bonds are reliable for controlling molecular

crystallization as they are robust and directional. Designing crystalline materials with predictable structures is one of the primary targets of crystal engineering. An effective approach is to design compounds with multiple hydrogen-bond acceptors and donors that are arrayed around a relatively rigid core, which can orient the hydrogen-bonding sites in ways that favour particular types of molecular assembly. A key reference in Etter's classic paper is to earlier work of Wuest et al, in which hydrogen bonding was used explicitly to direct molecular association in predictable ways. Related work was carried out by Ermer who studied the crystallization of adamantane-1,3,5,7-tetracarboxylic acid and showed that crystallization of this compound is controlled predictably by the self-association of tetrahedrally-oriented carboxyl groups which leads logically to the formation of a hydrogen-bonded network with diamondoid topology (Figure 5).[26]

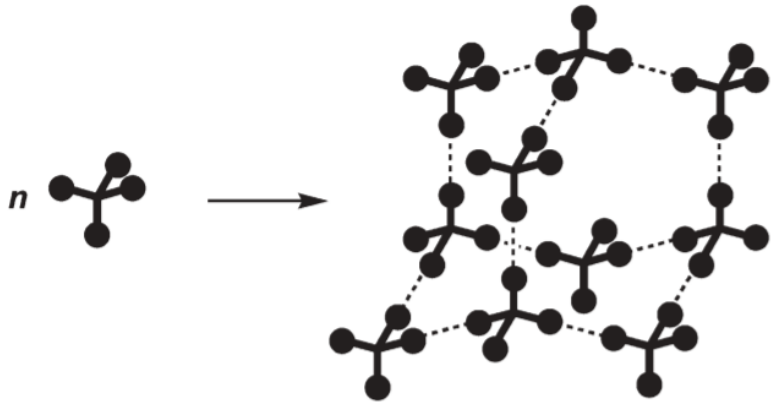

Figure 5. Hypothetical diamondoid network, constructed by association of functional groups connected to a rigid tetrahedral core (broken lines indicate directional intermolecular interactions).[24]

These early observations were the inspiration for increasingly ambitious modular construction, based on molecular subunits with well-defined structures and an ability to participate in a large number of hydrogen bonds. Examples include tetrapyridinones **1** and **2,** in which 2-pyridinone units are connected to a rigid tetrahedral core (Figure 6a).[27] 2-Pyridinone acts as a recognition group that tends to self-associate by forming hydrogen-bonded dimers (Figure 6b). The group thereby takes advantage of hydrogen bonds in order to place neighboring molecules in programmable positions and direct the molecular assembly. Moreover, the tetrahedral core orients this supramolecular structure, which results in predictable generation of diamondoid network.[26,27]

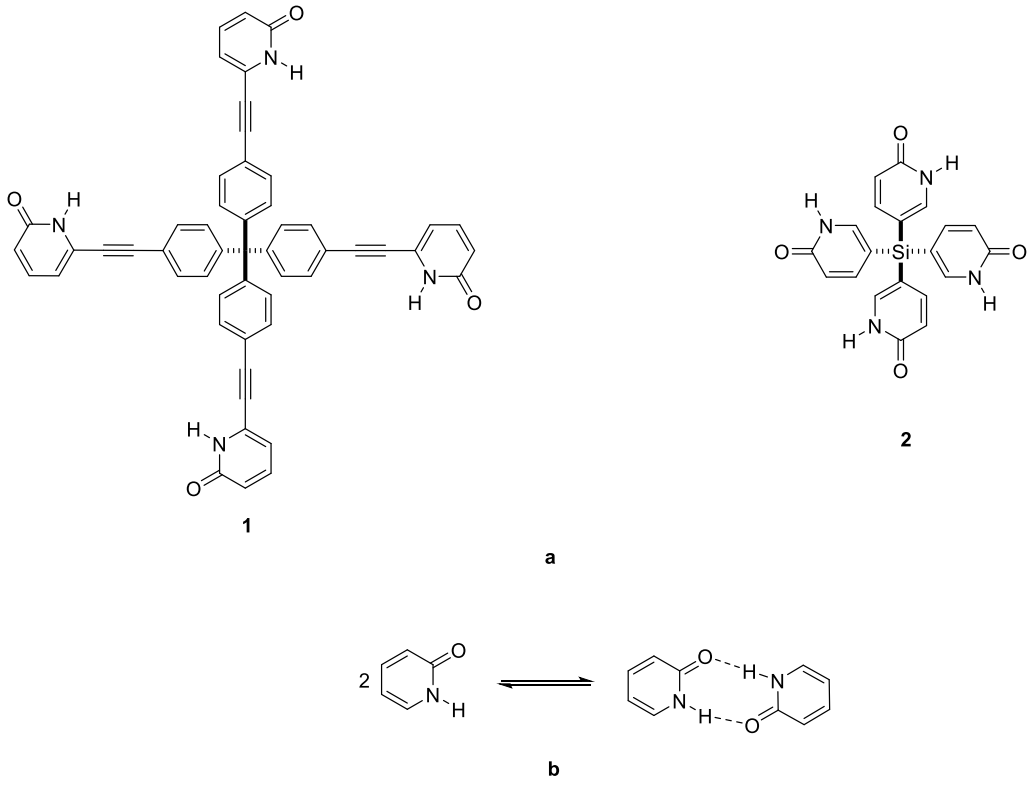

Figure 6. (a) Examples of modular construction based on association of 2-pyridinone groups connected to a rigid core. (b) Dimerization of 2-pyridinone.

Crystallization of tetrapyridinones **1** and **2** results in the formation of remarkably open networks held together by multiple hydrogen bonds. Both hydrogen-bonded networks formed by tetrapyridinones **1** and **2** are robust enough to retain their crystallinity during the exchange of guests, and the volume accessible to guests is high (up to 53%). This work validates the effectiveness of modular construction in crystal engineering as a tool for controlling the structure and properties of ordered solid materials. Crystallization of most molecules favours the formation of close-packed structures, which maximize the intermolecular interaction. Close-packed crystalline materials have no potential to include guests, and they only have small unfilled spaces between molecules that collectively add up to about 30% of the total volume of the crystals. In contrast, modular construction favours crystallization that does not normally lead to close packing because hydrogen bonding or other directional interactions prefer that the molecular components are arranged in other ways. Because, directional hydrogen bonding and close packing can not normally be optimized simultaneously, open networks are created. Therefore, modular construction is particular suitable for producing materials with high degrees of potential porosity. As a result, this strategy has revolutionized the engineering of highly ordered crystalline materials with large and open channels. Among these ordered crystalline materials are many that can retain their crystallinity after guests are partially or completely removed from the interior.

1.4.1 Porous Materials

Porous materials are a new class of materials with high structural rigidity and low density of mass. These materials are defined as a combination of solid phases with pores that make them

different from other materials.[33,34] Porous materials play a vital role in our daily life and industry. Some examples of their application are the purification of potable water, removing dust from gases, filtration, and molecular recognition. Porous materials can vary in composition and include both inorganic and organic frameworks. Zeolites are the first and example of microporous inorganic materials. Zeolites are aluminosilicates and are known for their potential to trap and store certain molecules like gases, for their utility as molecular sieves, and for their applications as catalysts. Zeolites contain Lewis acidic sites and can act as heterogeneous catalysts by activating specific reactions involving guest molecules inside the pores of the solid. These inorganic porous materials have well-defined pore sizes and are highly robust, and they can accommodate many gases and other small molecules (Figure 7).[35] Zeolites have high surface areas and offer resistance against high temperature, pressure, and chemical conditions, which justifies their wide usage in industry. Important examples include their use, as catalysts in the petroleum industry, as additives in detergents, and as ion-exchange materials.[33]

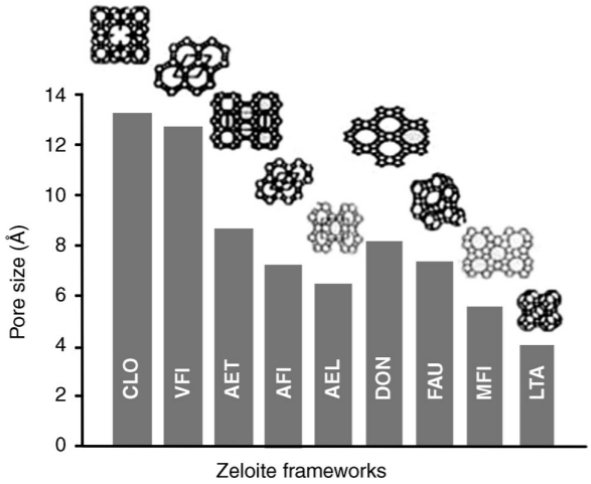

Figure 7. Different types of zeolites with different pore sizes.

The broad utility of zeolites provided a strong motivation for developing other porous ordered materials such as metal-organic frameworks (MOFs)[37,38] and covalent-organic frameworks (COFs).[39] MOFs are constructed from metal-containing subunits joined by organic linkers. MOFs offer highly open networks with permanent porosity and have applications in energy technologies, including fuel cells and catalytic conversion. COFs are constructed from organic molecules that undergo reactions leading to the formation of networks held together via covalent bonds. COFs typically have rigid structures with exceptional capacities for storing guests. Characterizing the structure of COFs is not as easy as for other porous materials since they do not typically form single crystals large enough to study by X-ray diffraction. However, despite the challenging characterization of COFs, they have useful applications in gas separation, energy storage, and electronics. Both MOFs and COFs (Figure **8a** and **8b,** respectively) have high thermal stability, due to the involvement of strong bonds that hold their frameworks in place.

Other porous ordered materials similar to zeolites, MOFs, and COFs are called "hydrogen-bonded organic frameworks (HOFs)." In contrast to other porous materials, frameworks of HOFs are held together by hydrogen bonds, and the modules used to construct HOFs are organic molecules. Each family of porous materials that have been produced by modular construction, including MOFs, COFs, and HOFs, has applications in gas storage, catalysts, and other areas that require porosity. However, each of these families of porous materials has individual properties that make them particularly suitable for use in specific areas. This subject will be discussed more in detail below.

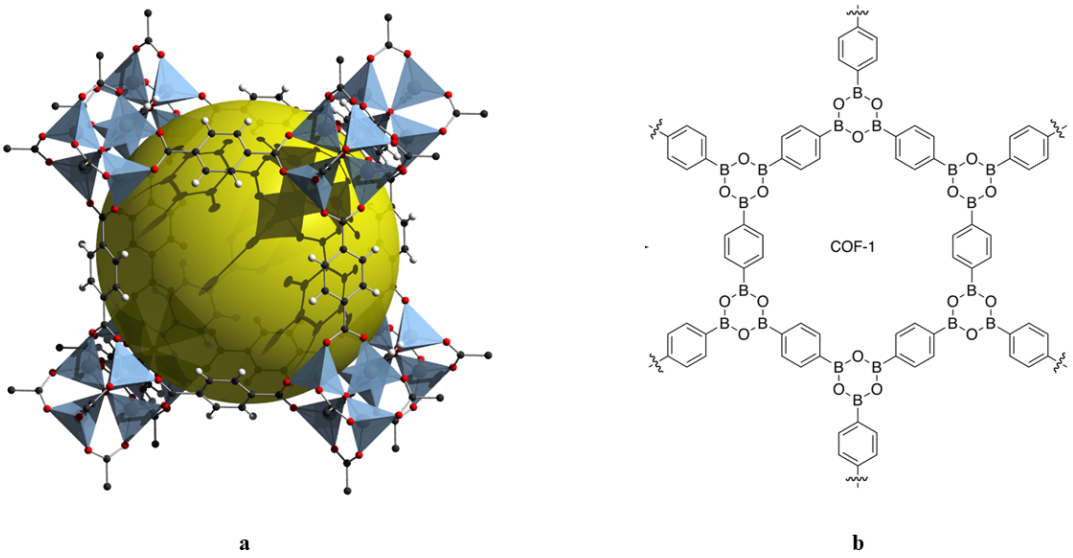

Figure 8. (a) Classic example of a MOF, called "MOF-5" with a large accessible volume represented in yellow. This metal-organic framework is obtained by the association of 1,4-benzenedicarboxylate with Zn^{2+}.[37] (b) An example of COFs, called "COF-1", which is obtained by linking three boronic acid groups to form six-membered rings of boroxine (B_3O_3).[40] Both of the frameworks remain crystalline after desolvation and show permanent porosity.

1.4.1.1 Hydrogen-Bonded Organic Frameworks (HOFs)

Hydrogen-bonded organic frameworks (HOFs) are organic porous materials, that have attracted much attention from crystal engineers during the past decades. HOFs are less known than MOFs and COFs because they are held together by relatively weak interactions, makes them inherently less stable. However, HOFs possess a high degree of crystallinity, because they are held together by hydrogen bonds, which can be broken and reformed reversibly to ensure that errors arising during crystallization are corrected. HOFs have several remarkable features that make them superior to other porous materials such as MOFs in certain applications. These

features include low density, self-healing by recrystallization, simple access by routine methods of crystallization, metal-free compositions, and a characteristic ability to deform in ways that promote the selective inclusion of guests. Nevertheless, hydrogen bonds are weaker than coordinative bonds in MOFs and COFs, so designing HOFs with high stability remains challenging. Removing guests from many open hydrogen-bonded frameworks will lead to the loss of their crystallinity, and their open structures will collapse. Over the years, many scientists have tried to design HOFs with permanent porosity and predictable structures similar to zeolites and MOFs. In order to meet the challenge of constructing HOFs with rigidity and stability, some factors should be taken into consideration. These factors include: 1) the need to incorporate multiple directional hydrogen-bonding units to ensure that the overall density of hydrogen bonds in the structure is high, 2) introducing stabilizing interactions between the building blocks and guests, and 3) using modules that have relatively little conformational freedom.[32]. Hydrogen bonds are individually weak, so multiple hydrogen bonds per module are needed to produce robust networks. Fortunately, various functional groups can be introduced to create multiple sites of hydrogen bonding per module. Examples of these functional groups include carboxylic acids, amidinium cations, benzimidazolones, diaminotriazines, amides, and others. As an example, Mastalerz and Oppel designed a highly ordered and open network constructed from triptycene trisbenzimidazolone **3,** in which imidazolone groups are grafted onto a rigid core of triptycene (Figure 9). The resulting porous network has a high surface area, which helps to increase the capacity for gas storage, and the volume accessible to guests is about 60%. This crystalline network is robust enough that it will retain its crystallinity after desolvation and results in a material with a high degree of permanent porosity.[39]

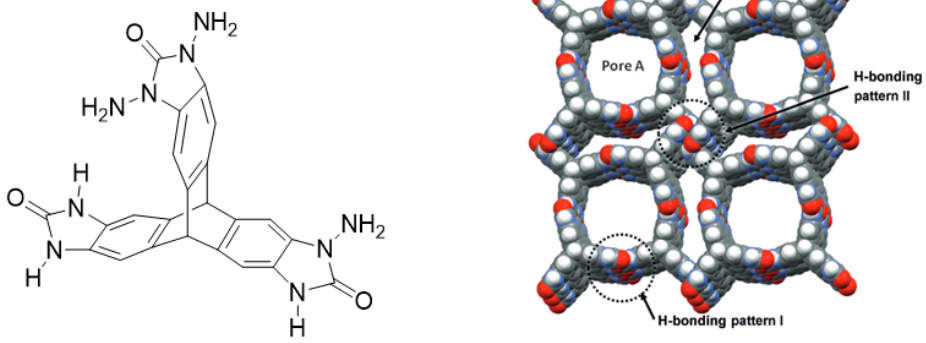

3

Figure 9. Example of a highly porous framework made by using the strategy of modular construction.

1.4.1.2 Porosity Measurement

In order to characterize porous materials, several parameters need to be measured, such as porosity, pore size, pore morphology, and specific surface area.[43] Porosity is the most important parameter among the others, as it influences the mechanical, physical, and chemical properties of the porous materials. The porosity value presents the volume occupied by guests compared to the total volume of the crystalline material, and it can vary in the range 0-100%. Depending on the size of the pores, there are various available methods for measuring porosity. If the size of pores is less than 2 nm (microporous), porosity can be measured by the adsorption of N_2 or other gases. On the other had, if the size of the pores is greater than 50 nm (macroporous) or in the rang 2-50 nm (mesoporous), three methods can be used. These methods are: 1) pycnometry, which measures the accurate mass-volume relation in solids or liquids. 2)

liquid intrusion, which is mostly measured by using Hg, and 3) gas adsorption, which is the most common method to measure porosity since this method has the potential to provide information on the size of the pores with a large defined surface area in materials.

The proof of permanent porosity can be obtained by the gas adsorption technique, which determines the reversible gas adsorption isotherm at low pressure and temperature. This isotherm represents the relationship between the adsorbed gas and the relative pressure. Measuring the adsorbed gas can occur by exposure of suitable gas such as N_2, Kr, or CO_2 to a porous sample that has been desolvated or been exchanged with another solvent that has a lower boiling point. Technically, the volume of the adsorbed gas can be measured at the boiling point of the appropriate gas. As soon as the sample comes into contact with the gas, and the gas reaches equilibrium with the surface, it is possible to measure the rational isotherm (Figure 10).[34]

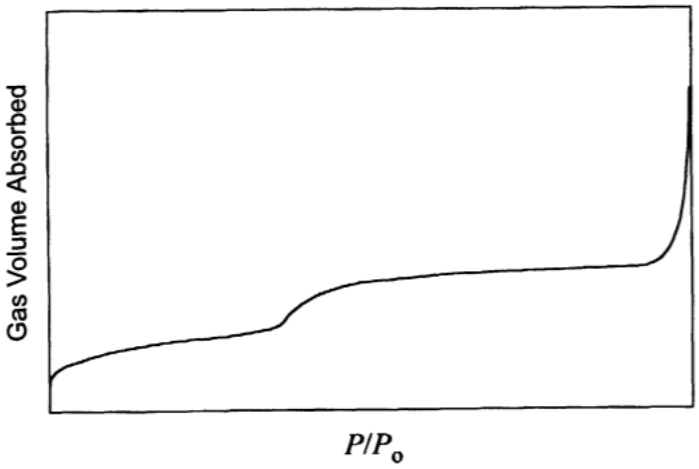

Figure 10. Typical gas adsorption isotherm graph

This gas adsorption isotherm also provides information on pore size, distribution of porous samples (quantity of each pore size in a relative volume of porous sample), and the specific

surface area. Specific surface area is another important feature of porous materials and, is defined as the total surface area of porous materials per unit of mass or volume. Measuring the surface area mostly measures the internal surface area in an open-cell porous material, and the external surface is very small and, can be neglected. Furthermore, there are several advantages to the internal surface area such as sound absorption, heat exchange, noise reduction, and catalysis. Depending on the size of the pores, there are several methods to measure the surface area, but the most common one is gas adsorption by using the BET isotherm. Brunauer-Emmett-Teller (BET) is a classical method to determine the gas adsorption data on a solid surface and to measure the specific surface area. The BET isotherm technique is based on Langmuir theory, which is only suitable for monolayer adsorption of gas molecules. Therefore, in 1938, Stephen Brunauer, Paul Hugh Emmett and Edward Teller extended this theory to provide a way to handle multilayer gas adsorption called the "BET method".[44] The porous sample in the gas adsorption BET method is either evacuated by heating under vacuum or degassed to remove unwanted species in the air, such moisture condensed on the pore surface. After this step, the gas, which is typically N_2, is absorbed on the surface at a low temperature in the adsorptive gas atmosphere and can be measured by the isotherm. It is worth mentioning that the results of Hg intrusion and gas adsorption are quite similar.

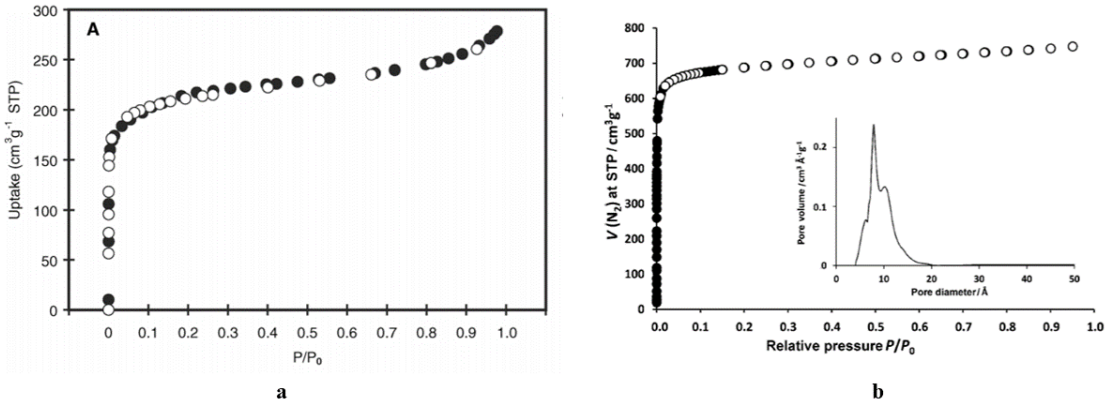

Figure 11. (a) Gas adsorption measurement by BET isotherm of COF-1 (Figure 8b). (b) BET isotherm of triptycene trisbenzimidazolone (Figure 9) as a HOF with a pore distribution diagram underneath. Both COF and HOF examples showed BET surface areas of 711 m^2/g and 2796 m^2/g respectively.

1.5 4,6-Diamino-1,3,5-triazinyl (DAT) Group

4,6-Diamino-1,3,5-triazinyl (DAT) groups are one of the most interesting recognition groups for use in the synthesis of hydrogen-bonded molecular complexes. DAT groups (**4**) are melamine derivatives, which are broadly useful in applications such as drug production, polymers, separation, and heterogenous catalysts. DAT groups are easily accessible, and they can be synthesized from the reaction between nitriles and dicyandiamide.[45,46]

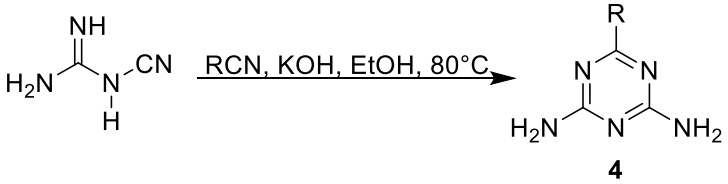

4

In addition, DAT groups have been extensively used in modular construction, since they can act as both hydrogen bond acceptors and donors, allowing them to take part in multiple hydrogen bonds according to reliable motifs. As a result, they are one of the most reliable functional groups for use in modular construction (Figure 6b). These motifs can be represented by structures **I-III** (Figure 12), which differ according to the relatively orientation of substituents. Because several motifs are possible, supramolecular assembly directed by DAT group will be far from being fully predictable. However, association is normally governed by one of the three patterns, and others are uncommon (Figure 12).[44] As a result, DAT groups have proven their ability to direct the construction of hydrogen-bonded organic frameworks (HOFs).

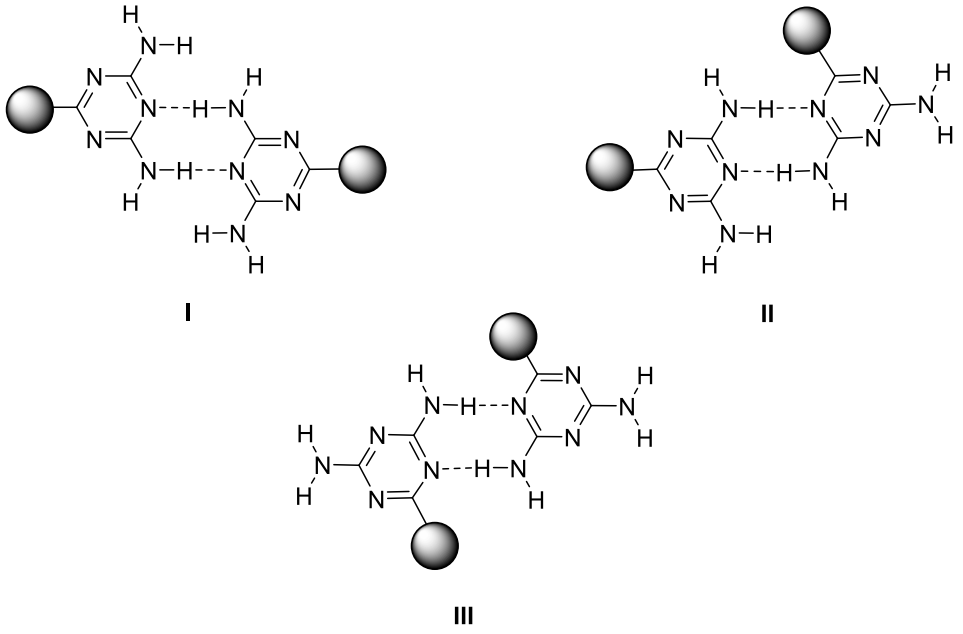

Figure 12. Hydrogen bonding motifs of DAT pairs. I. Face to face. II. Face to side. III. Side to side.[45]

Wuest and co-workers have developed various compounds containing DAT groups incorporated in well-defined molecular structures. One of the most interesting examples is hexakis[4-(2,4-diamino-1,3,5-triazin-6-yl)phenyl]benzene (**5a**), which acts as a module for the construction of a network in which each molecule is linked to six neighbors by hydrogen bonding of DAT groups. In the crystal structure of compound **5a**, hydrogen bond networks according to face to face motif I is favored, and the other two patterns are not observed, presumably for steric reasons.[46,47] Representations of the structure are provided in Figure 13.

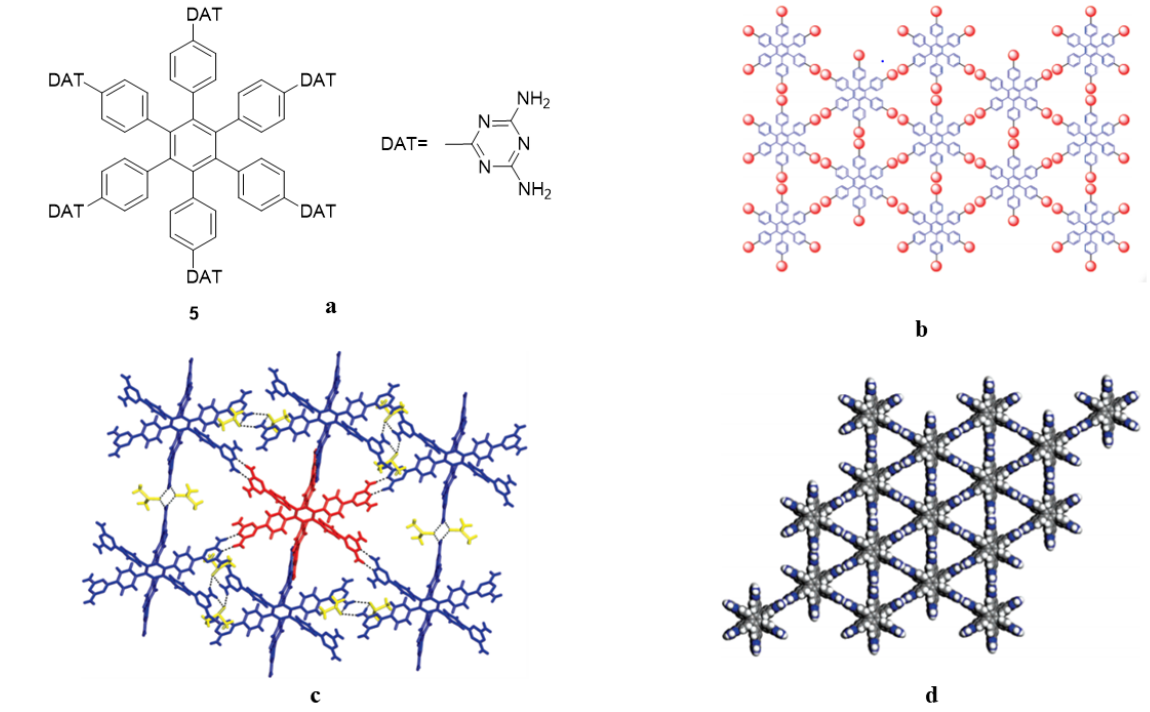

Figure 13. (a) Molecular structure of hexakis[4-(2,4-diamino-1,3,5-triazin-6-yl) phenyl]benzene **(5a).** (b) Representation of a possible network for compound **5a.** (c) Structure of crystals grown from DMSO/benzene, showing how each molecule is joined to its six neighbors through hydrogen bonds. (d) Representation of the open crystalline framework, with a guest accessible volume of 72%.

1.6 Purpose of this Study

Modular construction is able to provide predictably ordered materials with predetermined properties. The strategy is based on ensuring that molecular subunits engage in interactions that will hold neighboring modules in predetermined positions. Hydrogen bonds, due to their flexibility and directionality, have proven to be suitable for directing modular construction, despite being weaker than covalent bonds or coordinative interactions involving metals. As the number and the strength of hydrogen bonds increase, the resulting structures should become more robust and suitable for applications that require high stability. Therefore, our goal is to devise new modules for construction in which recognition groups that can be involved in unusually large numbers of hydrogen bonds are grafted to suitable molecular cores. Our work has been inspired by previous work in which DAT groups have played a key role in creating predictably ordered hydrogen-bonded organic frameworks (HOFs) with a high degree of permanent porosity. In this study, we have investigated a new recognition group related to DAT groups, but with a higher density of sites for hydrogen bonding. This new functional group has been grafted onto different rigid cores to generate unusually robust and open crystalline networks closely related to zeolites and MOFs.

1.7 References

(1) Lehn, J. Supramolecular Chemistry—Scope and Perspectives Molecules, Supermolecules, and Molecular Devices (Nobel Lecture). *Angew. Chem. Int. Ed. Engl.* **1988**, *27* (1), 89–112.

(2) Pedersen, C. J. The Discovery of Crown Ethers. *Science* **1988**, *241* (4865), 536–540.

(3) Cram, D. J. Cavitands: Organic Hosts with Enforced Cavities. *Science* **1983**, *219* (4589), 1177–1183.

(4) Stupp, S. I.; Palmer, L. C. Supramolecular Chemistry and Self-Assembly in Organic Materials Design. *Chem Mater* **2014**, 12.

(5) Whitesides, G. M.; Boncheva, M. Beyond Molecules: Self-Assembly of Mesoscopic and Macroscopic Components. *Proc. Natl. Acad. Sci. U. S. A.* **2002**, *99* (8), 4769–4774.

(6) Scofield, M. Nucleic Acids. In *xPharm: The Comprehensive Pharmacology Reference*; Enna, S. J., Bylund, D. B., Eds.; Elsevier: New York, 2007; pp 1–15.

(7) Pauling Linus. The Nature of the Chemical Bond. *Cornell Univ. Press Ithaca* **1939**, 131.

(8) Desiraju, G. R. Reflections on the Hydrogen Bond in Crystal Engineering. *Cryst. Growth Des.* **2011**, *11* (4), 896–898.

(9) Wang, L.-C.; Zheng, Q.-Y. Hydrogen Bonding in Supramolecular Crystal Engineering. In *Hydrogen Bonded Supramolecular Structures*; Li, Z.-T., Wu, L.-Z., Eds.; Lecture Notes in Chemistry; Springer Berlin Heidelberg: Berlin, Heidelberg, 2015; pp 69–113.

(10) Larson, J. W.; McMahon, T. B. Gas-Phase Bihalide and Pseudobihalide Ions. An Ion Cyclotron Resonance Determination of Hydrogen Bond Energies in XHY- Species (X, Y = F, Cl, Br, CN). *Inorg. Chem.* **1984**, *23* (14), 2029–2033.

(11) Emsley, J. Very Strong Hydrogen Bonding. *Chem Soc Rev* **1980**, *9* (1), 91–124.

(12) Langis-Barsetti, S.; Maris, T.; Wuest, J. D. Triptycene 1,2-Quinones and Quinols: Permeable Crystalline Redox-Active Molecular Solids. *J. Org. Chem.* **2018**, *83* (24), 15426–15437.

(13) Aitipamula, S.; Vangala, V. R. X-Ray Crystallography and Its Role in Understanding the Physicochemical Properties of Pharmaceutical Cocrystals. *J. Indian Inst. Sci.* **2017**, *97* (2), 227–243.

(14) Desiraju, G. R. Chemistry beyond the Molecule. *Nature* **2001**, *412* (6845), 397–400.

(15) Schmidt, G. M. J. Photodimerization in the Solid State. *Pure Appl. Chem.* **1971**, *27* (4), 647–678.

(16) Desiraju, G. R. *Crystal Engineering: The Design of Organic Solids*; Elsevier: Amsterdam; New York, 1989.

(17) Pepinsky, R. Crystal Engineering-New Concept in Crystallography; AMERICAN PHYSICAL SOC ONE PHYSICS ELLIPSE, COLLEGE PK, MD 20740-3844 USA, 1955; Vol. 100, pp 971–971.

(18) Kitaigorodskii, A. *Molecular Crystals and Molecules*, 1st ed.; Physical chemistry; New York, 1973; Vol. 29.

(19) Etter, M. C. Encoding and Decoding Hydrogen-Bond Patterns of Organic Compounds. *Acc. Chem. Res.* **1990**, *23* (4), 120–126.

(20) Desiraju, G. R. Supramolecular Synthons in Crystal Engineering—A New Organic Synthesis. *Angew. Chem. Int. Ed. Engl.* **1995**, *34* (21), 2311–2327.

(21) Desiraju, G. R. Crystal Engineering: From Molecule to Crystal. *J. Am. Chem. Soc.* **2013**, *135* (27), 9952–9967.

(22) Röntgen, W. *Phys Med Ges Würzbg.* **1895**, 137:132.

(23) Friedrich, W.; Knipping, P.; Laue, M. Interferenzerscheinungen Bei Röntgenstrahlen. *Ann. Phys.* **1913**, *346* (10), 971–988.

(24) Bragg, W. L. The Specular Reflection of X-Rays. *Nature* **1912**, *90* (2250), 410–410.

(25) Bragg, W. L.; Bragg, W. H. The Structure of Some Crystals as Indicated by Their Diffraction of X-Rays. *Proc. R. Soc. Lond. Ser. Contain. Pap. Math. Phys. Character* **1913**, *89* (610), 248–277.

(26) Lonsdale, K. The Structure of the Benzene Ring. *Nature* **1928**, *122* (3082), 810–810.

(27) Wuest, J. D. Engineering Crystals by the Strategy of Molecular Tectonics. *Chem. Commun.* **2005**, No. 47, 5830–5837.

(28) Wuest, J. D. Molecular Tectonics. In *Mesomolecules: From Molecules to Materials*; Mendenhall, G. D., Greenberg, A., Liebman, J. F., Eds.; Structure Energetics and Reactivity in Chemistry Series (SEARCH series); Springer Netherlands: Dordrecht, 1995; pp 107–131.

(29) Ermer, Otto. Five-Fold Diamond Structure of Adamantane-1,3,5,7-Tetracarboxylic Acid. *J. Am. Chem. Soc.* **1988**, *110* (12), 3747–3754.

(30) Ducharme, Y.; Wuest, J. D. Use of Hydrogen Bonds to Control Molecular Aggregation. Extensive, Self-Complementary Arrays of Donors and Acceptors. *J. Org. Chem.* **1988**, *53* (24), 5787–5789.

(31) Simard, M.; Su, D.; Wuest, J. D. Use of Hydrogen Bonds to Control Molecular Aggregation. Self-Assembly of Three-Dimensional Networks with Large Chambers. *J. Am. Chem. Soc.* **1991**, *113* (12), 4696–4698.

(32) Wang, X.; Simard, M.; Wuest, J. D. Molecular Tectonics. Three-Dimensional Organic Networks with Zeolitic Properties. *J. Am. Chem. Soc.* **1994**, *116* (26), 12119–12120.

(33) Liu, P. S.; Chen, G. F. Chapter One - General Introduction to Porous Materials. In *Porous Materials*; Liu, P. S., Chen, G. F., Eds.; Butterworth-Heinemann: Boston, 2014; pp 1–20.

(34) Ishizaki, K.; Komarneni, S.; Nanko, M. Applications of Porous Materials. In *Porous Materials: Process technology and applications*; Ishizaki, K., Komarneni, S., Nanko, M., Eds.; Materials Technology Series; Springer US: Boston, MA, 1998; pp 181–201.

(35) Espinal, L. Porosity and Its Measurement. In *Characterization of Materials*; American Cancer Society, 2012; pp 1–10.

(36) Huo, Q. Chapter 16 - Synthetic Chemistry of the Inorganic Ordered Porous Materials. In *Modern Inorganic Synthetic Chemistry*; Xu, R., Pang, W., Huo, Q., Eds.; Elsevier: Amsterdam, 2011; pp 339–373.

(37) Li, H.; Eddaoudi, M.; O'Keeffe, M.; Yaghi, O. M. Design and Synthesis of an Exceptionally Stable and Highly Porous Metal-Organic Framework. *Nature* **1999**, *402* (6759), 276–279.

(38) Furukawa, H.; Cordova, K. E.; O'Keeffe, M.; Yaghi, O. M. The Chemistry and Applications of Metal-Organic Frameworks. *Science* **2013**, *341* (6149), 1230444.

(39) Diercks, C. S.; Yaghi, O. M. The Atom, the Molecule, and the Covalent Organic Framework. *Science* **2017**, *355* (6328), eaal1585.

(40) Côté, A. P.; Benin, A. I.; Ockwig, N. W.; O'Keeffe, M.; Matzger, A. J.; Yaghi, O. M. Porous, Crystalline, Covalent Organic Frameworks. *Science* **2005**, *310* (5751), 1166–1170.

(41) Hisaki, I.; Xin, C.; Takahashi, K.; Nakamura, T. Designing Hydrogen-Bonded Organic Frameworks (HOFs) with Permanent Porosity. *Angew. Chem. Int. Ed.* **2019**, *58* (33), 11160–11170.

(42) Mastalerz, M.; Oppel, I. M. Rational Construction of an Extrinsic Porous Molecular Crystal with an Extraordinary High Specific Surface Area. *Angew. Chem. Int. Ed.* **2012**, *51* (21), 5252–5255.

(43) Liu, P. S.; Chen, G. F. Chapter Nine - Characterization Methods: Basic Factors. In *Porous Materials*; Liu, P. S., Chen, G. F., Eds.; Butterworth-Heinemann: Boston, 2014; pp 411–492.

(44) Brunauer, S.; Emmett, P. H.; Teller, E. Adsorption of Gases in Multimolecular Layers. *J. Am. Chem. Soc.* **1938**, *60* (2), 309–319.

(45) Bartholomew, D. 6.12 - 1,3,5-Triazines. In *Comprehensive Heterocyclic Chemistry II*; Katritzky, A. R., Rees, C. W., Scriven, E. F. V., Eds.; Pergamon: Oxford, 1996; pp 575–636.

(46) Blotny, G. Recent Applications of 2,4,6-Trichloro-1,3,5-Triazine and Its Derivatives in Organic Synthesis. *Tetrahedron* **2006**, *62* (41), 9507–9522.

(47) Fournier, J.-H.; Maris, T.; Wuest, J. D. Molecular Tectonics. Porous Hydrogen-Bonded Networks Built from Derivatives of 9,9‘-Spirobifluorene. *J. Org. Chem.* **2004**, *69* (6), 1762–1775.

Chapter 2. Modular Construction of Porous Hydrogen-Bonded Molecular Materials from Melams

2.1 Introduction

As summarized in Chapter 1, it is possible to design molecular compounds that crystallize to form highly open networks held together by hydrogen bonds. Modular construction is a powerful tool and has proven to be reliable strategy in which molecular subunits can be held in predetermined positions by multiple directional hydrogen bonds. Simple DAT groups have been used extensively for this purpose, and in favorable cases open networks held together by DAT groups can be desolvated to generate rigorously porous crystalline materials. To increase the robustness and porosity of the materials, we decided to examine the behaviour of related compounds with even higher densities of DAT groups. This led us to study complex derivatives of melam ($HN(DAT)_2$), which is the subject of the manuscript that is incorporated in Chapter 2.

Chapter 2 is presented in the form of an article describing the synthesis and associative behaviour of various molecular compounds incorporating multiple $N(DAT)_2$ units. The chapter shows that it is possible in this way to make highly porous networks that are held together by large numbers of hydrogen bonds. Selected examples can be converted by desolvation to give robust and stable HOFs with high degrees of permanent porosity.

Preliminary work, including the synthesis of various melams and analysis of their crystal structures, was carried out by Huy Che-Quang. I optimized the method of synthesis, made additional compounds, completed the characterizations, and wrote the experimental section. Dr Thierry Maris worked on the crystal structures. In addition, Prof. Ashlee Howarth and her

student Zvart Ajoyan at Concordia University measured the porosity of our materials. Prof. James Wuest supervised my work, and together we wrote the manuscript and experimental section.

In press in Chemistry -A European Journal

Modular Construction of Porous Hydrogen-Bonded Molecular Materials from Melams

Tinasadat Khadivjam,[†] Huy Che-Quang,[†] Thierry Maris,[†] Zvart Ajoyan,[‡]

Ashlee J. Howarth,[‡] and James D. Wuest*[,†]

[†]*Département de Chimie, Université de Montréal, Montréal, Québec H3C 3J7 Canada*

[‡]*Department of Chemistry & Biochemistry, Concordia University, Montréal, Québec H4B 1R6 Canada*

*Author to whom correspondence may be addressed. E-mail:

james.d.wuest@umontreal.ca

2.2 Abstract

Ordered materials with predictable structures and properties can be made by a modular approach, using molecules designed to interact with neighbors and hold them in predetermined positions. Incorporating 4,6-diamino-1,3,5-triazin-2-yl (DAT) groups in modules is an effective way to direct assembly because each DAT group can form multiple N–H···N hydrogen bonds according to established patterns. We have found that modules with high densities of N(DAT)2 groups can be made by base-induced double triazinylations of readily available amines. The resulting modules can form structures held together by remarkably large numbers of hydrogen bonds per molecule. Even simple modules with only 1–3 $N(DAT)_2$ groups and fewer than 70 non-hydrogen atoms can crystallize to form highly open networks in which each molecule engages in over 20 N–H···N hydrogen bonds, and more than 70% of the volume is available for accommodating guests. In favorable cases, guests can be removed to create rigorously porous crystalline solids analogous to zeolites and metal-organic framewroks.

2.3 Introduction

Modular construction has emerged as a powerful strategy for making ordered materials with predictable structures and properties. The strategy employs well-defined molecular modules designed to be joined to neighbors and held in predetermined positions. The properties of the individual modules can be varied according to need, and various chemical interactions can be chosen to direct the assembly. As a result, modular construction has unlimited scope for making useful new materials.

The rapid growth of modular construction in recent decades was triggered by two closely related advances. One, in organic chemistry, was the discovery that predictably ordered networks can be constructed from modules that engage in hydrogen bonding.[1–4] The other, in inorganic chemistry, was the related demonstration that coordination to metals can also be used to program assembly.[5] This early work revealed the special potential of modular construction as a way to make porous materials. When modules have little flexibility and favor directional interactions with neighbors, close packing and optimal intermolecular bonding cannot normally be achieved at the same time. Open structures are typically formed, with interstitial volumes occupied by molecules of solvent or other guests present during assembly. These observations provided a starting point for the subsequent development of important new classes of porous ordered materials, including metal-organic frameworks (MOFs),[6] covalent organic frameworks (COFs),[7,8] and hydrogen-bonded organic frameworks (HOFs).[9–11] All three classes share a key feature; specifically, they have open structures from which guests can be removed to create rigorously porous ordered materials. Together, MOFs, COFs, and HOFs already have many

applications, particularly in catalysis, separations, and the reversible inclusion of gases and other guests.

HOFs are less widely used than MOFs at present but offer unique advantages. For example, HOFs have metal-free porous structures of low density, and it may be possible to make biodegradable and biocompatible forms from renewable resources such as biomass. In addition, HOFs can show selective inclusion resulting from the special ability of hydrogen-bonded networks to deform in response to guests, and HOFs can be produced by low-energy solution-based methods of crystallization, purification, and processing. However, hydrogen bonds are typically weaker than the coordinative interactions present in MOFs, so removing guests from hydrogen-bonded networks to give well-ordered HOFs with significant levels of permanent porosity is inherently challenging.

An encouraging precedent, known for decades, is the behavior of hydroquinone as a module for constructing porous materials.[12] Each molecule in crystals of the β-form is hydrogen-bonded to four neighbors to create an open network, in which about 16% of the volume is available to accommodate guests. The network can be obtained either in porous guest-free form or as solvates, with small guests occupying the available volume. Although the porosity is low, the fact that it arises from modules of great simplicity hints at the latent potential of HOFs as porous materials. A breakthrough in the field of HOFs was the discovery that crystalline hydrogen-bonded molecular solids can have high permanent porosities similar to those of MOFs and purely inorganic analogues such as zeolites. In the first reported example of this type,[13,14] solvated crystals composed of hydrogen-bonded molecules of tetrakis(diaminotriazine) **1** were placed under vacuum, which led to the removal of guests and

the formation of a porous solid without loss of crystallinity, as confirmed initially by single-crystal X-ray diffraction and later by porosimetry. Subsequent work has revealed that other highly open hydrogen-bonded networks are robust enough to yield rigorously porous crystalline molecular solids after removal of guests.[15–19] As a result, HOFs cannot be dismissed as curiosities, and they can have properties that place them among the most remarkable porous materials known, including solvent-accessible volumes well above 70%, values of S_{BET} exceeding 3000 $m^2 g^{-1}$, and densities below 0.5 g cm^{-3}.[9–11,16,17]

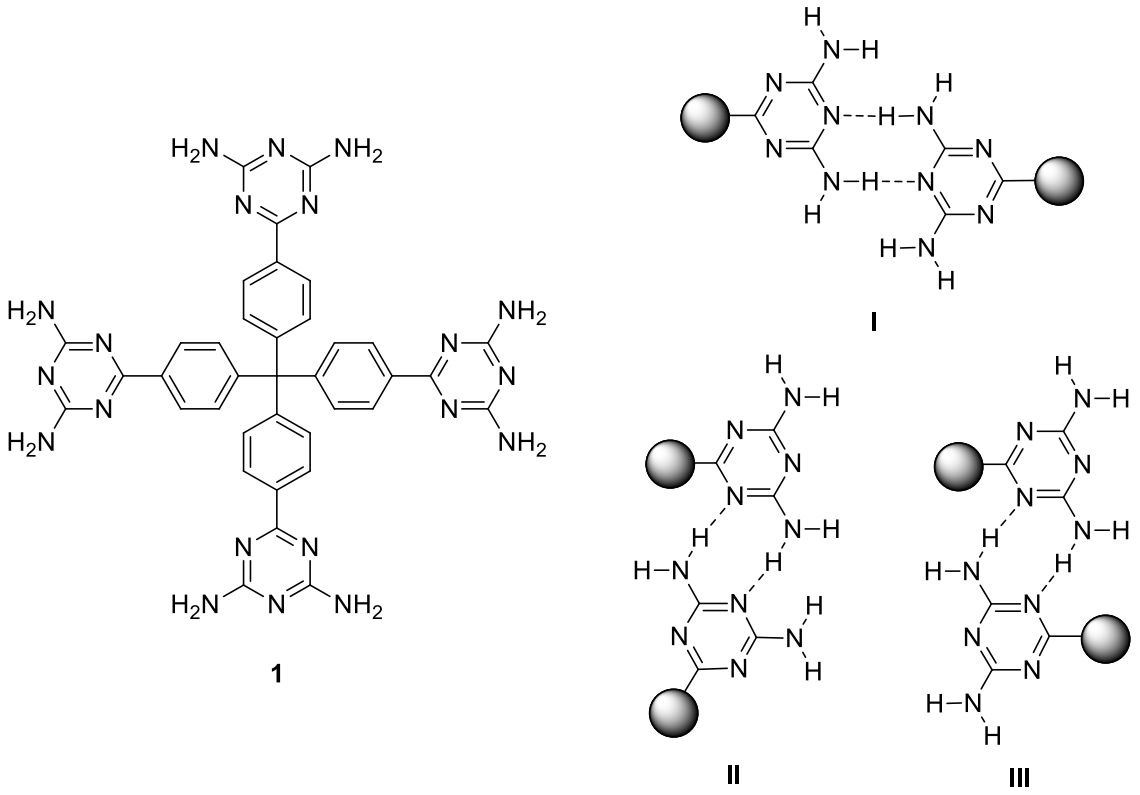

The structural integrity of such materials is maintained in large part by intermolecular hydrogen bonds, as assessed quantitatively by using DFT calculations to partition the lattice

energy of related solids into contributions from various sources, including hydrogen bonding.[20] Individual hydrogen bonds are weaker and less directional than covalent bonds and coordinative interactions involving metals. To compensate for this inherent disadvantage, each molecule in HOFs must normally engage in multiple hydrogen bonds. Diverse hydrogen-bonding functional groups can be used, but those that can serve simultaneously as donors and acceptors maximize the number of interactions per molecule. As illustrated by the behavior of compound **1** and many other examples, simple 4,6-diamino-1,3,5-triazin-2-yl (DAT) groups have proven to be particularly effective. Each group can form multiple hydrogen bonds according to three established motifs (**I**−**III**), which differ only in the relative orientation of the molecular cores (represented by gray spheres).[21]

The established ability of DAT groups to direct the assembly of HOFs and ensure their structural integrity provides a strong incentive to find ways to increase the density of DAT groups in molecules designed for use in modular construction. A special opportunity is suggested by the structure of melam (**2**), a compound first reported by Liebig in 1834.[19] In melam (**2**), two DAT groups are bonded to a central atom of nitrogen, thereby creating an $N(DAT)_2$ unit. Melam (**2**) is an intermediate in the formation of graphitic carbon nitrides by thermal condensation of melamine (**3**),[20–23] and it can also be obtained by other high-temperature methods.[24,25] However, substituted derivatives of melam (**2**) are virtually unknown. Devising ways to graft multiple $N(DAT)_2$ groups onto suitable molecular cores would allow the synthesis of compounds with exceptional capacities for forming hydrogen bonds. In this paper, we report simple ways to convert primary amines RNH_2 into the corresponding substituted melams $RN(DAT)_2$. In addition, we show that compounds with multiple $N(DAT)_2$

groups can be used as modules to construct remarkably open hydrogen-bonded networks, and we demonstrate that the resulting materials can be converted into HOFs with high porosity.

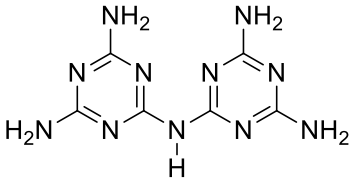

2

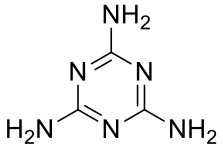

3

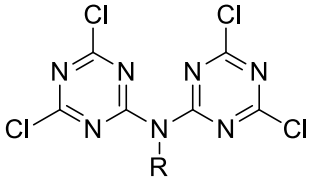

4

2.4 Results and Discussion

Conversion of Primary Amines RNH_2 into Substituted Melams $RN(DAT)_2$.

We found that primary amines RNH_2 can be converted into substituted melams $RN(DAT)_2$ by either of two straightforward procedures (Methods A and B in Scheme 1). Both methods are related to a process reported by Nohara et al. for triazinylating arylamines.[29] In our Method A, the amine is allowed to react with excess cyanuric chloride and sodium hydride at 25 °C in anhydrous THF, and the resulting intermediate is treated with concentrated aqueous NH_3 at 60 °C. In Method B, sodium hydride is replaced in the first step by diisopropylethylamine. In both methods, the initial step achieves bis(triazinylation) of the starting amine, as shown in representative cases by isolating bis(4,6-dichloro-1,3,5-triazin-2-yl)amines (**4**). Similar chlorotriazines were reported earlier by Nohara et al.[29] The chlorotriazines can normally be purified by crystallization or rapid column chromatography if desired but are susceptible to hydrolysis, so we typically converted them into substituted melams

by direct aminolysis, without isolation and purification. Method A was used to prepare melams **5**, **9**, and **10** in overall yields of 60, 40, and 40%, respectively, and Method B provided analogues **6**–**8** in overall yields of 53, 79, and 35%, respectively. Both methods are generally effective, and we simply selected the route that provided the higher yield, which appears to depend on factors that include the solubility and acidity of triazinylated intermediates. Melams **5**–**10** are all derived from arylamines, but Method A can also be used to make substituted melams from aliphatic amines, as illustrated by the conversion of benzylamine into melam **11** in 19% overall yield. As a result, our work provides simple ways to convert diverse primary amines into $N(DAT)_2$-substituted derivatives, thereby giving access to a promising new family of modules for constructing HOFs.

Scheme 1

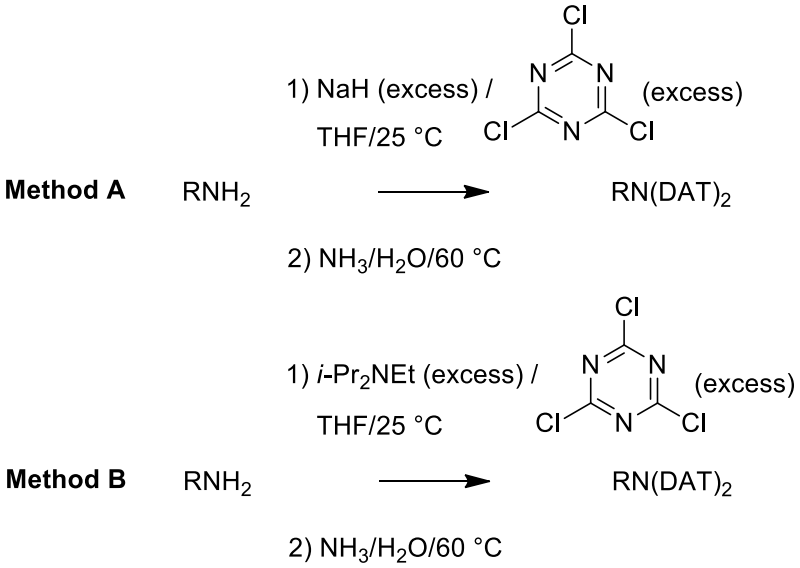

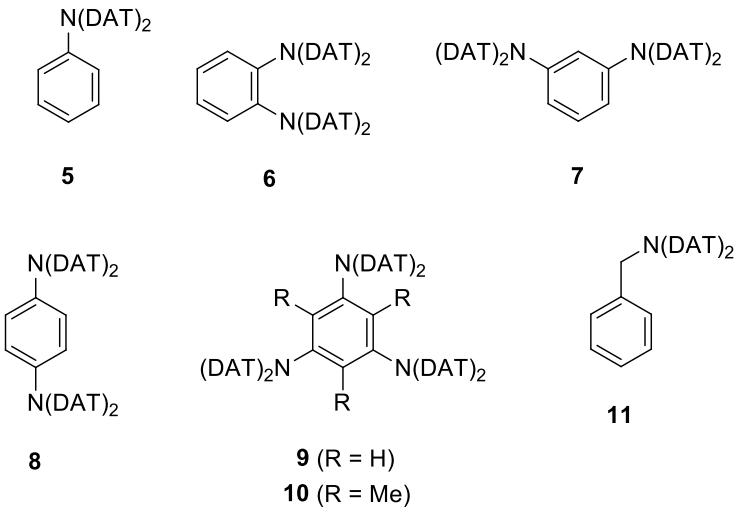

PhN(DAT)$_2$ (5)

Analysis by X-ray diffraction showed that crystals of melam **5** grown by cooling a hot solution in DMSO have the composition **5** • 3 DMSO and belong to the monoclinic space group *C*2/*c*. Other crystallographic data are provided in Table 1, views of the structure are shown in Figure 1, and selected parameters related to hydrogen bonding are collected in Table 2. As expected, compound **5** forms a network joined by multiple N–H···N hydrogen bonds characteristic of DAT groups, and interstitial volumes accommodate molecules of solvent. As shown in Figure 1a, each DAT group of compound **5** is linked to an essentially coplanar DAT group in two neighboring molecules, thereby giving rise to chains joined by a total of four hydrogen bonds of Type I per molecule (N···N distance = 2.968 Å). Association is reinforced by additional N–H···O hydrogen bonds involving well-ordered bridging molecules of DMSO (average N···O distance = 2.941 Å). Hydrogen-bonded chains of melam **5** pack to give corrugated sheets perpendicular to the *b*-axis (Figure 1b), and the sheets are stacked to give the

observed structure. Approximately 55% of the volume of the structure is accessible to guests.[30–32] As shown in Table 2, the density of N–H···N hydrogen bonds per unit of volume in the crystals (2.92×10^{-3} Å^{-3}) is substantially lower than that observed in the structure of the benchmark HOF derived from compound **1** (5.32×10^{-3} Å^{-3}).

Table 1. Crystallographic Data for Substituted Melams **5–8**

Compound	**5** • 3 DMSO	2 **6** • 2 DMSO • 9 H_2O	**7** • n DMSO (n = ~12–16)[a]	**7** • 4 DMSO	**8** • 3 DMSO • solvent	**8** • 5 DMSO • 2 C_6H_6
crystallization medium	DMSO	DMSO/H_2O	DMSO/EtOH	DMSO/Et_3NH^+ F^-	DMSO/EtOH	DMSO/C_6H_6
formula	$C_{18}H_{31}N_{11}O_3S_3$	$C_{40}H_{70}N_{44}O_{11}S_2$	$C_{18}H_{20}N_{22}$ + solvent	$C_{26}H_{44}N_{22}O_4S_4$	$C_{24}H_{38}N_{22}O_3S_3$ + solvent	$C_{40}H_{62}N_{22}O_5S_5$
crystal system	monoclinic	monoclinic	tetragonal	orthorhombic	orthorhombic	monoclinic
space group	*C*2/*c*	*C*2/*c*	$P4_32_12$	*Pbca*	*Pbcn*	$P2_1/c$
a (Å)	10.9174(4)	25.072(4)	21.2871(5)	16.7736(4)	22.6297(5)	16.7222(7)
b (Å)	18.9758(8)	13.115(2)	21.2871(5)	21.5283(5)	16.5486(4)	22.2116(9)
c (Å)	13.2699(5)	20.790(3)	32.0541(7)	22.2754(5)	21.7786(5)	16.9061(7)
α (°)	90	90	90	90	90	90
β (°)	93.486(2)	112.824(6)	90	90	90	119.267(2)
γ (°)	90	90	90	90	90	90
V (Å^3)	2743.99(18)	6300.7(18)	14525.0(8)	8043.8(3)	8155.9(3)	5477.8(4)
Z	4	4	8	8	8	4

Z'	0.5	0.5	1	1	1	1
T (K)	200	150	150	150	150	150
ρ_{calc} (g cm^{-3})	1.321	1.484	0.498[b]	1.415	1.269[b]	1.323
λ (Å)	1.54178	1.54178	1.34139	1.34139	1.54178	1.54178
μ (mm^{-1})	2.823	1.558	0.190[b]	1.778	2.139[b]	2.469
measured reflections	17420	43823	99948	101158	125544	76432
independent reflections	2709	5686	13667	8659	7393	10704
R_{int}	0.0492	0.0554	0.0648	0.0276	0.0438	0.0253
observed reflections	2489	5531	8222	7595	6925	9626
R_1, $I > 2\sigma(I)$	0.0573	0.0637	0.0470	0.0658	0.0855	0.0699
R_1, all data	0.0598	0.0645	0.0815	0.0716	0.0879	0.0735
wR_2, $I > 2\sigma(I)$	0.1573	0.1772	0.1487	0.1926	0.2383	0.2062
wR_2, all data	0.1544	0.1779	0.1709	0.1973	0.2397	0.2088
GoF	1.047	1.057	1.121	1.097	1.201	1.141

[a]Composition estimated by X-ray crystallography and NMR spectroscopy

[b]Calculated without contributions from disordered solvent molecules as determined using the mask/squeeze routine

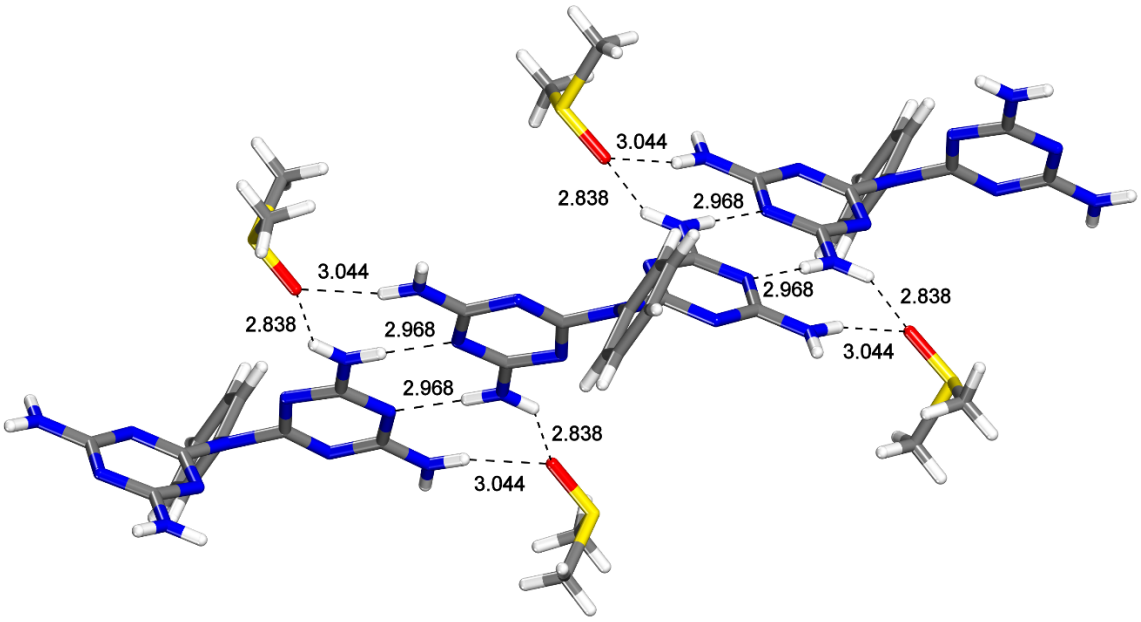

a

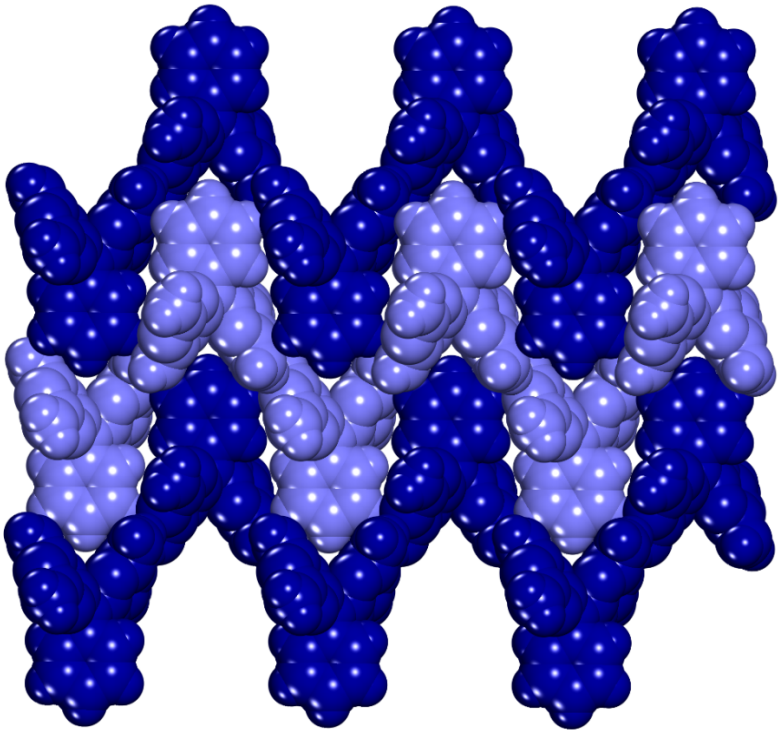

b

Figure 1. Representations of the structure obtained by crystallizing $PhN(DAT)_2$ **(5)** from DMSO. (a) View showing how molecules are linked into chains by N–H···N hydrogen bonds characteristic of DAT groups, reinforced by N–H···O hydrogen bonds involving bridging molecules of DMSO. Hydrogen bonds are represented by broken lines, with N···N and N···O distances given in Å. (b) View along the a-axis showing the cross sections of stacked corrugated sheets (in contrasting colors), each composed of parallel hydrogen-bonded chains packed along the a-axis. Unless noted otherwise, guest molecules of DMSO are omitted for clarity, and atoms of carbon are shown in gray, hydrogen in white, nitrogen in blue, oxygen in red, and sulfur in yellow.

Table 2. Selected Parameters Related to Hydrogen Bonding in the Structures of Compounds **1** and **5**–**10**

Compound	**DAT groups per molecule**	**N–H···N hydrogen bonds per molecule**[a]	**Hydrogen-bonded neighbors per molecule**	**N–H···N hydrogen bonds per unit volume** (10^{-3} Å^{-3})
1	4	16	8	5.32
5	2	4	2	2.92
6	4	14	3	8.89
7 ($P4_32_12$)	4	16	4	4.41

7 (*Pbca*)	4	22	7	10.94
8 (*Pbcn*)	4	22	7	10.79
8 ($P2_1/c$)	4	16	5	5.84
9	6	20	5	5.19
10	6	12	6	3.37

[a]An N–H···N hydrogen bond is considered to be formed when the measured N···N distance is less than 3.60 Å, the N···H distance is less than 2.65 Å, and the N–H···N angle is more than 120°.

In the structure, each molecule of $PhN(DAT)_2$ (**5)** adopts a nonplanar propeller-shaped conformation similar to those favored by triphenylamine and related triarylamines. The central atom of nitrogen is sp^2-hybridized (sum of C–N–C angles = 360.0°), defining a trigonal NC_3 core. The plane of this core lies at an angle of 46° with respect to the phenyl group, whereas the average angle between the plane of the core and the two triazinyl groups is 39°, reflecting slightly greater conjugation with the heterocyclic rings. Similarly, analysis of crystals of $HN(DAT)_2$ (**2**) shows that the two triazinyl groups are turned out of the plane of the NC_2 core, but in this case the central atom of nitrogen is only disubstituted, and the average angle of heteroaryl torsion is smaller (about 12°).[26]

Tautomer **5A** is favored in crystals of $PhN(DAT)_2$ **5**, instead of alternatives such as internally hydrogen-bonded structure **5B**. The average endocyclic carbon-nitrogen bond length

(1.343 Å) is similar to the length of exocyclic C–NH_2 bonds (1.336 Å), which are formally single. The longest carbon-nitrogen bonds in the $N(DAT)_2$ group of compound **5** (average length = 1.411 Å) are those involving the central atom of nitrogen, which is shared by two triazinyl rings. $HN(DAT)_2$ (**2**) shows analogous behavior, and its carbon-nitrogen bond lengths are similar to those observed in substituted derivative **5**. Although tautomer **5A** provides an adequate representation of the molecular structure of compound **5**, it is important to note that the carbon-nitrogen bonds in the $N(DAT)_2$ group, both endocyclic and exocyclic, all have significant double-bond character. In $PhN(DAT)_2$ **5**, the triazinyl rings are geometrically distorted, as they are in $HN(DAT)_2$ (**2**), in melamine, and even in 1,3,5-triazine itself,[33,34] and the average endocyclic N–C–N angle in compound **5** (126.12°) is much larger than the average C–N–C angle (113.82°).

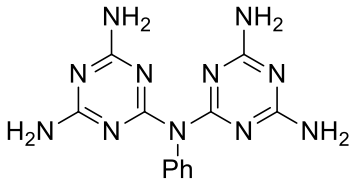

5A

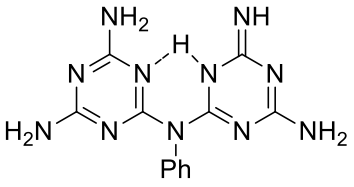

5B

1,2-Ph[N(DAT)$_2$]$_2$ (6)

Crystals of melam **6** were grown by allowing H_2O to diffuse slowly into a solution in DMSO. Analysis by X-ray diffraction established that the crystals have the composition 2 **6** • 2 DMSO • 9 H_2O and belong to the monoclinic space group *C*2/*c*. Table 1 presents additional crystallographic data, and Figure 2 provides views of the structure. Melam **6** generates an open

network joined by multiple N–H···N hydrogen bonds characteristic of DAT groups, and interstitial volumes accommodate guests. Figure 2a shows that molecules of compound **6** are linked along the *b*-axis to form chains held together by hydrogen bonds of Type III involving non-coplanar DAT groups (average N···N distance = 3.023 Å). Each molecule engages in a total of eight hydrogen bonds of this type. In addition, each molecule interacts with a third neighbor (Figure 2b) to form four N–H···N hydrogen bonds of Type I in which the DAT groups are non-coplanar (average N···N distance = 3.093 Å). The chains are thereby linked into *hcb* sheets aligned with the *bc*-plane (Figure 2c), and each molecule of melam **6** engages in a total of fourteen N–H···N hydrogen bonds. Approximately 31% of the volume of the structure is accessible to guests.[27–29]

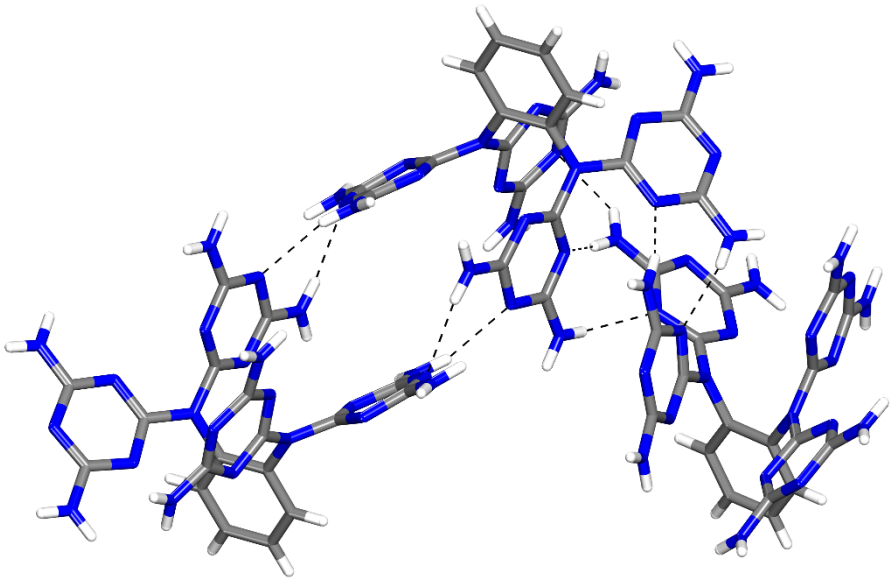

a

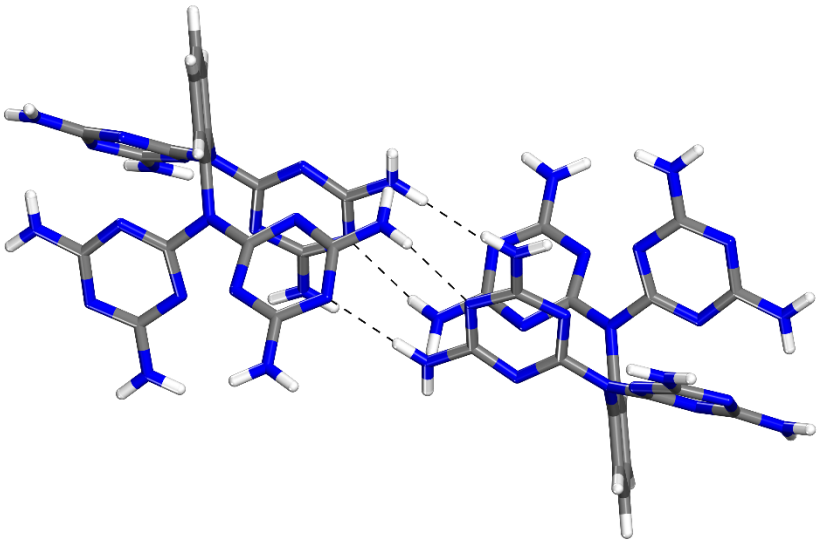

b

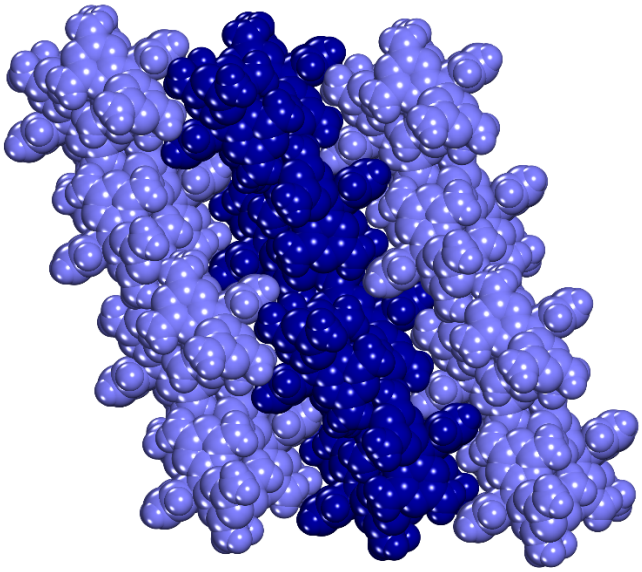

c

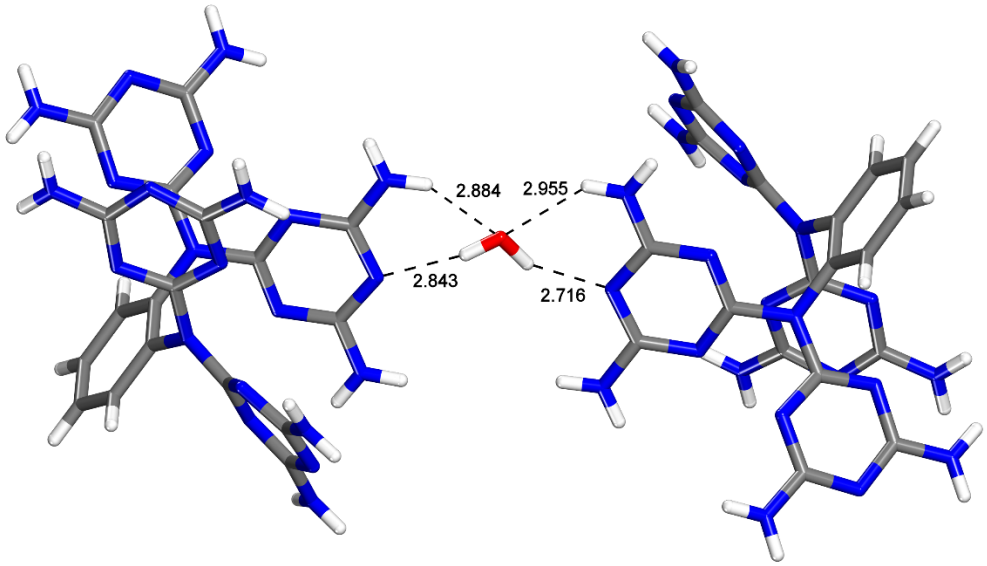

Figure 2. Representations of the structure obtained by crystallizing 1,2-Ph[N(DAT)$_2$]$_2$ (**6**) from DMSO/H_2O. (a) View showing part of a chain of molecules held together by distorted N–H···N hydrogen bonds of Type III. (b) View illustrating how each molecule also participates in distorted N–H···N hydrogen bonds of Type I, which link the chains into sheets parallel to the *bc*-plane. (c) View along the *b*-axis showing the cross sections of sheets parallel to the *bc*-plane (in contrasting colors). (d) View demonstrating how the structure is reinforced by additional N–H···O and O–H···N hydrogen bonds involving bridging molecules of H_2O. A single bridging molecule is shown in one of two statistically equivalent disordered positions. Hydrogen bonds are represented by broken lines (with N···O distances in Figure 2d given in Å). Unless noted otherwise, guest molecules are omitted for clarity, and atoms are shown in standard colors.

As shown in Table 2, the numbers of N–H···N hydrogen bonds and hydrogen-bonded neighbors per molecule are both lower in the structure of 1,2-Ph[N(DAT)$_2$]$_2$ (**6**) than in the

benchmark HOF derived from compound **1**, even though both compounds incorporate four DAT groups. In contrast, the density of hydrogen bonds is higher in melam **6**. In the observed structure, paired DAT groups appear to be prevented from achieving an optimal coplanar orientation by geometrical constraints resulting from the attachment of two DAT groups to a single atom of nitrogen in $N(DAT)_2$, as well as from the congested ortho-substitution of compound **6**. For these reasons, the four DAT groups in compound **6** cannot fully exploit their potential for forming N–H···N hydrogen bonds, and various sites are free to engage in additional N–H···O and O–H···N hydrogen bonds with included molecules of DMSO and H_2O. Of special note in the structure of melam **6** are bridging molecules of H_2O (Figure 2d).

As in the case of $PhN(DAT)_2$ (**5**), the central atom of nitrogen in each $N(DAT)_2$ group in compound $Ph[N(DAT)_2]_2$ (**6**) is sp^2-hybridized, the three aryl and heteroaryl substituents adopt a propeller-shaped conformation, and the preferred tautomer is analogous to structure **5A**. The dihedral angle between the planes defined by the NC_3 core and the phenyl group is increased from 46° in melam **5** to an average value of 61° in analogue **6** by the effect of ortho-substitution, and the average angle between the plane of the NC_3 core and the two triazinyl groups in compound **6** is significantly smaller (24°).

1,3-Ph[N(DAT)$_2$]$_2$ (7)

Allowing anhydrous EtOH to diffuse into a solution of melam **7** in DMSO produced crystals that were suitable for analysis by X-ray diffraction. The crystals proved to belong to the tetragonal space group $P4_32_12$ and to include disordered molecules of DMSO, with an

approximate composition **7** • ~12–16 DMSO as estimated by X-ray crystallography and NMR spectroscopy. Additional crystallographic data are summarized in Table 1, and views of the structure are presented in Figure 3. The central atom of nitrogen in the two $N(DAT)_2$ groups in compound **7** is sp^2-hybridized, its aryl and heteroaryl substituents adopt a propeller-shaped conformation, and the dihedral angles between each planar NC_3 core and the substituents are similar to those observed in simple melam $PhN(DAT)_2$ (**5**). Like analogues **5**–**6**, compound **7** gives rise to a network joined by multiple N–H···N hydrogen bonds characteristic of DAT groups.

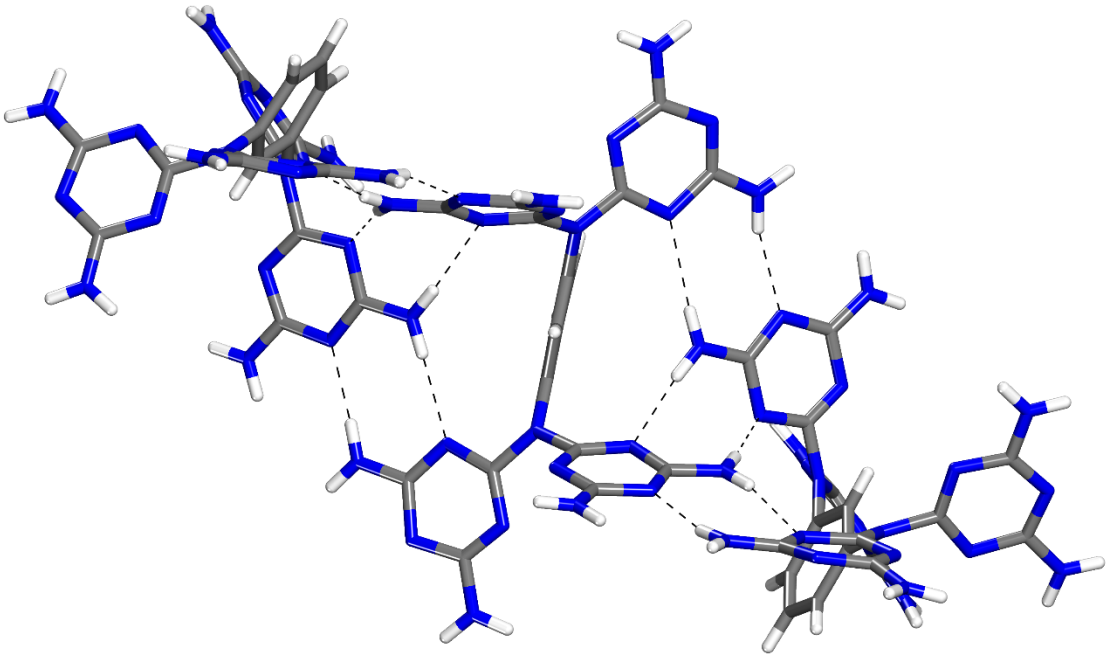

a

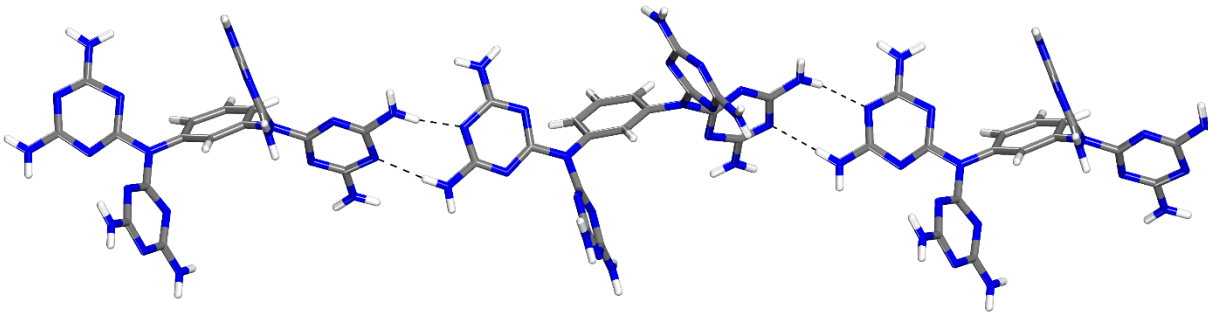

b

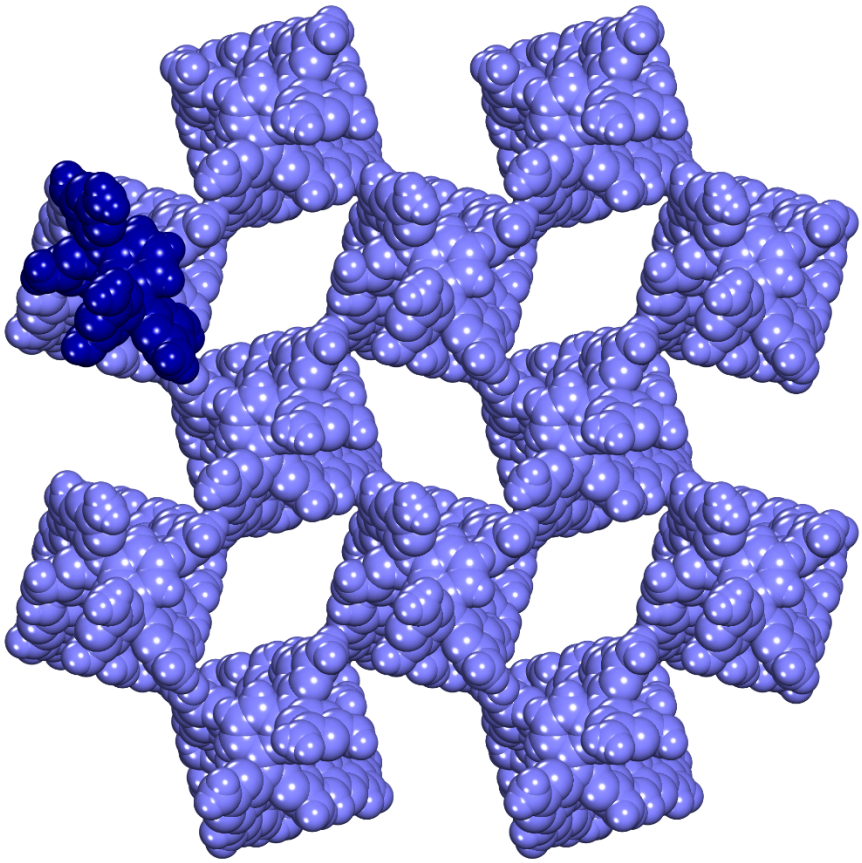

c

Figure 3. Representations of the structure produced by crystallizing 1,3-Ph[N(DAT)$_2$]$_2$ **(7)** from DMSO/EtOH. (a) View showing part of a chain of molecules with interdigitated DAT groups joined along the *c*-axis by distorted N–H···N hydrogen bonds of Types II and III. (b) Image showing how each molecule also participates in distorted N–H···N hydrogen bonds of Type I, which link the chains into a three-dimensional *cds* network. (c) Space-filling view along the *c*-axis showing the cross sections of channels, with a single molecule of compound **7** highlighted in a contrasting color. Hydrogen bonds are represented by broken lines, and guests are disordered and not shown. Unless noted otherwise, atoms are drawn in standard colors.

Figure 3a shows that interdigitation of non-coplanar DAT groups links 1,3-Ph[N(DAT)$_2$]$_2$ (**7**) into chains aligned with the *c*-axis and held together by twelve distorted hydrogen bonds of Types II and III per molecule (average N···N distance = 3.080 Å). Each molecule also forms four distorted N–H···N hydrogen bonds of Type I (average N···N distance = 2.935 Å) with two other neighbors (Figure 3b), thereby joining the chains into a three-dimensional *cds* network connected by a total of sixteen N–H···N hydrogen bonds per molecule of melam **7**. The resulting network is remarkably open, and conspicuous channels (8.4 × 16 Å^2) are aligned with the *c*-axis (Figure 3c). Approximately 74% of the volume of the structure is accessible to guests.[27–29] It is noteworthy that melam **7**, which is a small molecule with only 40 atoms other than hydrogen, can give rise to a network with such a high degree of openness. In contrast, the prototypic HOF derived from compound **1** is built from larger molecules (57 non-hydrogen atoms), yet only 42% of the volume of the structure can accommodate guests.

The behavior of 1,3-Ph[N(DAT)$_2$]$_2$ (**7**) reveals the special ability of multiple N(DAT)$_2$ groups to direct modular construction. Simpler analogue PhN(DAT)$_2$ (**5**) has only one N(DAT)$_2$

group, so chains are favored, with each molecule participating in only four N–H···N hydrogen bonds involving two neighbors (Table 2). In 1,2-Ph[N(DAT)$_2$]$_2$ (**6**), the presence of two N(DAT)$_2$ groups allows the construction of sheets instead of chains, with an increased number of N–H···N hydrogen bonds per molecule (twelve) and neighbors (three); however, steric obstacles created by ortho-substitution prevent the DAT groups from participating fully in hydrogen bonding. 1,3-Disubstitution in isomer **7** eliminates these obstacles and leads to the formation of a highly open three-dimensional network with more hydrogen bonds per molecule (sixteen) and interacting neighbors (four), as summarized in Table 2.

The high potential porosity of the structure derived from 1,3-Ph[N(DAT)$_2$]$_2$ (**7**) led us to attempt crystallizations under other conditions. In one such experiment, the compound was found to crystallize from DMSO containing a dissolved salt (Et_3NH^+ F^-), and a related hydrogen-bonded network was formed. The crystals proved to have the composition **7** • 4 DMSO and to belong to the orthorhombic space group *Pbca*. Et_3NH^+ F^- is not included in the observed structure but appears to play a role in the crystallization. Table 1 includes additional crystallographic information, and Figure 4 provides views of the structure. Interdigitated DAT groups join compound **7** into chains aligned with the *a*-axis and held together by ten N–H···N hydrogen bonds per molecule (four of Type II, four of Type III, and two single N–H···N interactions), with an average N···N distance of 3.113 Å (Figure 4a). Each molecule interacts simultaneously with five other neighbors to form seven additional N–H···N hydrogen bonds (five single bonds and two of Type I) with an average N···N distance of 3.084 Å. The result is a three-dimensional *vco* network joined by a total of twenty-two N–H···N hydrogen bonds per molecule of melam **7**. Six of the set of seven hydrogen-bonded neighbors lie approximately in

the *ab*-plane and define sheets, which are linked by hydrogen bonds of Type I involving the seventh neighbor (Figure 4b). Approximately 50% of the volume of the structure is accessible to guests.[30–32] Additional cohesion is provided by N–H···O hydrogen bonds involving bridging molecules of DMSO (Figure 4c), as shown in Figure 1a in the case of simple analogue $PhN(DAT)_2$ (**5**).

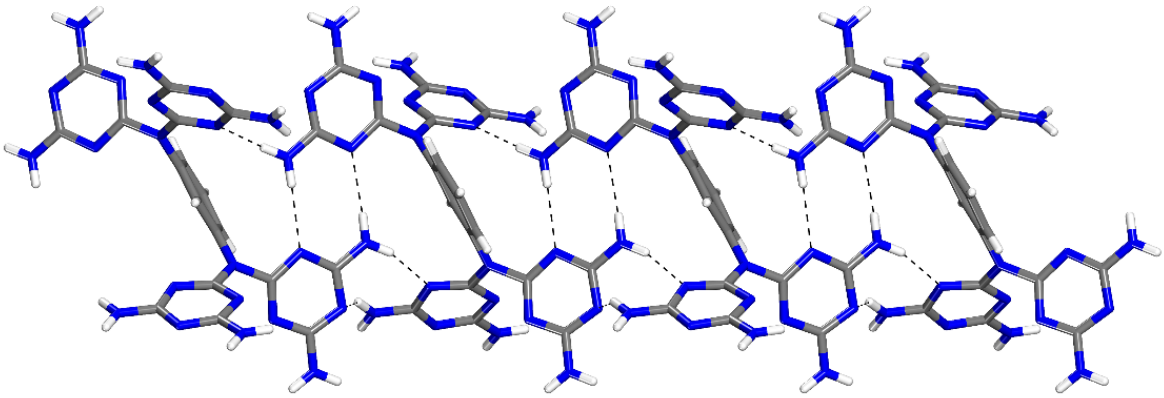

a

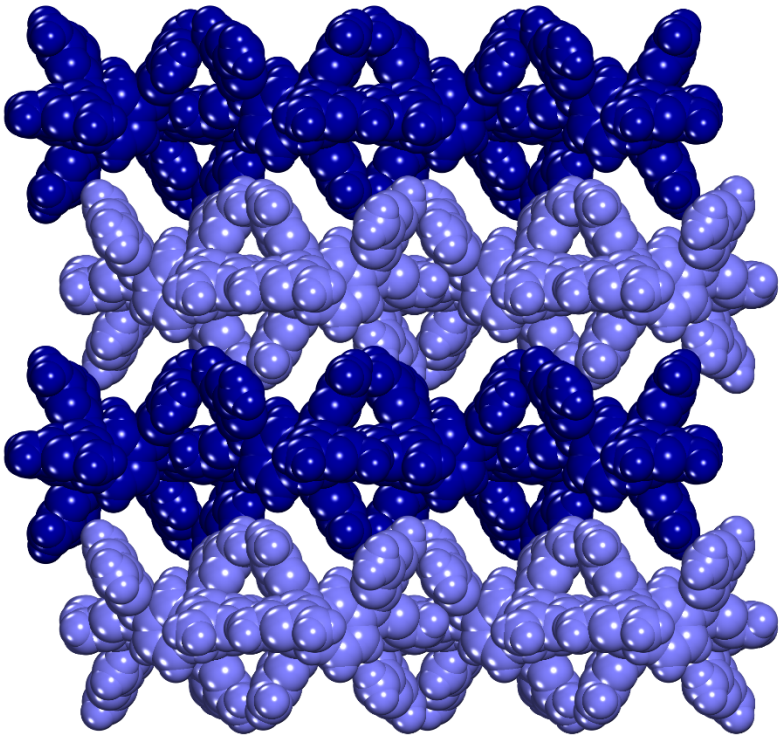

b

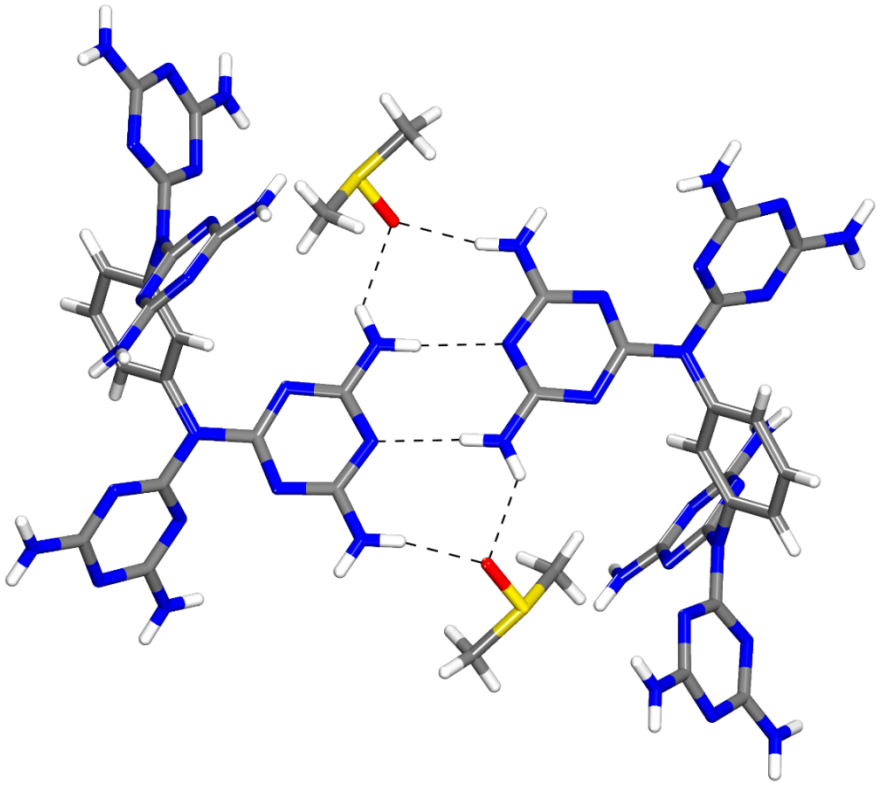

c

Figure 4. Representations of the structure obtained by crystallizing 1,3-Ph[N(DAT)$_2$]$_2$ (**7**) from DMSO in the presence of Et_3NH^+ F^-. (a) View showing part of a chain of molecules with interdigitated DAT groups joined along the *a*-axis by N–H···N hydrogen bonds of various types. (b) Space-filling view along the *a*-axis showing the cross sections of sheets parallel to the *ab*-plane (in contrasting colors). (c) Image showing reinforcing N–H···O hydrogen bonds involving bridging molecules of DMSO. Hydrogen bonds are represented by broken lines. Unless noted otherwise, guests are omitted for clarity, and atoms are drawn in standard colors.

The ability of 1,3-Ph[N(DAT)$_2$]$_2$ (**7**) to form at least two different hydrogen-bonded networks is not surprising and can be attributed to multiple factors, including (1) the

conformational flexibility of compound **7**; (2) the ability of simple DAT groups to engage in several characteristic patterns of coplanar hydrogen bonding (I–III), as well as non-planar variants; and (3) access to additional interdigitated hydrogen-bonding motifs arising from the special features of $N(DAT)_2$ groups in proximity. These factors may make the structures of compounds with multiple $N(DAT)_2$ groups hard to foresee, but they also ensure that a single module can give rise to potentially porous crystalline materials with diverse architectures, depending on the conditions of crystallization. Crystallizations of melam **7** in pure DMSO and in DMSO containing Et_3NH^+ F^- may differ because of the special ability of fluoride to form hydrogen bonds.

It is instructive to compare key features of the *vco* network formed by crystallizing 1,3-$Ph[N(DAT)_2]_2$ (**7)** in DMSO/ Et_3NH^+ F^- with those of the prototypic HOF derived from compound **1**. Compounds **1** and **7** both incorporate four DAT groups, and the numbers of N–H···N hydrogen bonds per molecule and close neighbors are similar (Table 2). Nevertheless, the density of hydrogen bonds in the *vco* network generated by melam **7** (10.94×10^{-3} $Å^{-3}$) is substantially higher than the corresponding value for the HOF built from compound **1** (5.32×10^{-3} $Å^{-3}$). This difference identifies compounds with multiple $N(DAT)_2$ groups as promising modules for constructing porous crystalline materials that are more robust than those held together by simple DAT groups.

1,4-Ph[N(DAT)$_2$]$_2$ (8)

Crystals were grown by allowing anhydrous EtOH or diethyl ether to diffuse into solutions of melam **8** in DMSO. Analysis by X-ray diffraction revealed that the crystals have

the approximate composition **8** • 3 DMSO and belong to the orthorhombic space group *Pbcn*. Table 1 presents additional crystallographic data, and Figure 5 provides views of the structure. The conformational and tautomeric preferences of the $N(DAT)_2$ groups in melam **8** are similar to those observed in analogues **5** and **7**, and compound **8** gives rise to a network joined by multiple N–H···N hydrogen bonds characteristic of DAT groups. In particular, each molecule interacts with two neighbors along the *b*-axis to form a distinctive motif with interdigitated DAT groups (Figure 5a), which creates a total of ten hydrogen bonds (average N···N distance = 3.200 Å), including four of Type II, four of Type III, and two additional simple N–H···N hydrogen bonds. As in the case of isomeric 1,3-disubstituted analogue **7**, achieving compact interdigitation in the structure of 1,4-disubstituted melam **8** appears to require the formation of Type II and III N–H···N hydrogen bonds in which the participating DAT groups deviate significantly from optimal coplanarity. Each molecule of melam **8** is also linked to five other neighbors by a total of ten additional hydrogen bonds (two of Type I and eight simple N–H···N hydrogen bonds). Six of the total of seven neighbors lie approximately in the *bc*-plane, defining sheets (Figure 5b), and the seventh neighbor (connected by paired N–H···N hydrogen bonds of Type I) is incorporated in an adjacent sheet. This yields a three-dimensional *vcg* network, in which each molecule is joined to its neighbors by a total of twenty-two N–H···N hydrogen bonds. The structure is remarkably similar to the one formed by isomeric 1,3-disubstituted melam **7** (Figure 4b), and the density of hydrogen bonds (10.79×10^{-3} $Å^{-3}$) is even higher (Table 2). Included molecules of DMSO form additional hydrogen bonds with melam **8**, and approximately 51% of the volume is accessible to guests.[30-32]

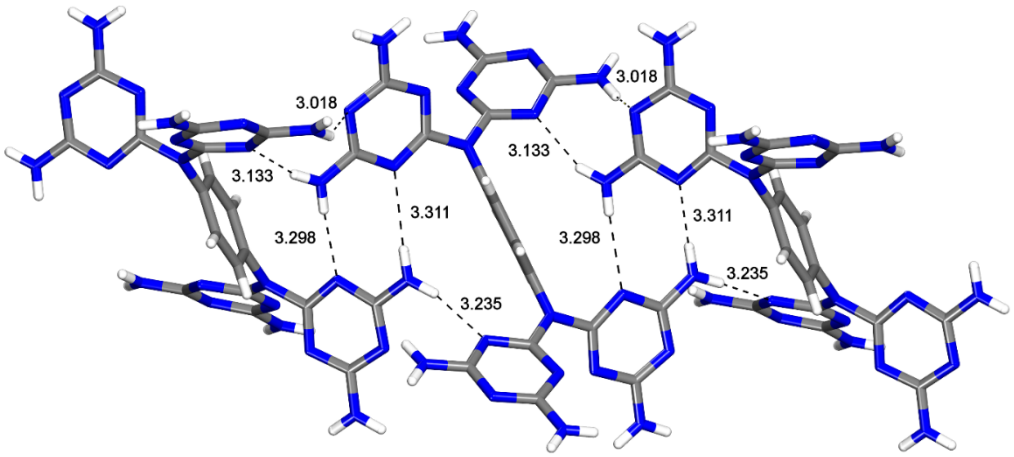

a

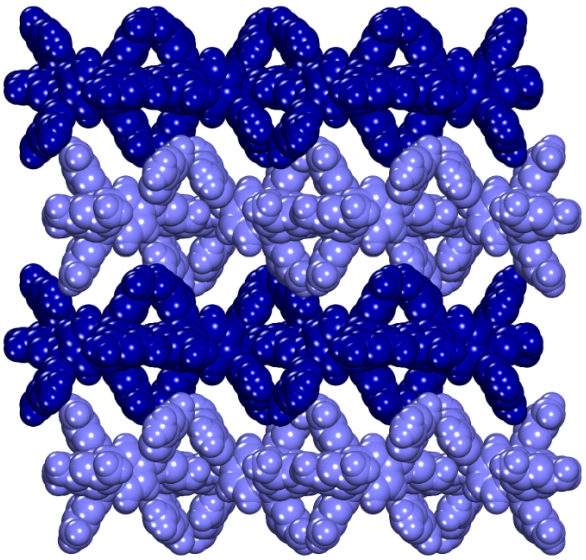

b

Figure 5. Representations of the structure produced by crystallizing 1,4-Ph[N(DAT)$_2$]$_2$ (**8**) grown from DMSO/EtOH. (a) Part of a chain of interdigitated molecules joined along the *b*-axis by distorted N–H···N hydrogen bonds of Types II and III, as well as by simple hydrogen bonds.

(b) Space-filling view along the *b*-axis showing the cross sections of sheets parallel to the *bc*-plane (in contrasting colors). Hydrogen bonds are represented by broken lines, with N···N distances given in Å. Guests are omitted for clarity, and atoms are shown in standard colors, unless noted otherwise

Crystals also resulted when benzene was allowed to diffuse into solutions of 1,4-Ph[N(DAT)$_2$]$_2$ (**8)** in DMSO. The crystals were found to have the composition **8** • 5 DMSO • 2 C_6H_6 and to belong to the monoclinic space group $P2_1/c$. Additional crystallographic data are summarized in Table 1, and views of the structure appear in Figure 6. Molecules with interdigitated DAT groups are linked into chains along the *c*-axis by distorted N–H···N hydrogen bonds of Types II and III, with an average N···N distance of 3.175 Å (Figure 6a). Two additional neighbors are joined to each molecule of melam **8** by a total of three hydrogen bonds (two of Type I and one simple N–H···N hydrogen bond), yielding an open three-dimensional *noy* network in which each molecule is joined to five neighbors by a total of sixteen hydrogen bonds. Significant channels (6.3 × 13 Å^2) are aligned with the *a*-axis (Figure 6b), and approximately 65% of the volume is accessible to guests.[27–29] Included molecules of solvent are largely ordered, and DMSO forms additional hydrogen bonds with melam **8**.

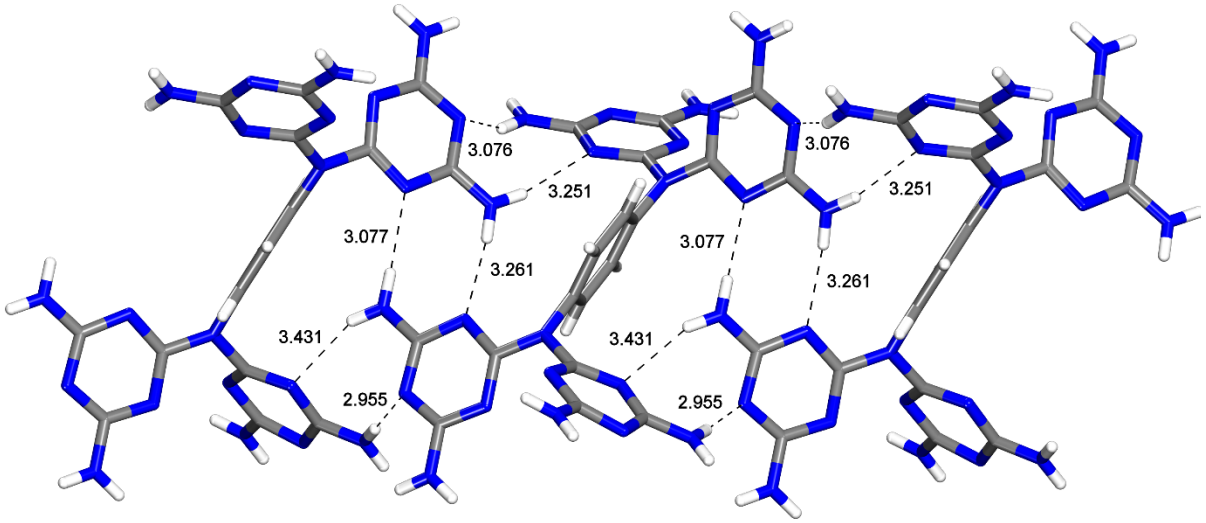

a

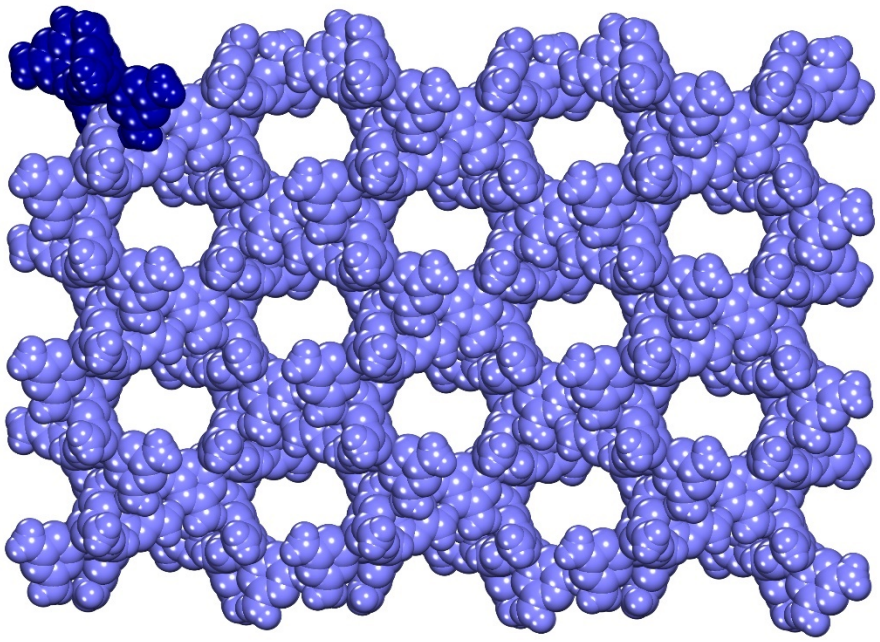

b

Figure 6. Representations of the structure obtained by crystallizing 1,4-Ph[N(DAT)$_2$]$_2$ **(8)** from DMSO/C_6H_6. (a) Part of a chain of interdigitated molecules joined along the *c*-axis by distorted

N–H···N hydrogen bonds of Types II and III. (b) Space-filling view along the *a*-axis showing the cross sections of channels. A single molecule of compound **8** is shown in a contrasting color. Hydrogen bonds are represented by broken lines, with N···N distances given in Å. Guests are omitted for clarity and atoms are drawn in normal colors, unless noted otherwise.

1,3,5-Ph[N(DAT)$_2$]$_3$ (9)

Melams **6**–**8** incorporate two N(DAT)$_2$ groups and consistently produce networks in which N–H···N hydrogen bonding is a major cohesive force, as measured both by the density of hydrogen bonds per unit volume and by the number per molecule. Of particular note is the behavior of melams **7**–**8**, in which suitably oriented N(DAT)$_2$ groups form special interdigitated associative motifs. These patterns of association led us to study the behavior of 1,3,5-Ph[N(DAT)$_2$]$_3$ (**9**), in which three N(DAT)$_2$ groups are positioned in similar ways.

Crystals of melam **9** grown from DMSO/MeOH proved to have the approximate composition **9** • 11 DMSO and to belong to the monoclinic space group *C*2/*c*. Table 3 provides additional crystallographic data, and Figure 7 shows views of the structure. The three N(DAT)$_2$ groups of compound **9** favor conformations like those observed in simpler analogues **5**, **7**, and **8**. Each molecule of melam **9** is linked to two neighbors by interactions involving interdigitated N(DAT)$_2$ groups (Figure 7a–b), leading to the formation of chains held together by a total of fourteen N–H···N hydrogen bonds per molecule (eight of Type II and six of Type III, with an average N···N distance of 3.128 Å). As shown in Figure 7c, three other neighbors are joined to each molecule of melam **9** by a total of six hydrogen bonds of Type I (average N···N distance

= 2.994 Å). These interactions give rise to a highly open three-dimensional *noy* network in which the number of hydrogen-bonded neighbors (five), the number of N–H···N hydrogen bonds per molecule (twenty), and the density of hydrogen bonds (5.19×10^{-3} Å^{-3}) all have high values (Table 2). Approximately 68% of the volume of the structure is accessible to guests,[30–32] included molecules of DMSO are disordered, and very large channels (12×13 Å^2) are aligned with the *c*-axis (Figure 7d).

Table 3. Crystallographic Data for Substituted Melams **9–10**

Compound	**9**	**10**
crystallization medium	DMSO/MeOH	DMSO/EtOH
formula	$C_{24}H_{27}N_{33}$ + solvent	$C_{27}H_{33}N_{33}$ + solvent
crystal system	monoclinic	trigonal
space group	*C*2/*c*	$P\bar{3}c1$
a (Å)	29.648(3)	22.8270(11)
b (Å)	34.503(3)	22.8270(11)
c (Å)	17.4110(5)	21.2262(7)
α (°)	90	90
β (°)	107.839(4)	90
γ (°)	90	90

V (Å^3)	16954(3)	14234.3(12)
Z	8	6
Z'	1	0.5
T (K)	150	100
ρ_{calc} (g cm^{-3})	0.609*	0.574*
λ (Å)	1.54178	1.54178
μ (mm^{-1})	0.372*	0.344*
measured reflections	175817	64830
independent reflections	13025	8793
R_{int}	0.0495	0.0366
observed reflections	13025	4978
R_1, I > 2σ(I)	0.0969	0.0927
R_1, all data	0.1043	0.1187
wR_2, I > 2σ(I)	0.3721	0.2953
wR_2, all data	0.3901	0.3123
GoF	1.083	1.016

*Calculated without contributions from disordered solvent molecules as determined using the mask/squeeze routine

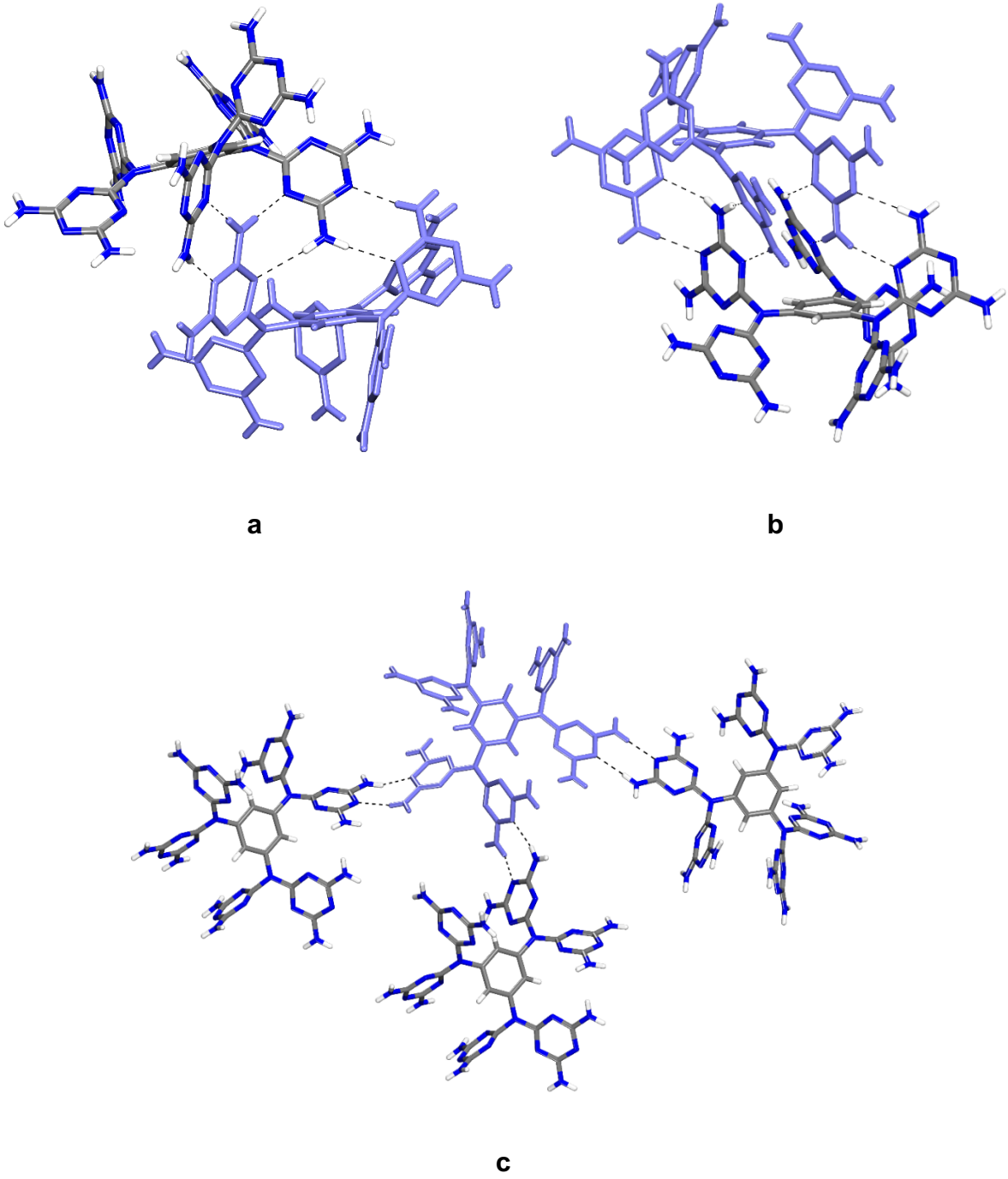

a **b**

c

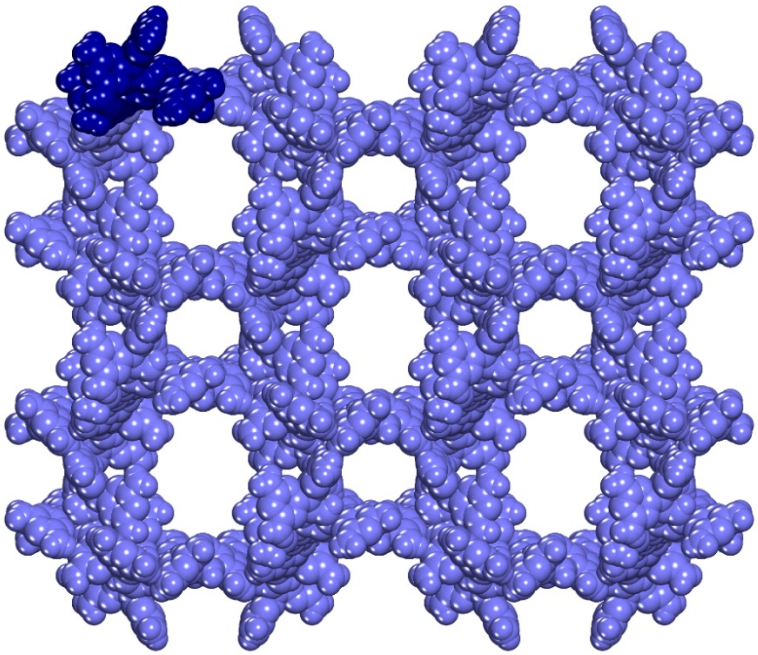

d

Figure 7. Representations of the structure produced by crystallizing 1,3,5-Ph[N(DAT)$_2$]$_3$ (**9**) from DMSO/MeOH. (a) View showing a central molecule of compound **9** (light blue) and one of two neighbors that engage in hydrogen bonds involving interdigitated N(DAT)$_2$ groups. (b) Image showing the same central molecule (light blue) and a second neighbor with interdigitated N(DAT)$_2$ groups. (c) View showing how the central molecule (light blue) and three additional neighbors are linked by N–H···N hydrogen bonds of Type I. (d) Space-filling view along the *c*-axis showing the cross sections of channels, with a single molecule of compound **9** highlighted in a contrasting color. Hydrogen bonds are represented by broken lines, disordered guests are not shown, and atoms are drawn in standard colors, unless noted otherwise.

1,3,5-Me_3-1,3,5-Ph[$N(DAT)_2$]$_3$ (10)

The consistent behavior of substituted melams **7**–**9** suggests that well-oriented $N(DAT)_2$ groups can direct modular construction with certain elements of predictability. In particular, the groups yield networks held together by unusually large numbers of N–H···N hydrogen bonds per molecule, and normal patterns of association characteristic of DAT groups are observed, as well as more complex versions arising from interdigitation. However, other organizational details, such as the precise number of hydrogen-bonded neighbors or hydrogen bonds per molecule, cannot yet be foreseen with confidence. Nevertheless, it is clear that compounds with multiple $N(DAT)_2$ groups are well-suited for the modular construction of hydrogen-bonded materials.

The behavior of 1,3,5-Me_3-1,3,5-Ph[$N(DAT)_2$]$_3$ (**9)** encouraged us to study its methyl-substituted analogue **10**. Crystals suitable for analysis by X-ray diffraction were grown by allowing anhydrous EtOH to diffuse into solutions of melam **10** in DMSO. The crystals were found to have the approximate composition **10** • 7 DMSO and to belong to the trigonal space group $P\bar{3}c1$. Other crystallographic data are summarized in Table 3, and views of the structure are presented in Figure 8. The three $N(DAT)_2$ groups of compound **10** favor conformations similar to those observed in simpler analogues; however, the average angle (75.6°) between the plane of the aryl core and the NC_2 plane defined by the central atom of nitrogen and the two bonded atoms of carbon in each $N(DAT)_2$ group is significantly increased by the effect of the flanking methyl groups. The nearly orthogonal orientation of the $N(DAT)_2$ groups disfavors interdigitation of the type observed in the structures of melams **7**–**9**. Instead, each molecule of compound **10** is joined to six neighbors by a total of twelve N–H···N hydrogen bonds of Type

I (average N···N distance = 2.976 Å), forming chains aligned with the *c*-axis (Figure 8a). This yields a highly open three-dimensional *cds* network in which approximately 69% of the volume is accessible to guests,[27–29] and large channels (10 × 11 $Å^2$) are aligned with the *c*-axis (Figure 8b).

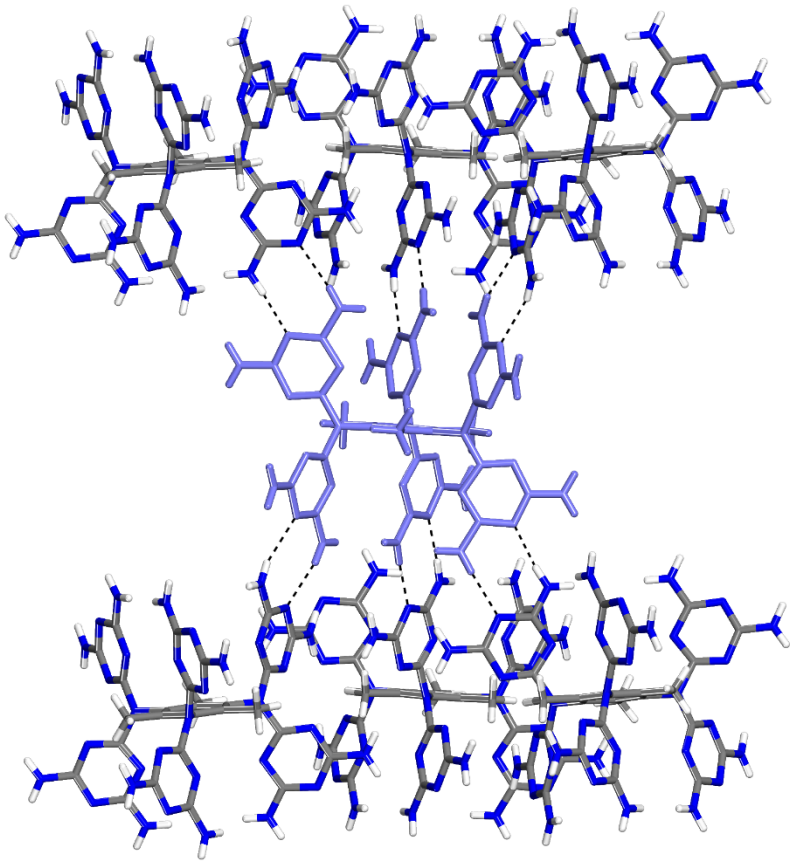

a

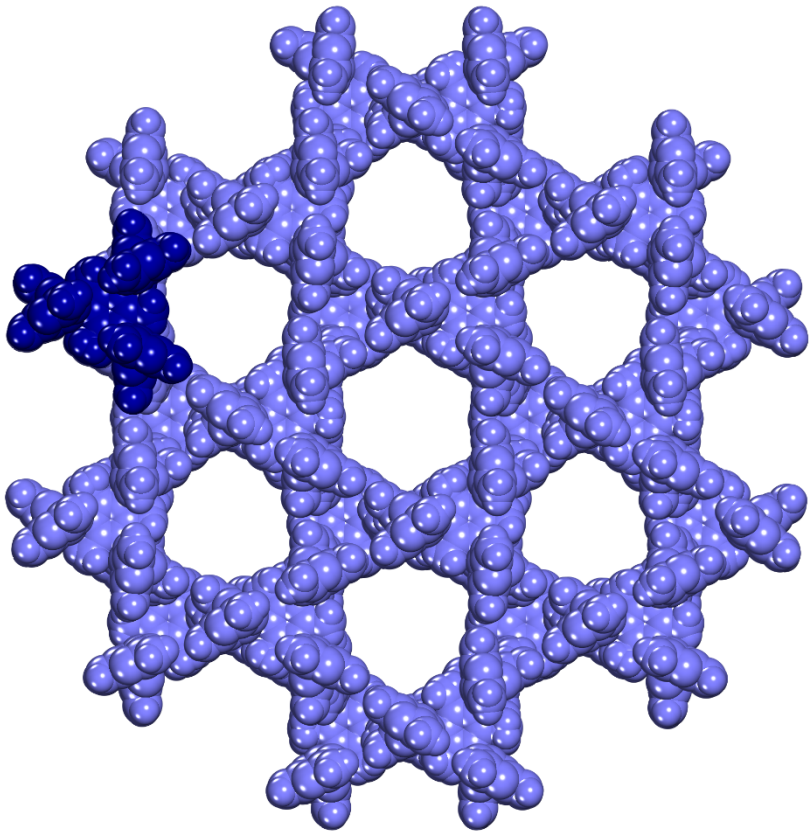

b

Figure 8. Representations of the structure obtained by crystallizing melam **10** from DMSO/EtOH. (a) View showing how a central molecule (light blue) is joined to six neighbors by a total of twelve N–H···N hydrogen bonds of Type I to form chains aligned with the *c*-axis. (b) Space-filling view along the *c*-axis showing the cross sections of channels. A single molecule of compound **10** is shown in a contrasting color. Hydrogen bonds are represented by broken lines, disordered guests are not shown, and atoms are drawn in normal colors, unless noted otherwise.

Demonstrating Porosity in Materials Constructed from Complex Melams

The integrity of the prototypic HOF derived from compound **1** is maintained primarily by N–H···N hydrogen bonds involving four simple DAT groups. As summarized in Table 2, each molecule of compound **1** forms sixteen hydrogen bonds with eight neighbors. In the $P4_32_12$ structure of 1,3-Ph[N(DAT)$_2$]$_2$ (**7**), with a total of four DAT groups incorporated in two N(DAT)$_2$ units, each molecule takes part in the formation of sixteen N–H···N hydrogen bonds involving four neighbors. In crystals of melam **10**, with three N(DAT)$_2$ groups, each molecule forms twelve N–H···N hydrogen bonds involving six neighbors. Table 2 shows that the densities of N–H···N hydrogen bonds in the structures derived from compounds **1**, **7**, and **10** are similar (5.32, 4.41, and 3.37 × 10^{-3} Å^{-3}, respectively). For this reason, we thought that desolvating crystals of melams **7** or **10** might yield HOFs, even though the percentage of guest-accessible volume in the observed structures (74% and 68%, respectively) is substantially higher than that in the structure of compound **1** (42%), making the formation of an open guest-free framework from compounds **7** and **10** correspondingly more challenging.

Unfortunately, all attempts to produce ordered solids with permanent porosity by removing solvent from the $P4_32_12$ crystals of 1,3-Ph[N(DAT)$_2$]$_2$ (**7**), were unsuccessful. Desolvation could be achieved by placing crystals containing DMSO under vacuum at 25 °C, but the resulting material proved to be amorphous and nonporous. Crystals were also immersed in DMSO/EtOH (1:1), then exposed to pure EtOH, and finally placed under vacuum at 25 °C, but the residual solid was again amorphous and nonporous. In addition, we were unable to convert crystals of melam **7** into a porous activated form by exposure to supercritical CO_2 ($scCO_2$).

We turned to melam **10** and desolvated crystals grown from DMSO/EtOH by placing them in EtOH to effect exchange, followed by removing included solvent under vacuum at 25 °C. Analysis by powder X-ray diffraction confirmed that the resulting material was crystalline (Figure 9), but the structure of the solvated form was not retained, and exposure to solvent did not regenerate the original form. Efforts to obtain desolvated material in the form of single crystals suitable for structural analysis by X-ray diffraction have not yet been successful. Material with a similar powder diffraction pattern was obtained by exposing crystals of melam **10** to $scCO_2$,[35] and the resulting solid proved to be porous. Reversible adsorption/desorption of N_2 at 77 K is shown in Figure 10, and the Brunauer–Emmett–Teller (BET) surface area was determined to be 515 $m^2\ g^{-1}$. The observed surface area exceeds that found for the prototypic HOF prepared from compound **1** (359 $m^2\ g^{-1}$ as measured by sorption of CO_2 at 196 K)[14] and is the highest reported for a HOF held together primarily by N–H···N hydrogen bonds.

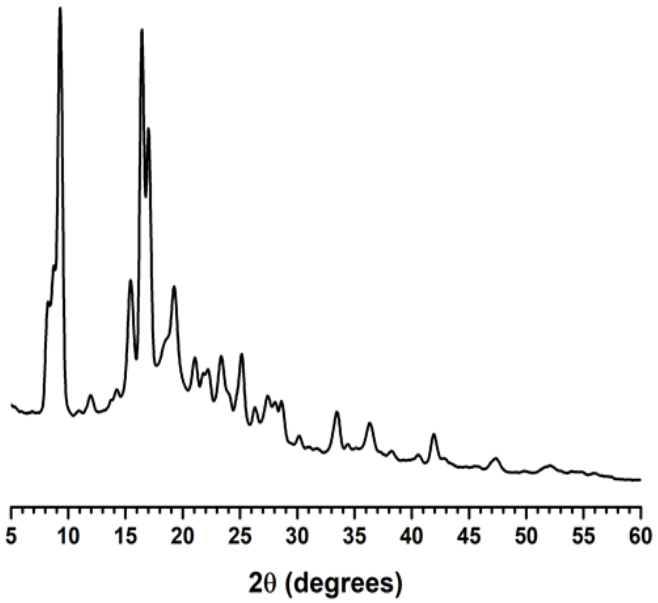

Figure 9. Powder X-ray diffraction pattern of the porous solid obtained by subjecting crystals of melam **10** grown from DMSO/EtOH to exchange and desolvation under vacuum at 25 °C.

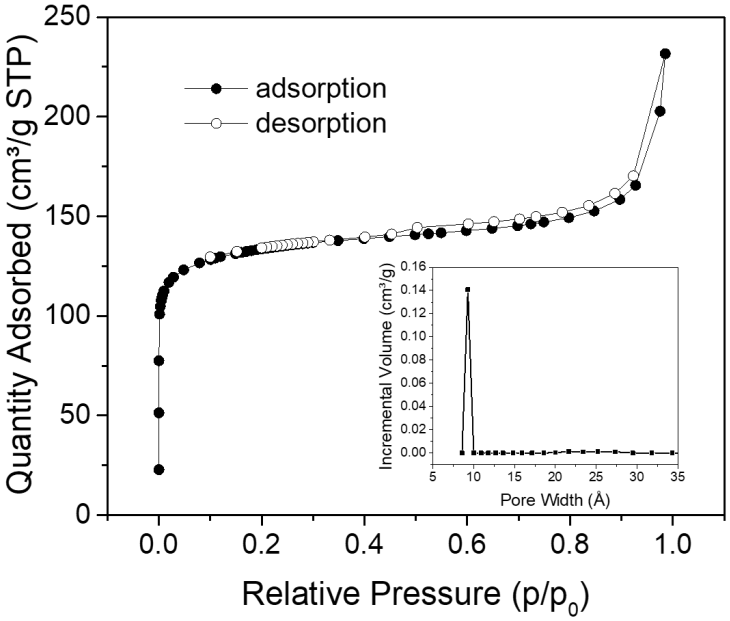

Figure 10. N_2 sorption isotherm at 77 K for crystals of melam **10** desolvated by exposure to $scCO_2$. Inset: Distribution of pore sizes as estimated by DFT.

The observed Type I N_2 sorption isotherm indicates that the new HOF is microporous, and further analysis of the data by DFT suggests the presence of pores 9.3 Å in diameter (Figure 10, inset). The desolvated HOF and the solvated framework initially produced by crystallizing melam **10** from DMSO/EtOH have structures that are not identical, but they appear to be related because both have pores of similar diameter (9.3 Å as measured by porosimetry and 10–11 Å as found by X-ray crystallography). However, the experimentally determined BET surface area (515 $m^2\ g^{-1}$) is much smaller than the value (3000 $m^2\ g^{-1}$) estimated by MOF Explorer for hypothetical solvent-free crystals of melam **10** grown from DMSO/EtOH.[36,37] In the case of the prototypic HOF derived from compound **1**, the measured surface area (359 $m^2\ g^{-1}$) is also much lower than the estimated value (1650 $m^2\ g^{-1}$). These changes reveal that both frameworks

respond to desolvation by undergoing deformations that reduce accessible surface substantially. Figure 8 shows that channels in the structure of crystals of melam **10** are aligned with the *c*-axis. Because similar channels appear to be retained in the corresponding HOF, we conclude that forces induced by desolvation are exerted primarily along the *c*-axis, which is the principal direction of N–H···N hydrogen bonding and presumably the least resistant to compression.

The porous crystalline solid constructed from melam **10** is especially noteworthy because most previously reported HOFs, including the prototypic HOF formed from compound **1**, show little or no adsorption of N_2 at 77 K.[38–42] The porosity of HOFs produced from compound **1** and melam **10** appears to be largely one-dimensional, with access limited to channels parallel to the *c*-axis in both structures. The special ability of the HOF derived from melam **10** to sorb N_2 may be due to the significantly larger diameter of its channels.

Solvated crystals formed by compounds **1**, **7**, and **10** have similar densities of N–H···N hydrogen bonds, all formed by interacting DAT groups (Table 2), yet the consequences of desolvation differ markedly. In the cases of benchmark compound **1** and melam **10**, structural changes occur but porous crystalline solids are nevertheless obtained. In contrast, desolvation of crystals of 1,3-Ph[$N(DAT)_2]_2$ (**7**) produces amorphous nonporous materials under all conditions examined. These intriguing differences in behavior appear to result from various factors. In particular, the percentage of guest-accessible volume is much higher in crystals of melams **7** and **10**, making it inherently more difficult for the desolvated forms to remain crystalline and to maintain open structures. In addition, N–H···N hydrogen bonds that maintain the structure of crystals of compounds **1**, **7**, and **10** have similar overall densities but may vary in strength or in the degree of non-isotropic spatial distribution, which may make the

frameworks vulnerable to stresses applied in certain directions. Differences in the behavior of the three compounds may also reflect structure-reinforcing effects of hydrogen bonding with included molecules of solvent, and specific architectural features may also affect the ease of repositioning neighboring molecules. For example, compound **1** has a nearly rigid tetraphenylmethyl core, and DAT groups normally lie close to the plane of aryl substituents to allow the formation of intramolecular C–H···N interactions.[21] As a result, compound **1** has a well-defined shape, whereas melams **7** and **10** can adopt diverse conformations that differ according to the torsional angles formed by the planar NC_3 core of each $N(DAT)_2$ group with respect to the aryl and triazinyl substituents.

At present, the relative importance of these various factors is not clear. Further study is needed to reveal why melam **10** yields a HOF with record porosity for frameworks held together primarily by N–H···N hydrogen bonds, despite the potential disadvantages of a high percentage of accessible volume and significant molecular flexibility. We believe that the simplicity of making complex melams, combined with the apparent ease of crystallizing them, will give rise to a large new family of HOFs, allowing systematic comparisons of the type needed to reveal how to control porosity by design. These studies may help lead to HOFs that can rival or surpass other classes of porous materials in performance.

2.5 Conclusions

Our work provides straightforward ways to convert amines RNH_2 into the corresponding melams $RN(DAT)_2$ by base-induced triazinylations and subsequent reactions with NH_3. Complex melams have a special ability to form structures held together by large numbers of N–

H···N hydrogen bonds per molecule. When suitably designed, even simple compounds with only 1–3 $N(DAT)_2$ groups and no more than 70 non-hydrogen atoms can crystallize to form highly open networks in which each molecule engages in over 20 N–H···N hydrogen bonds and more than 70% of the volume is available for accommodating guests. In favorable cases, guests can be removed to create rigorously porous crystalline hydrogen-bonded frameworks. In principle, any compound with multiple NH_2 groups can be converted into a derivative with an equal number of $N(DAT)_2$ groups and a greatly enhanced ability to engage in intermolecular hydrogen bonds. As a result, our work is expected to lead to a broad new family of compounds suitable for the modular construction of HOFs with unusually high degrees of robustness, porosity, and other useful properties.

2.6 Experimental Section

All reagents and solvents were obtained from commercial sources and used without further purification unless otherwise indicated.

***N*^{2}-(4,6-Diamino-1,3,5-triazin-2-yl)-*N*^{2}-phenyl-1,3,5-triazine-2,4,6-triamine (5).** Aniline (0.19 g, 2.0 mmol), cyanuric chloride (3.6 g, 20 mmol), and sodium hydride (60% by weight in oil, 1.6 g, 40 mmol) were combined in anhydrous oxygen-free THF (10 mL), and the mixture was stirred at 25 °C overnight under an atmosphere of N_2. The resulting yellow suspension was filtered, the separated solid was washed with THF, and volatiles were then removed from the combined filtrate and washings by evaporation under reduced pressure. The residual yellow

solid was transferred to a sealable tube and treated with aqueous NH_3 (14 M, 12 mL, 170 mmol). The tube was closed, and the mixture was stirred at 60 °C for 72 h to give a suspension of colorless solid. The solid was separated by filtration and was washed with hot H_2O, MeOH, and anhydrous EtOH. The washed solid was then dried in vacuo to give a colorless sample of compound **5** (0.38 g, 1.2 mmol, 60%). Further purification could achieved by crystallization from hot DMSO: mp > 300 °C; FTIR (ATR) 3473, 3304, 3138, 1629, 1527, 1334, 1015, 802, 625 cm^{-1}; ^1H NMR (300 MHz, DMSO-d_6) δ 7.27 (t, ^3J = 7.3 Hz, 2H), 7.08 (t, ^3J = 7.3 Hz, 1H), 7.05 (d, ^3J = 7.3 Hz, 2H), 6.60 (bs, 8H); ^{13}C NMR (100 MHz, DMSO-d_6) δ 169.29, 168.77, 143.51, 129.31, 127.43, 125.46; HRMS (ESI-TOF) *m/z* $[M + H]^+$ calcd for $C_{12}H_{14}N_{11}$ 312.14282, found 312.14309.

N^2,$N^{2'}$-(1,2-Phenylene)bis(N^2-(4,6-diamino-1,3,5-triazin-2-yl)-1,3,5-triazine-2,4,6-triamine (6). 1,2-Benzenediamine (0.21 g, 1.9 mmol), cyanuric chloride (1.5 g, 8.1 mmol), and diisopropylethylamine (1.4 mL, 8.0 mmol) were combined in anhydrous oxygen-free THF (10 mL), and the mixture was stirred at 25 °C overnight under an atmosphere of N_2. The resulting yellow suspension was filtered, the separated solid was washed with THF, and volatiles were then removed from the combined filtrate and washings by evaporation under reduced pressure. The residual yellow solid was transferred to a sealable tube and was treated with aqueous NH_3 (14 M, 11 mL, 150 mmol). The tube was closed, and the mixture was stirred at 60 °C for 72 h to give a suspension of colorless solid. The solid was separated by filtration and was washed with hot H_2O, MeOH, and anhydrous EtOH. The washed solid was then dried in vacuo to give a colorless sample of compound **6** (0.56 g, 1.0 mmol, 53%). Further purification could achieved by crystallization from hot DMSO: mp > 300 °C; FTIR (ATR) 3455, 3322, 3189, 1619, 807,

1528, 1331, 807 cm^{-1}; ^{1}H NMR (300 MHz, DMSO-d_6) δ 7.03 (m, 2H), 6.91 (m, 2H), 6.23 (s, 16H); ^{13}C NMR (100 MHz, DMSO-d_6) δ 168.54, 168.25, 140.27, 129.15, 125.67; HRMS (ESI-TOF) *m/z* $[M + H]^+$ calcd for $C_{18}H_{21}N_{22}$ 545.23141, found 545.23061.

N^2,$N^{2'}$-(1,3-Phenylene)bis(N^2-(4,6-diamino-1,3,5-triazin-2-yl)-1,3,5-triazine-2,4,6-triamine (7). 1,3-Benzenediamine (0.21 g, 1.9 mmol), cyanuric chloride (1.5 g, 8.1 mmol), and diisopropylethylamine (1.4 mL, 8.0 mmol) were combined in anhydrous oxygen-free THF (10 mL), and the mixture was stirred at 25 °C overnight under an atmosphere of N_2. The resulting yellow suspension was filtered, the separated solid was washed with THF, and volatiles were then removed from the combined filtrate and washings by evaporation under reduced pressure. The residual yellow solid was transferred to a sealable tube and was treated with aqueous NH_3 (14 M, 10 mL, 150 mmol). The tube was closed, and the mixture was stirred at 60 °C for 72 h to give a suspension of colorless solid. The solid was separated by filtration and was washed with hot H_2O, MeOH, and anhydrous EtOH. The washed solid was then dried in vacuo to give a colorless sample of compound **7** (0.83 g, 1.5 mmol, 79%). Further purification could achieved by crystallization induced by allowing anhydrous EtOH to diffuse slowly into a saturated solution in DMSO: mp > 300 °C; FTIR (ATR) 3316, 3187, 1623, 1525, 1341, 1015, 809, 756 cm^{-1}; ^{1}H NMR (400 MHz, DMSO-d_6) δ 7.19 (t, ^{3}J = 8.0 Hz, 1H), 6.88 (dd, ^{3}J = 8.0 Hz, ^{4}J =2.0 Hz, 2H), 6.73 (t, ^{4}J = 2.0 Hz, 1H), 6.60 (s, 16H); ^{13}C NMR (175 MHz, DMSO-d_6) δ 168.56, 168.26, 142.77, 128.85, 124.23, 123.96; HRMS (ESI-TOF) *m/z* $[M + H]^+$ calcd for $C_{18}H_{21}N_{22}$ 545.23141, found 545.23203.

N^2,$N^{2'}$-(1,4-Phenylene)bis(N^2-(4,6-diamino-1,3,5-triazin-2-yl)-1,3,5-triazine-2,4,6-triamine (8). 1,4-Benzenediamine (0.21 g, 1.9 mmol), cyanuric chloride (1.5 g, 8.1 mmol), and

diisopropylethylamine (1.4 mL, 8.0 mmol) were combined in anhydrous oxygen-free THF (10 mL), and the mixture was stirred at 25 °C overnight under an atmosphere of N_2. The resulting yellow suspension was filtered, the separated solid was washed with THF, and volatiles were then removed from the combined filtrate and washings by evaporation under reduced pressure. The residual yellow solid was transferred to a sealable tube and was treated with aqueous NH_3 (14 M, 11 mL, 150 mmol). The tube was closed, and the mixture was stirred at 60 °C for 24 h to give a suspension of colorless solid. The solid was separated by filtration and was washed with hot H_2O, MeOH, and anhydrous EtOH. The washed solid was then dried in vacuo. Crystallization of the solid was induced by allowing anhydrous EtOH to diffuse into a solution in DMSO, followed by slow evaporation of the mixture. This yielded compound **8** (0.36 g, 0.66 mmol, 35%) as a colorless solid: mp > 300 °C; FTIR (ATR) 3314, 3188, 1620, 1527, 1333, 1017, 813 cm^{-1}; ^1H NMR (400 MHz, DMSO-d_6) δ 7.04 (s, 4H), 6.57 (s, 16H); ^{13}C NMR (100 MHz, DMSO-d_6) δ 169.04, 168.78, 139.62, 127.35; HRMS (ESI-TOF) *m/z* $[M + H]^+$ calcd for $C_{18}H_{21}N_{22}$ 545.23141, found 545.23104.

1,3,5-Benzenetriamine Trihydrochloride. 1,3,5-Benzenetriamine was prepared by the Pd/C-catalyzed reduction of 3,5-dinitroaniline by hydrazine, using a published method.[43] After the reaction mixture was filtered through Celite, the Celite was washed with MeOH, and the combined filtrate and washings were treated with concentrated aqueous HCl (20–50 mL). The resulting colorless precipitate was separated by filtration and dried in vacuo to afford 1,3,5-benzenetriamine trihydrochloride: ^1H NMR (400 MHz, DMSO-d_6) δ 6.7 (br s, 9H), 6.6 (s, 3H).

***N*²,*N*²',*N*²''-(Benzene-1,3,5-triyl)tris[*N*²-(4,6-diamino-1,3,5-triazin-2-yl)-1,3,5-triazine-2,4,6-triamine] (9).** 1,3,5-Benzenetriamine trihydrochloride (0.46 g, 2.0 mmol), cyanuric chloride (3.4 g, 18 mmol), and sodium hydride (60% by weight in oil, 1.6 g, 40 mmol) were

combined in anhydrous oxygen-free THF (10 mL), and the mixture was stirred at 25 °C for 72 h under an atmosphere of N_2. The resulting yellow suspension was filtered, the separated solid was washed with THF, and volatiles were then removed from the combined filtrate and washings by evaporation under reduced pressure. The residual yellow solid was transferred to a sealable tube and was treated with aqueous NH_3 (14 M, 12 mL, 170 mmol). The tube was closed, and the mixture was stirred at 60 °C for 72 h to give a suspension of colorless solid. The solid was separated by filtration and was washed with hot H_2O, MeOH, and anhydrous EtOH. The washed solid was then dried in vacuo and was crystallized from hot DMSO. The resulting crystals were separated by filtration, washed with H_2O, and dried in vacuo to afford compound **9** (0.62 g, 0.80 mmol, 40%) as a colorless solid: mp > 300 °C; FTIR (ATR) 3315, 3187, 1619, 1525, 1342, 1011, 814, 462 cm^{-1}; ^1H NMR (400 MHz, DMSO-d_6) δ 6.66 (s, 3H), 6.56 (s, 24H); ^{13}C NMR (100 MHz, DMSO-d_6) δ 168.63, 168.56, 141.86, 121.53; HRMS (ESI-TOF) *m/z* [M + H]$^+$ calcd for $C_{24}H_{28}N_{33}$ 778.31999, found 778.32019.

***N*^{2},*N*$^{2'}$,*N*$^{2''}$-(2,4,6-Trimethylbenzene-1,3,5-triyl)tris[*N*^{2}-(4,6-diamino-1,3,5-triazin-2-yl)-1,3,5-triazine-2,4,6-triamine] (10).** 2,4,6-Trimethyl-1,3,5-benzenetriamine (0.33 g, 2.0 mmol),[44–46] cyanuric chloride (3.4 g, 18 mmol), and sodium hydride (60% in oil, 0.72 g, 18 mmol) were combined in anhydrous oxygen-free THF (10 mL), and the mixture was stirred at 25 °C for 48 h under an atmosphere of N_2. The resulting yellow suspension was filtered, the separated solid was washed with THF, and volatiles were then removed from the combined filtrate and washings by evaporation under reduced pressure. The residual yellow solid was transferred to a sealable tube and was treated with aqueous NH_3 (14 M, 11 ml, 150 mmol). The tube was closed, and the mixture was stirred at 60 °C for 48 h to give a suspension of colorless

solid. The solid was separated by filtration and was washed with hot H_2O, MeOH, and anhydrous EtOH. The washed solid was then dried in vacuo to give a colorless sample of compound **10** (0.65 g, 0.79 mmol, 40%). Further purification could be achieved by crystallization induced by allowing anhydrous EtOH to diffuse slowly into a saturated solution in DMSO: mp > 300 °C; FTIR (ATR) 3320, 3197, 1614, 1530, 1445, 813, 1345 cm^{-1}; ^1H NMR (400 MHz, DMSO-d_6) δ 6.40 (s, 24H), 1.97 (s, 9H); ^{13}C NMR (175 MHz, DMSO-d_6) δ 168.57, 168.15, 138.26, 136.84, 15.50; HRMS (ESI-TOF) *m/z* $[M + H]^+$ calcd for $C_{27}H_{34}N_{33}$ 820.36694, found 820.36583.

***N*-Benzyl-4,6-dichloro-1,3,5-triazin-2-amine.** *N*-Benzyl-4,6-dichloro-1,3,5-triazin-2-amine was prepared by a published procedure[47] and crystallized from hot hexane. The crystals were separated by filtration, washed with hexane, and dried in vacuo to afford *N*-benzyl-4,6-dichloro-1,3,5-triazin-2-amine (3.69 g, 14.5 mmol, 78%) as a colorless solid: ^1H NMR (400 MHz, $CDCl_3$) δ 7.41-7.31 (m, 5H), 6.30 (bs, 1H), 4.70 (d, ^3J = 6.1 Hz, 2H).

***N*^{2}-Benzyl-*N*^{2}-(4,6-diamino-1,3,5-triazin-2-yl)-1,3,5-triazine-2,4,6-triamine (11).** *N*-Benzyl-4,6-dichloro-1,3,5-triazin-2-amine (0.995 g, 3.90 mmol), cyanuric chloride (2.17 g, 11.8 mmol), and sodium hydride (60% by weight in oil, 0.470 g, 11.8 mmol) were combined in anhydrous oxygen-free THF (10 mL), and the mixture was stirred at 25 °C for 48 h under an atmosphere of N_2. The resulting yellow suspension was filtered, the separated solid was washed with THF, and volatiles were then removed from the combined filtrate and washings by evaporation under reduced pressure. The residual solid was transferred to a sealable tube and was treated with aqueous NH_3 (14 M, 12 mL, 170 mmol). The tube was closed, and the mixture was stirred at 80 °C for 72 h to give a suspension of colorless solid. The solid was separated by filtration and was

washed with hot H_2O, MeOH, and anhydrous EtOH. The washed solid was then dried in vacuo to give a colorless sample of compound **11** (0.30 g, 0.92 mmol, 24%). Further purification could be achieved by crystallization induced by allowing $CHCl_3$ to diffuse slowly into a saturated solution in DMSO: mp 266 °C; FTIR (ATR) 3323, 3137, 1629, 1530, 1450, 1378, 1283, 1015, 946, 814 cm^{-1}; ^1H NMR (400 MHz, DMSO-d_6) δ 7.34 (d, ^3J = 7.3 Hz, 2H), 7.25 (t, ^3J = 7.3 Hz, 2H), 7.17 (t, ^3J = 7.3 Hz, 1H), 6.45 (s, 8H), 5.13 (s, 2H); ^{13}C NMR (100 MHz, DMSO-d_6) δ 168.75, 168.47, 140.50, 128.75, 128.12, 127.18, 50.33; HRMS (ESI-TOF) *m/z* $[M + H]^+$ calcd for $C_{13}H_{16}N_{11}$ 326.15847, found 326.15836.

Homogeneity of Crystalline Samples of Melams 5–11

Typically, crystallizations of compounds **5**–**11** were efficient and yielded small, well-formed single crystals that appeared to be homogeneous when examined by polarized light microscopy. Diffusion of EtOH into a solution of melam **5** (0.0205 g) in DMSO (2 mL) induced the formation of 0.0149 g of crystals (73%, assuming that the initial and recrystallized solid samples are equally solvated). Crystallizations of melams **6**, **7**, **9**, and **10** on similar scales provided crystals in 98%, 61%, 83%, and 65% yields, respectively. Crystallization of melam **8** on a somewhat larger scale (0.90 g) from DMSO (15–18 mL) provided 0.36 g of crystals (40%). In general, removal of crystals of melams **5**–**11** from the mother liquors, followed by drying, led to rapid loss of crystallinity and the formation of amorphous solids, so it was not possible to confirm by powder X-ray diffraction that the bulk samples consisted largely of a single crystalline phase.

Supporting Information Available: Additional details, including descriptions of porosimetric experiments, discussions of crystallographic analyses, ORTEP drawings, and NMR spectra of compounds **5**–**11**. Deposition Numbers 1970867–970874 contain supplementary crystallographic data for this paper. These data are provided free of charge by the joint Cambridge Crystallographic Data Centre and Fachinformationszentrum Karlsruhe Access Structures service www.ccdc.cam.ac.uk/structures.

Acknowledgments. We are grateful to the Natural Sciences and Engineering Research Council of Canada, the Ministère de l'Éducation du Québec, the Canada Foundation for Innovation, the Canada Research Chairs Program, and Université de Montréal for financial support. In addition, we thank Dr. Sophie Langis-Barsetti and reviewers for helpful suggestions. Dr. Pedro M. Aguiar provided valuable assistance in obtaining satisfactory NMR spectra.

Notes. The authors declare no competing financial interest.

2.7 References

1. O. Ermer, *J. Am. Chem. Soc*. **1988**, *110*, 3747.
2. Y. Ducharme, J. D. Wuest, *J. Org. Chem.* **1988**, *53*, 5787.
3. M. Simard, D. Su, J. D. Wuest, *J. Am. Chem. Soc.* **1991**, 113, 4696.
4. M. C. Etter, *Acc. Chem. Res.* **1990**, *23*, 120.

5. B. F. Hoskins, R. Robson, *J. Am. Chem. Soc.* **1989**, *111*, 5962.

6. H. Furukawa, K. E. Cordova, M. O'Keeffe, O. M. Yaghi, *Science* **2013**, *341*, 1230444.

7. M. S. Lohse, T. Bein, *Adv. Funct. Mater.* **2018**, *28*, 1705553.

8. C. S. Diercks, O. M. Yaghi, *Science* **2017**, *355*, 6328.

9. I. Hisaki, C. Xin, K. Takahashi, T. Nakamura, *Angew. Chem. Int. Ed.* **2019**, *58*, 11160; *Angew. Chem.* **2019**, *131*, 11278.

10. R.-B. Lin, Y. He, P. Li, H. Wang, W. Zhou, B. Chen, *Chem. Soc. Rev.* **2019**, *48*, 1362.

11. J. Luo, J.-W. Wang, J.-H. Zhang, S. Lai, D.-C. Zhong, *CrystEngComm* **2018**, *20*, 5884.

12. D. E. Palin, H. M. Powell, *J. Chem. Soc.* **1948**, 815.

13. P. Brunet, M. Simard, J. D. Wuest, *J. Am. Chem. Soc.* **1997**, *119*, 2737.

14. Y. He, S. Xiang, B. Chen, *J. Am. Chem. Soc.* **2011**, *133*, 14570.

15. I. Brekalo, D. E. Deliz, L. J. Barbour, M. D. Ward, T. Friščić, K. T. Holman, *Angew. Chem. Int. Ed.* **2020**, *59*, 1997; *Angew. Chem.* **2020**, *132*, 2013.

16. P. Li, P. Li, M. R. Ryder, Z. Liu, C. L. Stern, O. K. Farha, J. F. Stoddart, *Angew. Chem. Int. Ed.* **2019**, *58*, 1664; *Angew. Chem.* **2019**, *131*, 1678.

17. A. Pulido, L. Chen, T. Kaczorowski, D. Holden, M. A. Little, S. Y. Chong, B. J. Slater, D. P. McMahon, B. Bonillo, C. J. Stackhouse, A. Stephenson, C. M. Kane, R. Clowes, T. Hasell, A. I. Cooper, G. M. Day, *Nature* **2017**, *543*, 657.

18. A. Comotti, S. Bracco, A. Yamamoto, M. Beretta, T. Hirukawa, N. Tohnai, M. Miyata, P. Sozzani, *J. Am. Chem. Soc.* **2014**, *136*, 618.

19. M. Mastalerz, I. M. Oppel, *Angew. Chem. Int. Ed.* **2012**, *51*, 5252; *Angew. Chem.* **2012**, *124*, 5345.

20. C. Trolliet, G. Poulet, A. Tuel, J. D. Wuest, P. Sautet, *J. Am. Chem. Soc.* **2007**, *129*, 3621.

21. K. E. Maly, E. Gagnon, T. Maris, J. D. Wuest, *J. Am. Chem. Soc.* **2007**, *129*, 4306.

22. J. Liebig, *Ann. Pharm.* **1834**, 10, 1.

23. B. Bann, S. A. Miller, *Chem. Rev.* **1958**, *58*, 131.

24. X. Li, S. T. A. G. Melissen, T. Le Bahers, P. Sautet, A. F. Masters, S. N. Steinmann, T. Maschmeyer, *Chem. Mater.* **2018**, *30*, 4253.

25. A. Schwarzer, T. Saplinova, E. Kroke, *Coord. Chem. Rev.* **2013**, *257*, 2032.

26. B. V. Lotsch, W. Schnick, *Chem. Eur. J.* **2007**, *13*, 4956.

27. E. Wirnhier, M. B. Mesch, J. Senker, W. Schnick, *Chem. Eur. J.* **2013**, *19*, 2041.

28. N. E. Braml, A. Sattler, W. Schnick, *Chem. Eur. J.* **2012**, *18*, 1811.

29. N. Nohara, S. Sekiguchi, K. Matsui, *J. Heterocycl. Chem.* **1970**, *7*, 519.

30. The percentage of volume accessible to guests was estimated by the PLATON program.[28,29] PLATON calculates the accessible volume by allowing a spherical probe of variable radius to roll over the van der Waals surface of the network. PLATON uses a default value of 1.20 Å for the radius of the probe, which is an appropriate model for small guests such as water. The van der Waals radii used to define surfaces for these calculations are C: 1.70 Å, H: 1.20 Å, and N: 1.55 Å. The percentage of accessible volume is given by $100V_g/V$, where V is the volume of the unit cell and V_g is the guest-accessible volume as calculated by PLATON.

31. A. L. Spek, *PLATON, A Multipurpose Crystallographic Tool*; Utrecht University: Utrecht, The Netherlands, 2001.

32. P. van der Sluis, A. L. Spek, *Acta Crystallogr.* **1990**, *A46*, 194.

33. R. D. Allington, D. Attwood, I. Hamerton, J. N. Hay, B. J. Howlin, *Comput. Theor. Polym. Sci.* **2001**, 11, 467.

34. C. A. Morrison, B. A. Smart, D. W. H. Rankin, H. E. Robertson, M. Pfeffer, W. Bodenmüller, R. Ruber, B. Macht, A. Ruoff, V. Typke, *J. Phys. Chem. A* **1997**, *101*, 10029.

35. See the Supporting Information for details.

36. Surface areas for the adsorption of N_2 were estimated by using MOF Explorer,[34] with 5000 probes per atom of diameter 3.72 Å.

37. M. Usdin, Y. Chung, R. Snurr, https://doi.org/10.5281/zenodo.3567067.

38. W. Yang, W. Zhou, B. Chen, *Cryst. Growth Des*. **2019**, *19*, 5184.

39. D.-D. Zhou, Y.-T. Xu, R.-B. Lin, Z.-W. Mo, W.-X. Zhang, J.-P. Zhang, *Chem. Commun*. **2016**, *52*, 4991.

40. J. Lü, C. Perez-Krap, M. Suyetin, N. H. Alsmail, Y. Yan, S. Yang, W. Lewis, E. Bichoutskaia, C. C. Tang, A. J. Blake, R. Cao, M. Schröder, *J. Am. Chem. Soc.* **2014**, *136*, 12828.

41. P. S. Nugent, V. L. Rhodus, T. Pham, K. Forrest, L. Wojtas, B. Space, M. J. Zaworotko, *J. Am. Chem. Soc.* **2013**, *135*, 10950.

42. B. D. Chandler, D. T. Cramb, G. K. H. Shimizu, *J. Am. Chem. Soc.* **2006**, *128*, 10403.

43. A. S. Lukas, S. E. Miller, M. R. Wasielewski, *J. Phys. Chem. B* **2000**, *104*, 931.

44. M. Havlík, B. Dolenský, J. Kessler, I. Císařová, V. Král, *Supramol. Chem.* **2012**, *24*, 127.

45. D. Parker, K. Senanayake, J. Vepsailainen, S. Williams, A. S. Batsanov, J. A. Howard, *J. Chem. Soc., Perkin Trans. 2* **1997**, 1445.

46. G. A. Adamson, C. W. Rees, *J. Chem. Soc., Perkin Trans. 1* **1996**, 1535.

47. A. Fatona, R. M. Berry, M. A. Brook, J. M. Moran-Mirabal, *Chem. Mater.* **2018**, 30, 2424.

Table of Contents Graphic

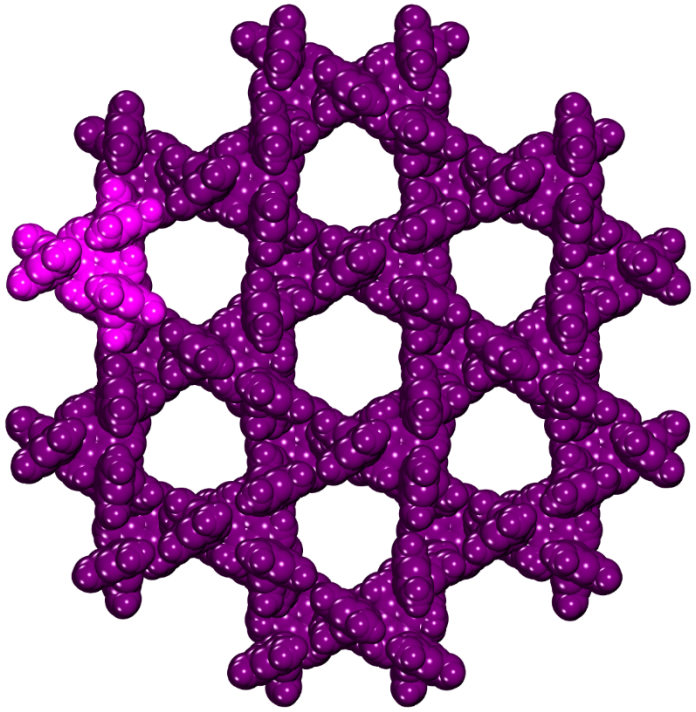

Complex melams made by simple triazinylations of amines can be used as modules to construct highly porous crystalline molecular materials held together by hydrogen bonds.

Keywords: Crystal engineering, hydrogen bonding, melams, porous material

Chapter 3. Conclusions and Perspectives

In previous chapters, we have shown that the strategy of the modular construction can be used in conjunction with $N(DAT)_2$ units to generate well-defined highly open hydrogen-bonded networks. Hydrogen bonds have a crucial role in this work since they are robust and directional. $N(DAT)_2$ groups have a strong potential to direct the self-assembly of frameworks that are held together by numerous N-H···N bonds per module. Our work has proven that even simple structures, such as those containing only one or two $N(DAT)_2$ groups, can still form highly open networks. The results also show that as more hydrogen bonds are involved in these frameworks, the volume accessible to guests can reach or even surpass 70%. The architectures resulting from self-assembly of compounds containing $N(DAT)_2$ units are robust and in favorable cases can retain their crystallinity after removing guests by desolvation. This allows the exchange of guests as well as the formation of unusually open-hydrogen-bonded frameworks (HOFs) with a high robustness, significant porosity, and other valuable properties. As an example, in our work melams **7** and **10** showed particularly high solvent-accessible volumes and high potential porosity. We examined both materials to see if they could be converted into permanently porous HOFs. In fact, melam **10** yielded a crystalline porous HOF, but melam **7** resulted in amorphous material. At this stage of our work, there is no clear answer why the open framework of melam **7** collapses when solvent is removed and fails to yield a porous crystalline HOF. Melam **10** is microporous and has channels with a large diameter (9.3 Å), which may facilitate the loss of guests under mild conditions and allow conversion into a HOF without loss of crystallinity. Melam **10** showed a small surface area (515 m^2/g) compared to other types of HOFs such as those ones built from modules held together by N−H···O hydrogen bonds. For

example, Mastalerz generated a HOF by grafting imidazolone units onto a rigid core of triptycene, and the resulting desolvated material showed a surface area of 2796 m^2/g (Chapter 1, Figure 10). We are optimistic that the relatively small surface area of our compound will result in high selectivity toward specific gas species such as CO_2. As a result, our work is expected to lead to a broad new family of compounds suitable for the modular construction of HOFs with unusually high degrees of robustness, porosity, and other useful properties.

By deepening our understanding of the self-assembly of $N(DAT)_2$ groups, our research opens new doors in the design and synthesis of frameworks based on $N(DAT)_2$ functionality. Such compounds are likely to be highly porous and may thus prove to be useful materials. There are a large number of new compounds that can be targeted as part of future work. As an example, hexaphenylbenzene is an interesting compound that can be used as a core onto which $N(DAT)_2$ groups can be grafted, giving compound **1**. An analogue of this compound with one DAT group appended to each phenyl ring has been examined before by the Wuest group and found to give a robust open hydrogen-bonded network. We expect the addition of multiple $N(DAT)_2$ groups will produce a molecule with a remarkable ability to engage in multiple hydrogen bonds and produce highly porous frameworks.[1]

Another promising class of compounds that have proven to generate highly open networks by other strategies are those with tetraphenylmethane cores. Potential new targets include compounds **2** and **3**, which are rigid and structurally well-defined.[2] Another interesting target can be achieved by grafting $N(DAT)_2$ groups onto a tetraphenyl orthocarbonate core (**4**).[3] Target **4** is particularly attractive because the Wuest group has developed significant expertise in the synthesis of aryl orthocarbonates, and we believe that compound **4** and analogues can be

made from readily available phenols in two or three steps. Moreover, these compounds can participate in unusually large numbers of intermolecular hydrogen bonds, leading to the generation of robust and highly open networks. Similarly, $N(DAT)_2$ functionalized bicyclooxacalixarene cages **5**, are realistic targets that are expected to have a high potential for producing robust networks that can retain their crystallinity after desolvation, as well as its analogues did.[4,5]

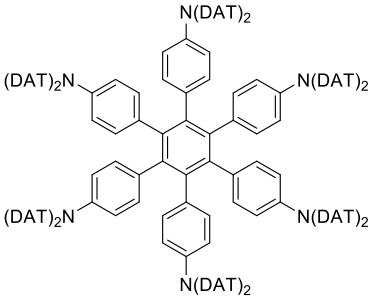

1

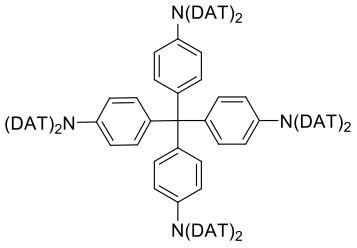

2

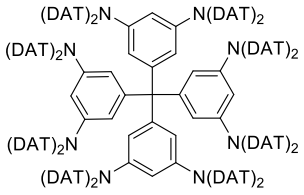

3

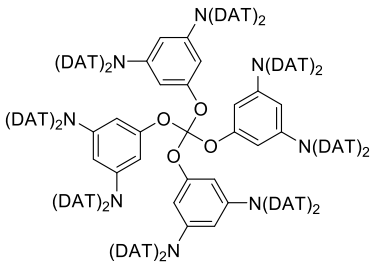

4

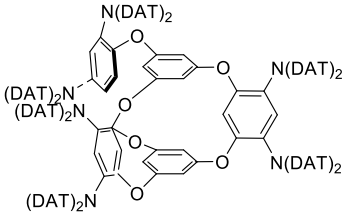

5

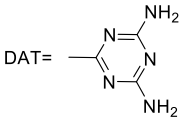

We expect that materials built from these compounds will have a strong potential utility because of their porous nature and additional favorable properties, such as low density relative to other porous materials such as MOFs and zeolites. Moreover, because compounds with $N(DAT)_2$ groups associate by hydrogen bonding, they are expected to give porous materials

with structures that can deform in response to the requirements of guests, leading to a potential for selective inclusion. As a result, future targets **1-5** are likely to be particularly effective for use in separations and the selective storage of guests.

An important challenge for the future is to identify permanently porous ordered organic materials that can be produced cheaply on a large scale. Converting the $–NH_2$ group into the $N(DAT)_2$ group is a simple one-pot operation that uses inexpensive reagents, so commercial production of new materials held together by the interactions of multiple $–N(DAT)_2$ groups should be feasible, starting from various readily-available compounds with multiple $–NH_2$ groups. Particularly attractive possibilities include the conversion of polyamines such as (aminomethyl)polystyrene or poly(vinylamine) into the corresponding derivatives in which the $–NH_2$ groups have been transformed into $–N(DAT)_2$ groups. Strong but reversible inter-chain interactions based on hydrogen bonding should give rise to the formation of networks with high intrinsic porosity.

In such ways, hydrogen-bonded organic frameworks (HOFs) may eventually have an important practical impact. By studying and working on these types of materials, we have built new types of HOFs with novel properties. We believe that the approach we have used will lead to many more classes of compounds that can generate porous organic materials.

3.1 References

(1) Maly, K. E.; Gagnon, E.; Maris, T.; Wuest, J. D. Engineering Hydrogen-Bonded Molecular Crystals Built from Derivatives of Hexaphenylbenzene and Related Compounds. *J. Am. Chem. Soc.* **2007**, *129* (14), 4306–4322.

(2) Brunet, P.; Simard, M.; Wuest, J. D. Molecular Tectonics. Porous Hydrogen-Bonded Networks with Unprecedented Structural Integrity. *J. Am. Chem. Soc.* **1997**, *119* (11), 2737–2738.

(3) Matsumura, S.; Inata, H. Process for Producing Porous, Film-like or Fibrous Structure of Aromatic Polyester. US4419308A, December 6, **1983**.

(4) Naseer, M. M.; Wang, D.-X.; Zhao, L.; Huang, Z.-T.; Wang, M.-X. Synthesis and Functionalization of Heteroatom-Bridged Bicyclocalixaromatics, Large Molecular Triangular Prisms with Electron-Rich and -Deficient Aromatic Interiors. *J. Org. Chem.* **2011**, *76* (6), 1804–1813.

(5) Wang, Z.; Luo, Y.; Zhai, T.-L.; Ma, H.; Chen, J.-J.; Shu, Y.; Zhang, C. Porous Triphenylbenzene-Based Bicyclooxacalixarene Cage for Selective Adsorption of CO_2/N_2. *Org. Lett.* **2016**, *18* (18), 4574–4577.

Annex A

Supplementary information

Chapter 2

Modular Construction of Porous Hydrogen-Bonded

Molecular Materials from Melams

Modular Construction of Porous Hydrogen-Bonded Molecular Materials from Melams

Tinasadat Khadivjam,[†] Huy Che-Quang,[†] Thierry Maris,[†] Zvart Ajoyan,[‡]

Ashlee J. Howarth,[‡] and James D. Wuest*[,†]

[†]*Département de Chimie, Université de Montréal, Montréal, Québec H3C 3J7 Canada*

[‡]*Department of Chemistry & Biochemistry, Concordia University, Montréal, Québec H4B 1R6 Canada*

*Author to whom correspondence may be addressed. E-mail:

james.d.wuest@umontreal.ca

Contents **Page**

I. Methods of Activation and Measurements of Porosity

Equipment: Vacuum activation was performed using a Micromeritics Smart VacPrep equipped with a hybrid turbo vacuum pump. Drying with supercritical CO_2 ($scCO_2$) was carried out using a Tousimis Samdri-PVT-3D manual critical-point dryer. N_2 adsorption-desorption isotherms were collected at 77 K using a Micromeritics Tristar II Plus instrument.

Attempted Methods of Activation: With a Pasteur pipet, mother liquors (DMSO/EtOH) were removed from freshly crystallized samples of melams **7** ($P4_32_12$ form) and **10** (~100 mg each), and the residual solids were placed under vacuum at 25 °C for 5 h prior to N_2 adsorption-desorption measurements. Samples prepared in this way did not sorb N_2, so they were placed under vacuum at 25 °C for an additional 24 h. After this additional treatment, the samples still did not demonstrate permanent porosity. Freshly-crystallized samples of melams **7** and **10** were

also exposed twice for 5 min to EtOH (10 mL) to promote exchange of included solvent, but no permanent porosity was observed after the exchanged samples were dried under vacuum.

Supercritical Activation: With a Pasteur pipet, mother liquors (DMSO/EtOH) were removed from freshly crystallized samples of melams **7** ($P4_32_12$ form) and **10** (~100 mg each), and the residual solids were exposed twice for 5 min to EtOH (10 mL) to promote exchange of included solvent. The two resulting samples were then transferred to supercritical drying dishes, placed in a supercritical drying chamber, and subjected to exchange with liquid CO_2 for 2 h. The samples were each purged once after 10 min and again after 2 h, before being heated to the supercritical point of CO_2 (31.1 °C at 1071 psi). The samples were each left in supercritical CO_2 for 15 min before the supercritical drying chamber was bled at a rate of 0.5 cm^3 min^{-1}.

Measurements of Porosity: Figure S1 shows the BET plot obtained for samples of melam **10** activated by $scCO_2$. Figure S2 shows the powder X-ray diffraction patterns of materials prepared by subjecting solvated crystals of melam **10** grown from DMSO/EtOH to two methods of activation: (1) Initial exposure of the crystals to 1:1 DMSO/EtOH, subsequent exposure to pure EtOH, and desolvation at 25 °C under vacuum and (2) initial exposure of the crystals to EtOH, followed by supercritical activation as described above.

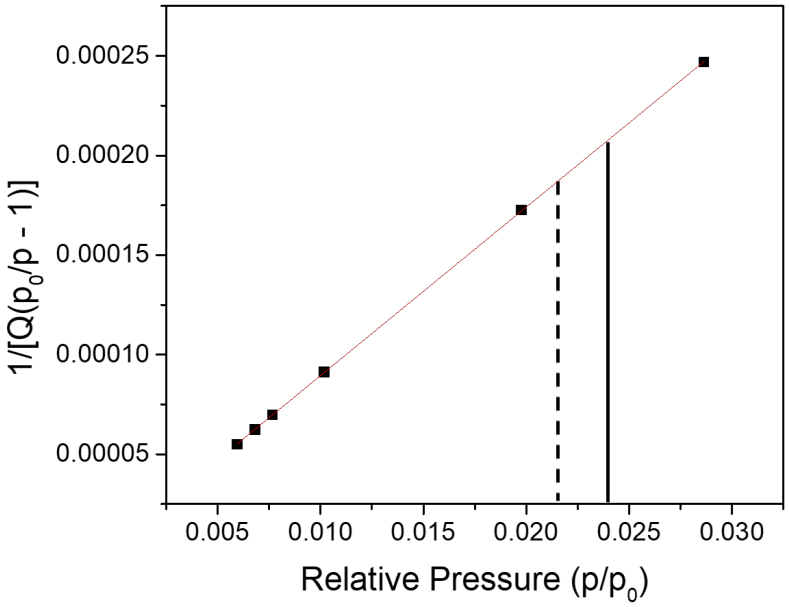

Figure S1. BET plot for crystalline melam **10** activated by scCO2. The solid black line corresponds to p/p_0 at the monolayer capacity (n_m), and the dotted line corresponds to the calculated value for monolayer formation $(\sqrt{C} + 1)^{-1}$.

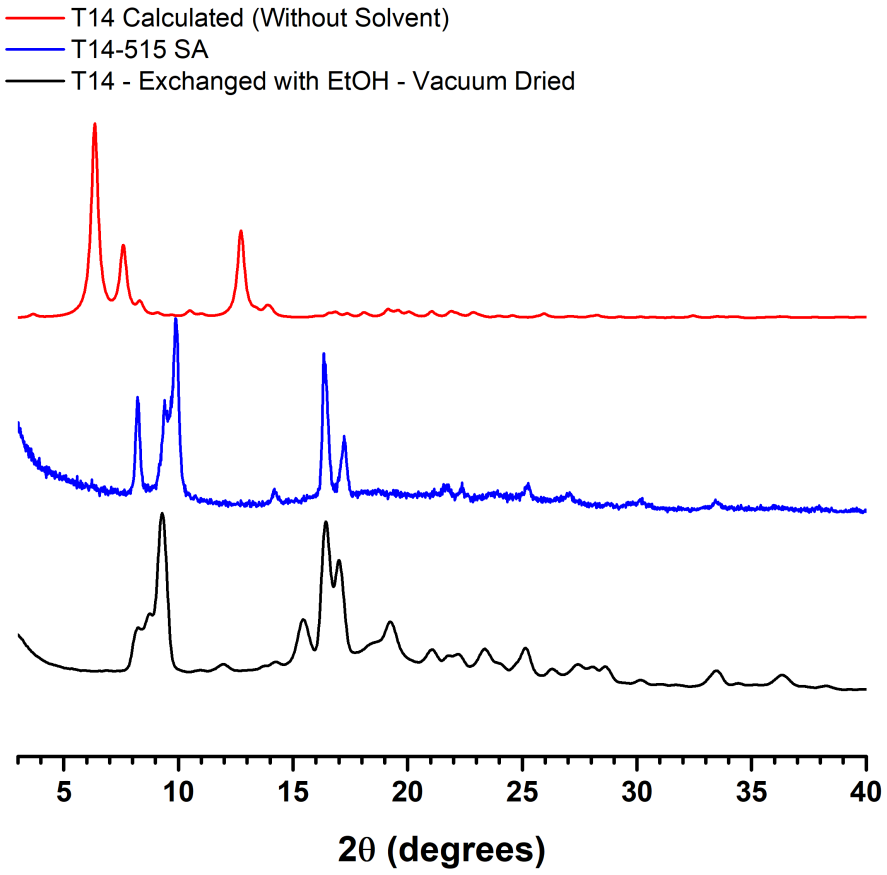

Figure S2. Powder X-ray diffraction patterns, as simulated for the hypothetical solvent-free form of crystals of melam **10** grown from DMSO/EtOH (red), as measured for crystals exposed to pure EtOH and then subjected to activation by supercritical CO_2 (blue), and as measured for crystals exposed to 1:1 DMSO/EtOH and then to pure EtOH, followed by desolvation at 25 °C under vacuum (black).

II. Additional Crystallographic Information

Data collection was carried out on a Bruker Venture Metaljet diffractometer using GaKα radiation (λ = 1.34139 Å). During all experiments, the samples were cooled using an Oxford Cryostream liquid-nitrogen device at 150 K. The cell lattice parameters were determined using reflections taken from three sets of 104 frames measured and harvested within the APEX3 suite of programs.[1] Integration of frames was performed using *SAINT*,[7] and a semiempirical absorption correction was applied with *SADABS*.[2] The structures were solved using a dual space and intrinsic phasing approach with *SHELXT*,[3] and the refinement was carried out using *SHELXL*-2018/3.[4]

Many of the crystal structure refinements were challenging because of the presence of disordered molecules of solvent, which resulted in weak reflections at high angles. For melam **8** crystallized from DMSO/EtOH, certain molecules of solvent proved to be disordered in ways that prevented the use of models with reasonable geometries. The refinement was carried out by including disordered molecules of DMSO molecules refined with partial occupancy factors, while the remaining disordered solvent contribution was modeled by applying the mask/*squeeze* routine implemented in *OLEX2*.[5,6] A total of 392 electrons was found in the unit cell, corresponding (with $Z = 4$) to roughly two molecules of DMSO and one molecule of H_2O for each molecule of melam **8**. For melams **9** and **10**, as well as for melam **7** crystallized from DMSO/EtOH, the entire solvent contribution was treated with the mask/squeeze routine. Totals of 4086, 3664, and 3625 electrons per cell were found for melams **7**, **9**, and **10**, respectively. This corresponds roughly to 96, 87, and 86 molecules of DMSO in the unit cells, respectively, giving 12 molecules of DMSO per molecule of melam **7** ($Z = 8$), 11 for melam **9** (Z = 8), and 7

for melam **10** (Z = 12). Crystals of melam **10** grown from DMSO/EtOH were highly unstable. They decomposed within seconds when removed from their mother liquors and yielded a new crystalline form when kept at 25 °C in contact with the mother liquors for several days.

Solvent-accessible volumes were evaluated using the *VOID* routine in *PLATON*,[5] and hydrogen-bonded network topologies were investigated using *TOPOS*.[7] Structural data have been deposited at The Cambridge Crystallographic Data Centre with deposition numbers CCDC 1970867–1970874. These data can be obtained free of charge via www.ccdc.cam.ac.uk/data_request/cif, by emailing data_request@ccdc.cam.ac.uk, or by contacting The Cambridge Crystallographic Data Centre, 12 Union Road, Cambridge CB2 1EZ, UK; fax: +44 1223 336033.

III. ORTEP Diagrams

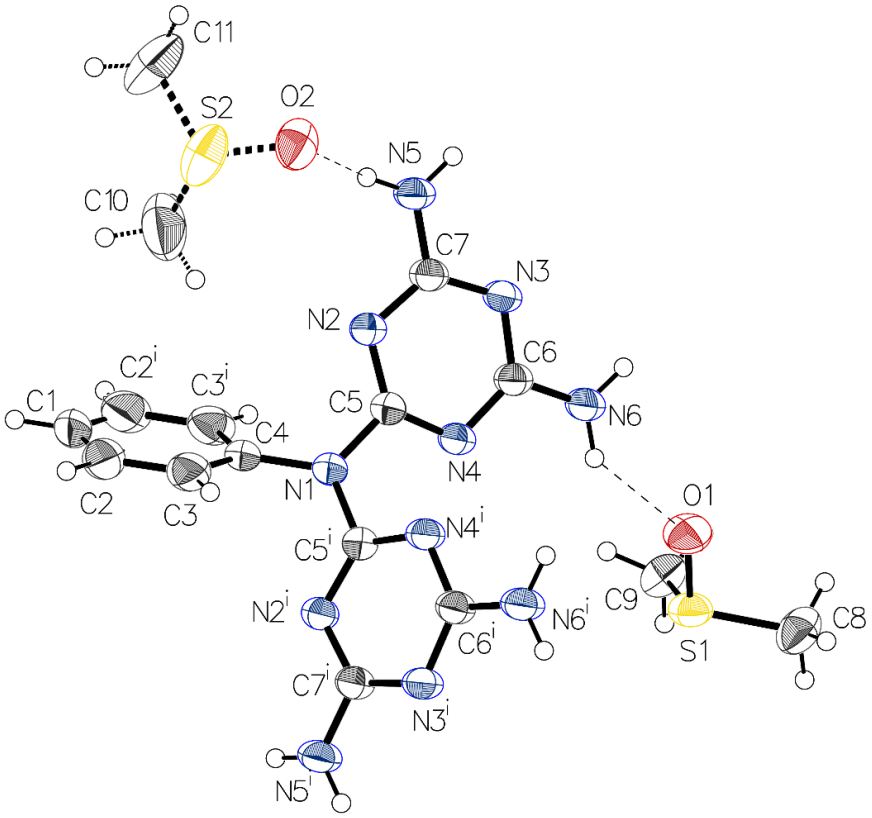

Figure S2. Thermal atomic displacement ellipsoid plot of the structure obtained by crystallizing $PhN(DAT)_2$ (**5**) from DMSO. The ellipsoids of non-hydrogen atoms are drawn at the 50% probability level, and hydrogen atoms are represented by a sphere of arbitrary size. Symmetry code (i): 1-x, y, ½-z.

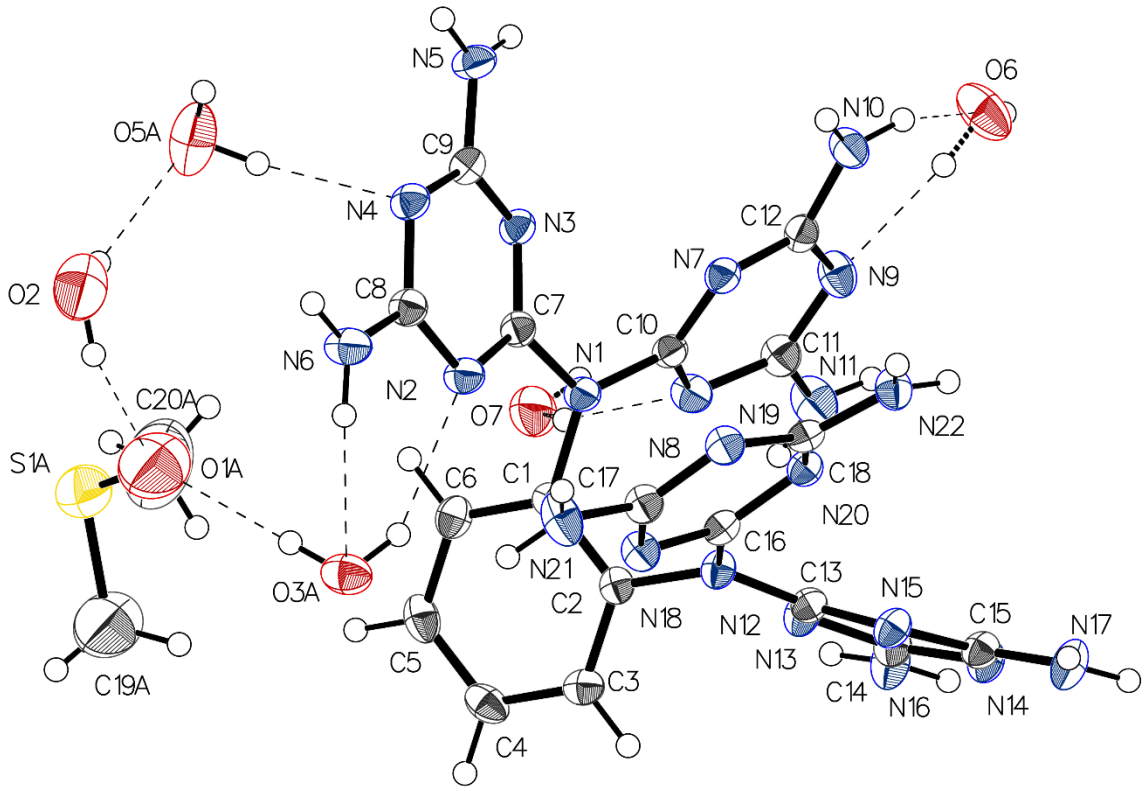

Figure S3. Thermal atomic displacement ellipsoid plot of the structure obtained by crystallizing 1,2-Ph[N(DAT)$_2$]$_2$ (**6**) from DMSO/H_2O. The ellipsoids of non-hydrogen atoms are drawn at the 50% probability level, and hydrogen atoms are represented by a sphere of arbitrary size. Only the major component of the disordered solvent molecule is shown.

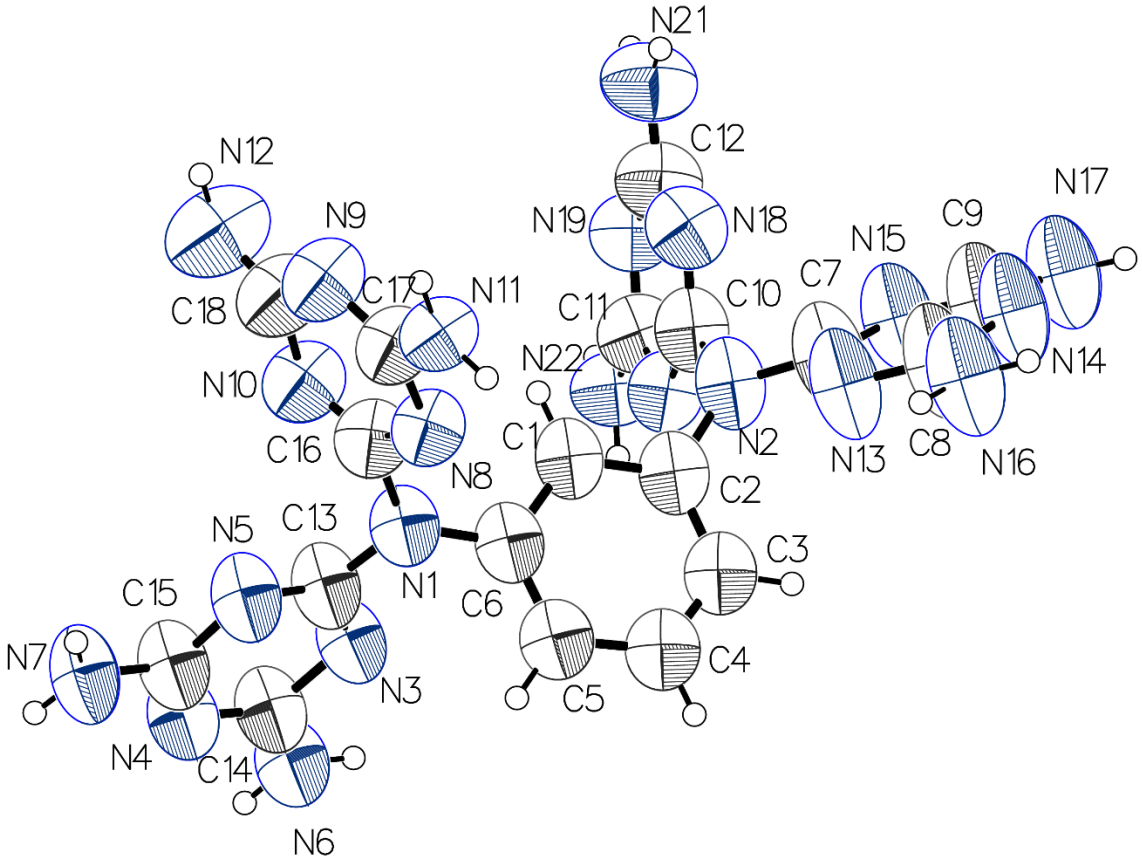

Figure S4. Thermal atomic displacement ellipsoid plot of the structure produced by crystallizing 1,3-Ph[N(DAT)$_2$]$_2$ (**7**) from DMSO/EtOH. The ellipsoids of non-hydrogen atoms are drawn at the 50% probability level, and hydrogen atoms are represented by a sphere of arbitrary size.

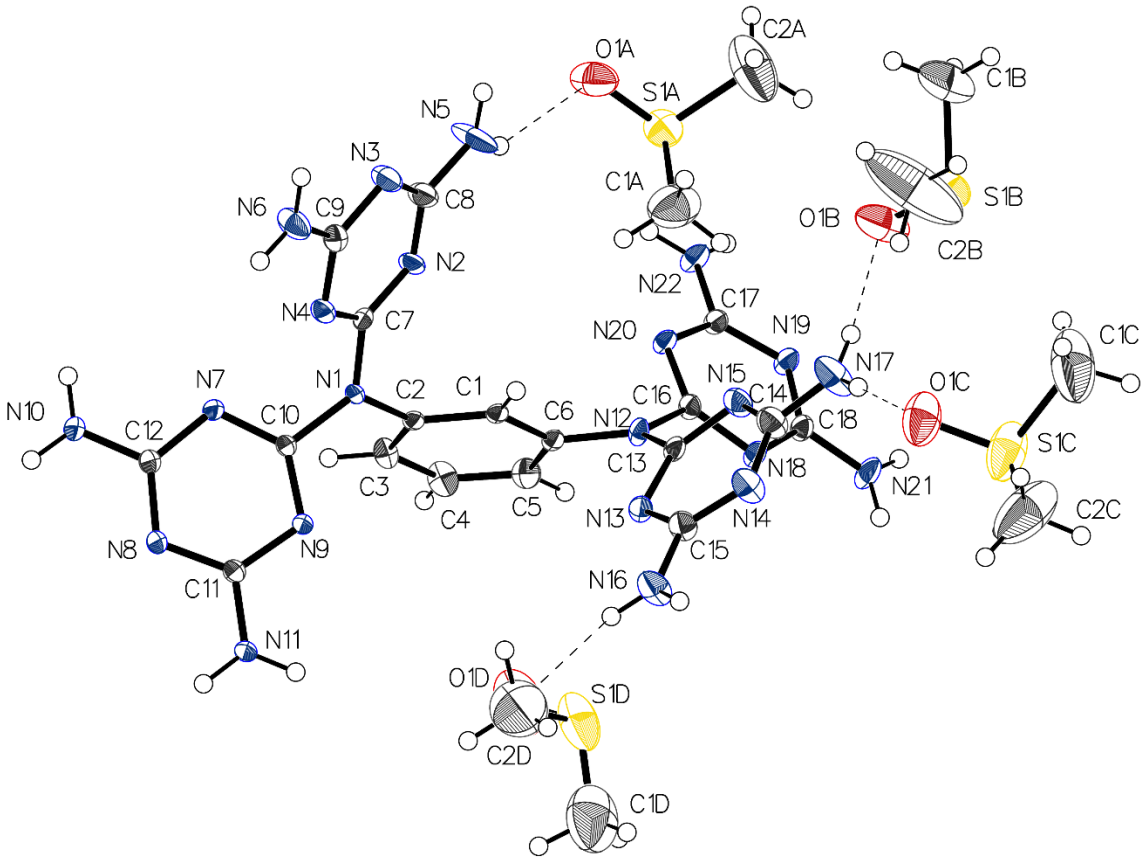

Figure S5. Thermal atomic displacement ellipsoid plot of the structure obtained by crystallizing 1,3-Ph[N(DAT)$_2$]$_2$ (**7**) from DMSO in the presence of Et_3NH^+ F^-. The ellipsoids of non-hydrogen atoms are drawn at the 50% probability level, and hydrogen atoms are represented by a sphere of arbitrary size. Only the major component of the disordered solvent molecule is shown.

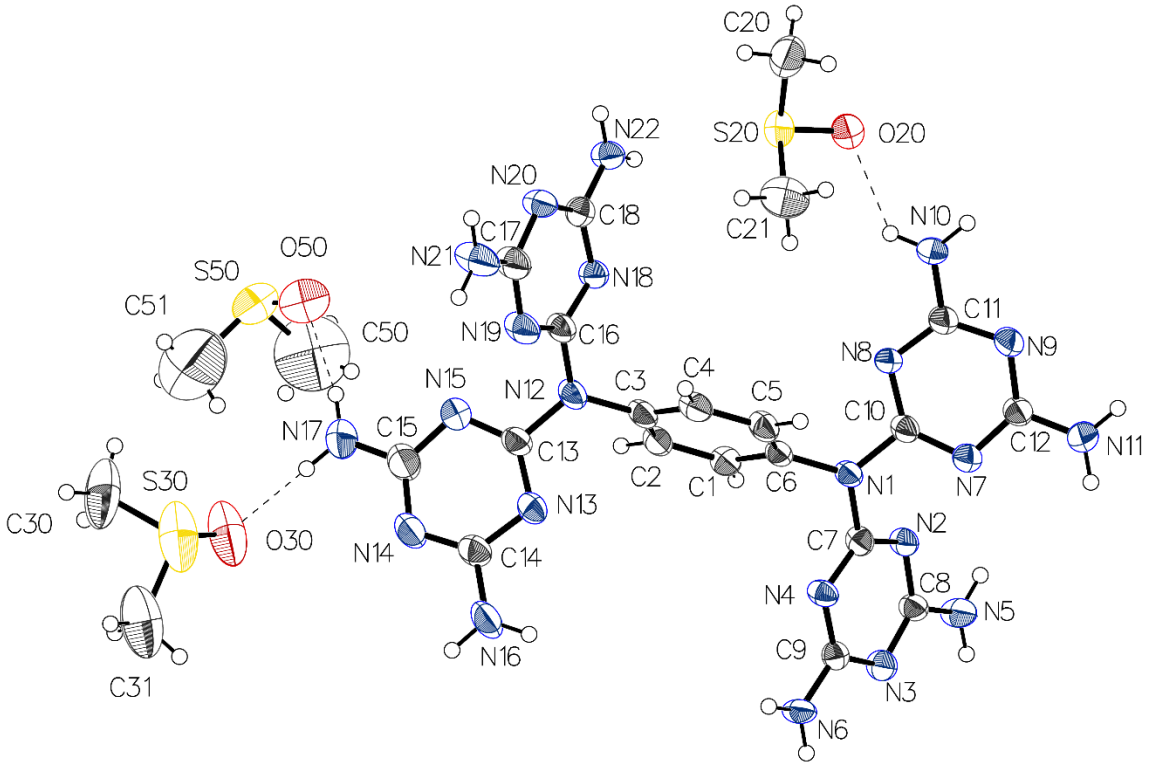

Figure S6. Thermal atomic displacement ellipsoid plot of the structure produced by crystallizing 1,4-Ph[N(DAT)$_2$]$_2$ (**8**) from DMSO/EtOH. The ellipsoids of non-hydrogen atoms are drawn at the 50% probability level, and hydrogen atoms are represented by a sphere of arbitrary size. Only the major component of the disordered solvent molecule is shown.

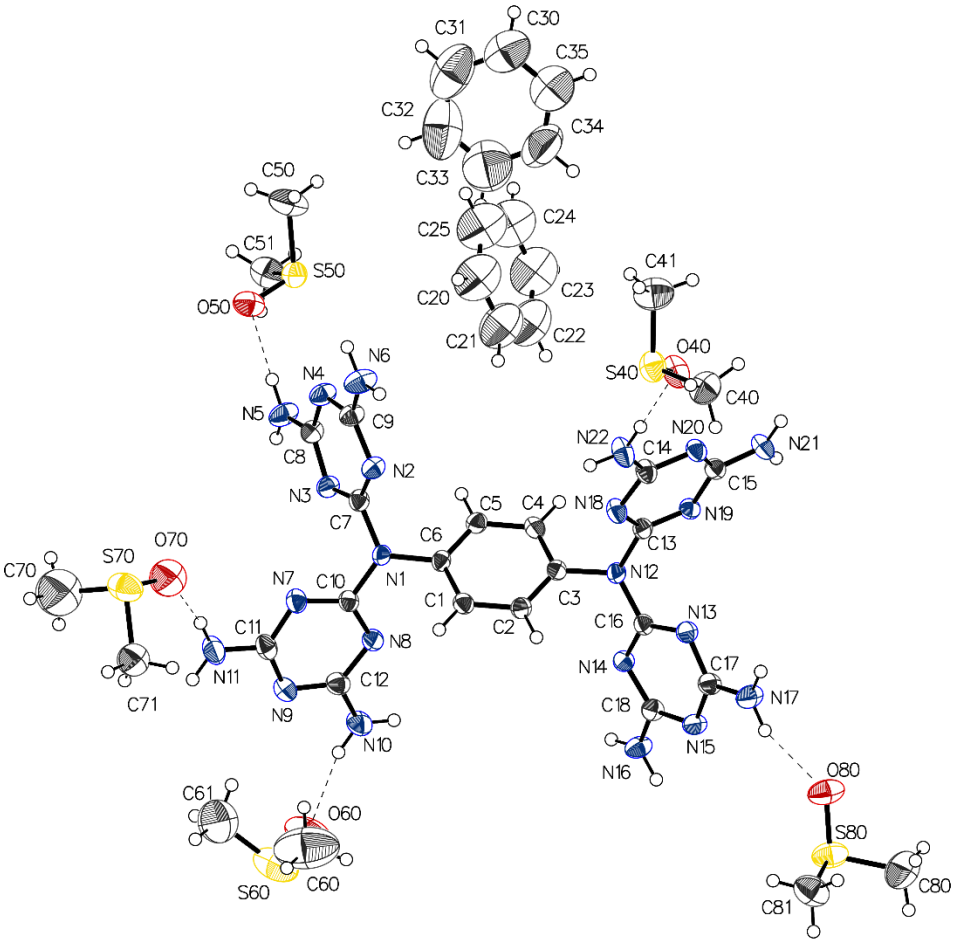

Figure S7. Thermal atomic displacement ellipsoid plot of the structure obtained by crystallizing 1,4-Ph[N(DAT)$_2$]$_2$ (**8**) from DMSO/C_6H_6. The ellipsoids of non-hydrogen atoms are drawn at the 50% probability level, and hydrogen atoms are represented by a sphere of arbitrary size. Only the major component of the disordered solvent molecule is shown.

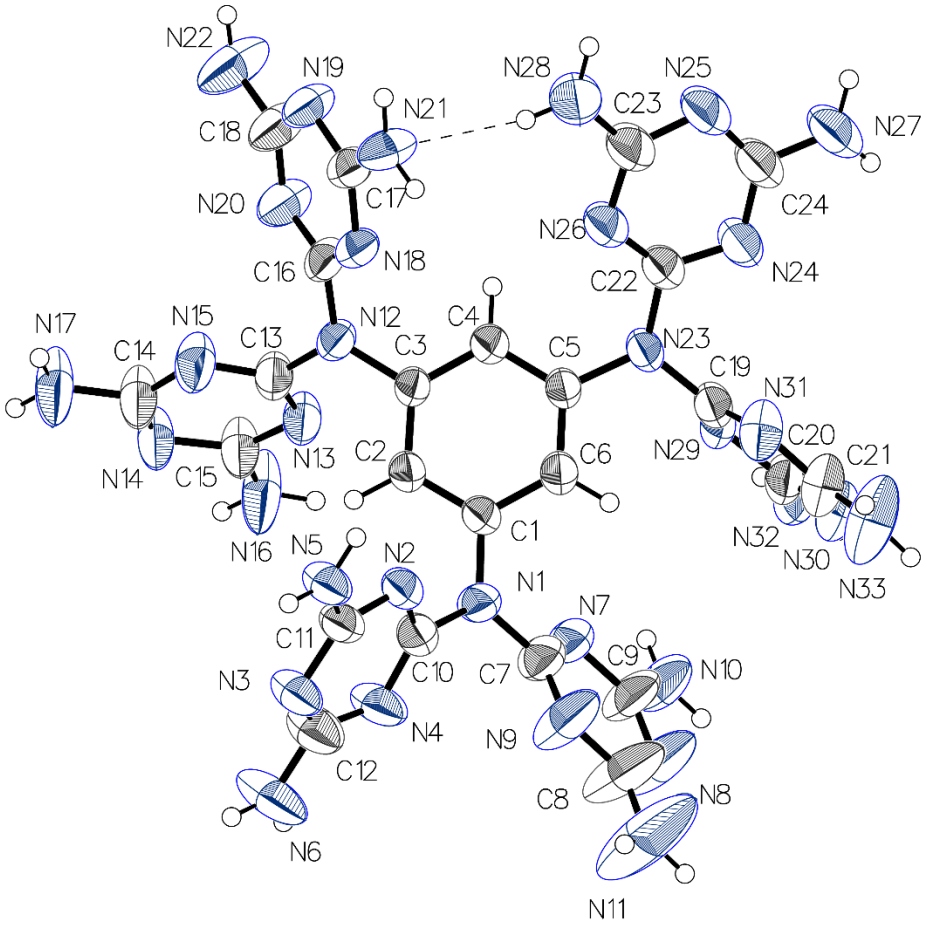

Figure S8. Thermal atomic displacement ellipsoid plot of the structure produced by crystallizing 1,3,5-Ph[N(DAT)$_2$]$_3$ (**9**) from DMSO/MeOH. The ellipsoids of non-hydrogen atoms are drawn at the 50% probability level, and hydrogen atoms are represented by a sphere of arbitrary size.

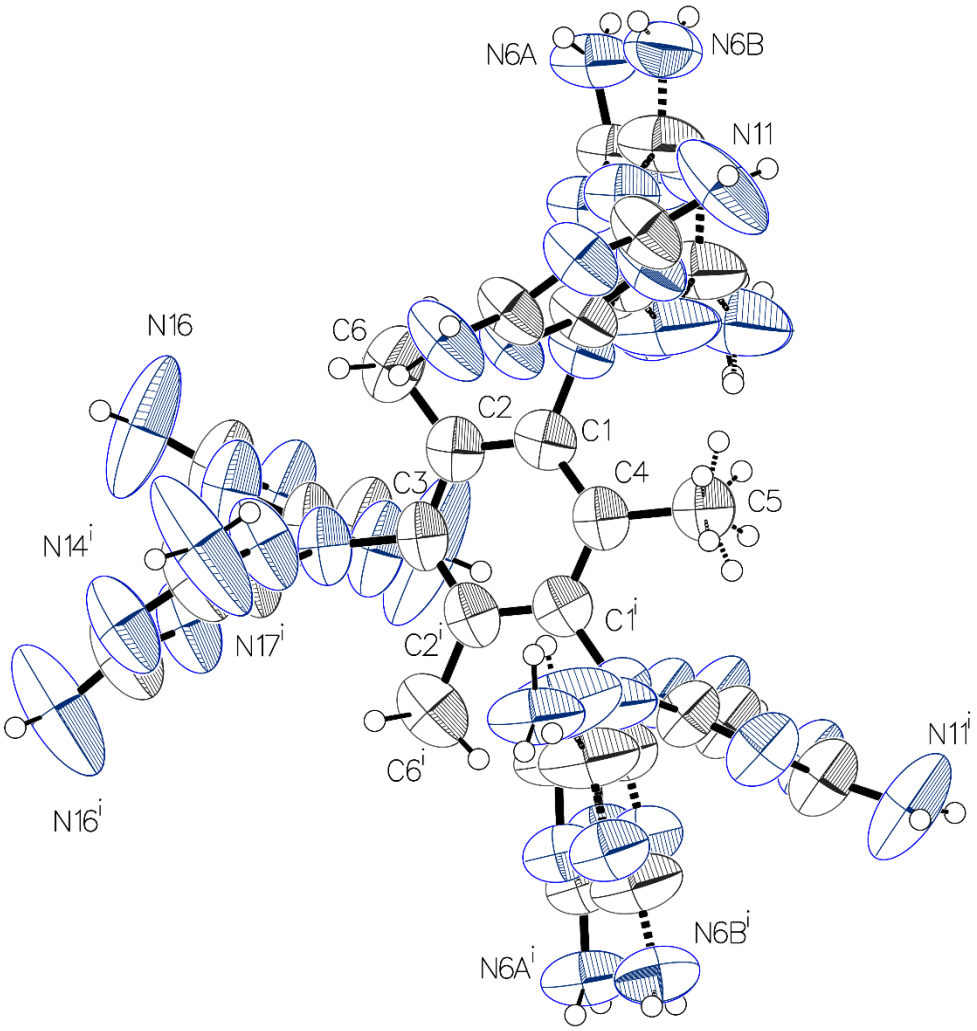

Figure S9. Thermal atomic displacement ellipsoid plot of the structure obtained by crystallizing melam **10** from DMSO/EtOH. The ellipsoids of non-hydrogen atoms are drawn at the 50% probability level, and hydrogen atoms are represented by a sphere of arbitrary size. Symmetry code (i): x-y, -y, 1/2-z.

IV. ^{1}H and ^{13}C NMR Spectra of Melams 5–11

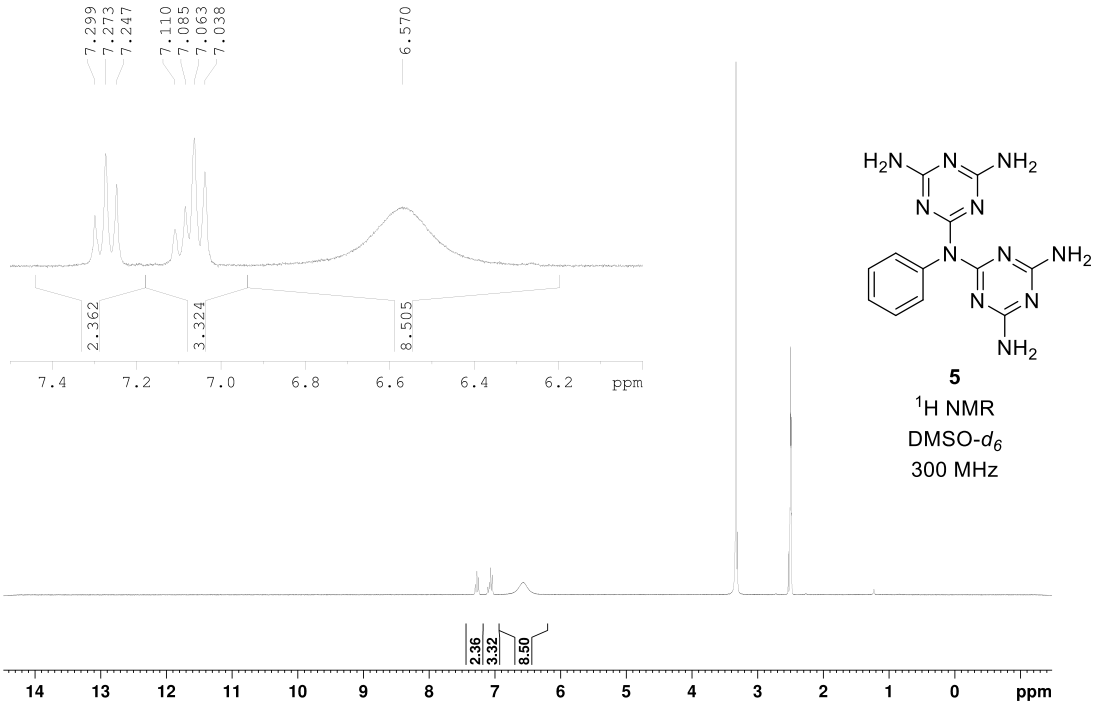

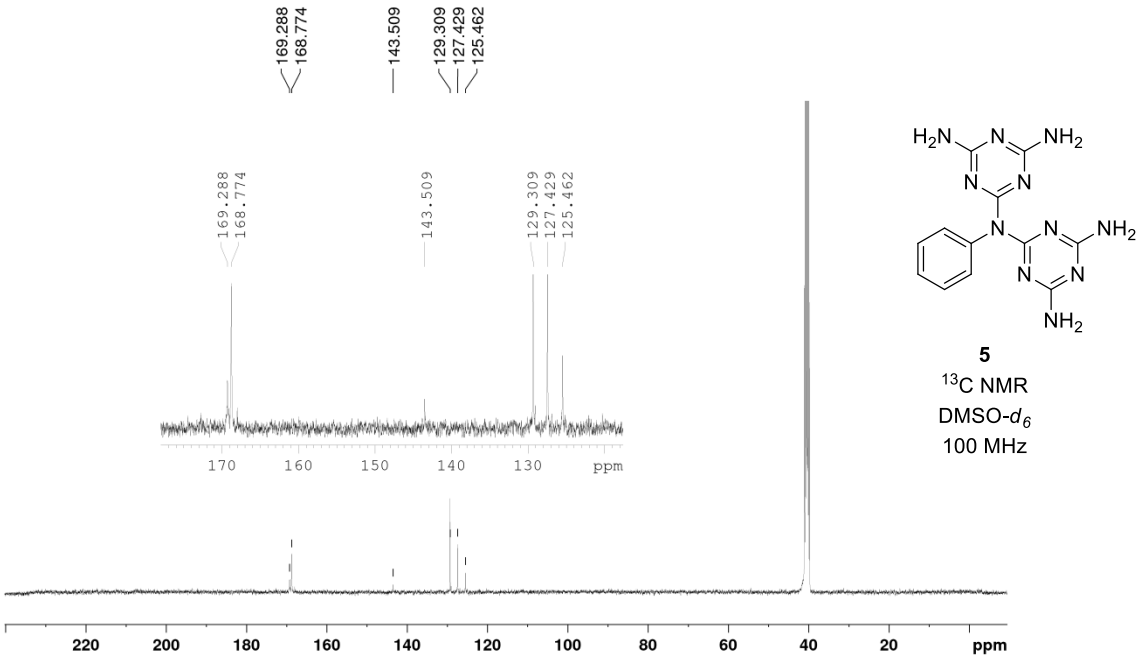
169.288
168.774
143.509
129.309
127.429
125.462
220
200
180
160
140
120
100
80
60
40
20
ppm
170
160
150
140
130
ppm
H2N
NH2
NH2
NH2
5
13C NMR
DMSO-d6
100 MHz

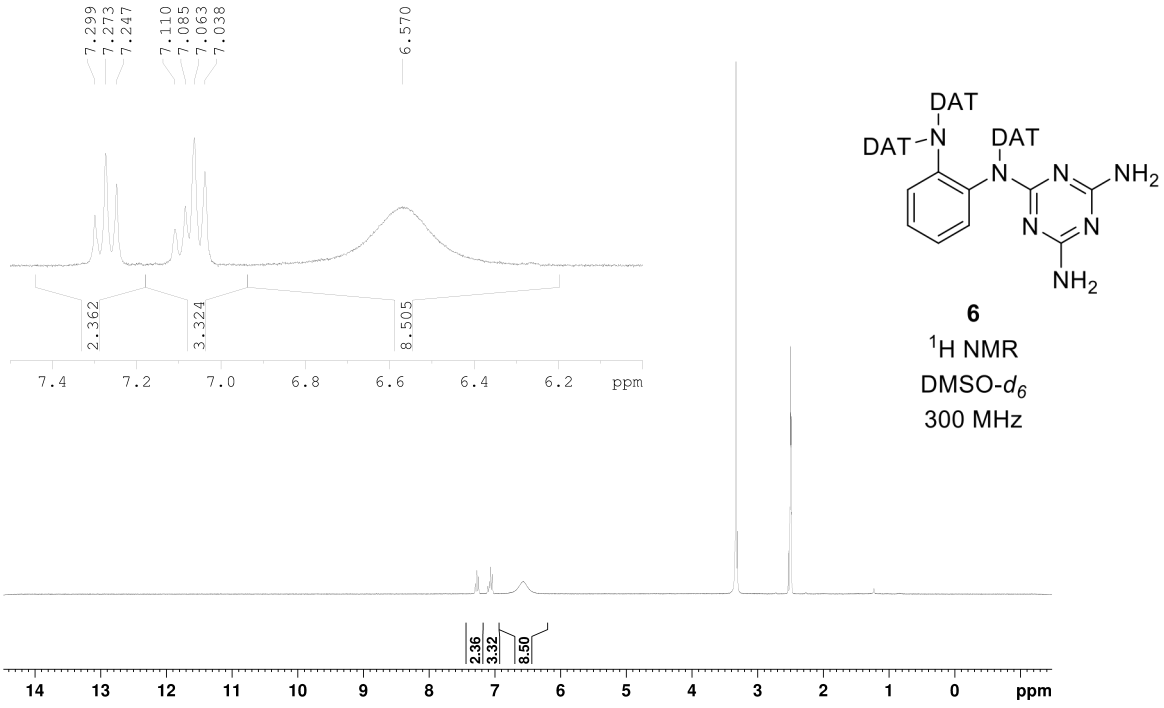
7.299
7.273
7.247
7.110
7.085
7.063
7.038
6.570
2.362
3.324
8.505
7.4
7.2
7.0
6.8
6.6
6.4
6.2
ppm
DAT
DAT
DAT
NH2
NH2
6
1H NMR
DMSO-d6
300 MHz
2.36
3.32
8.50
14
13
12
11
10
9
8
7
6
5
4
3
2
1
0
ppm

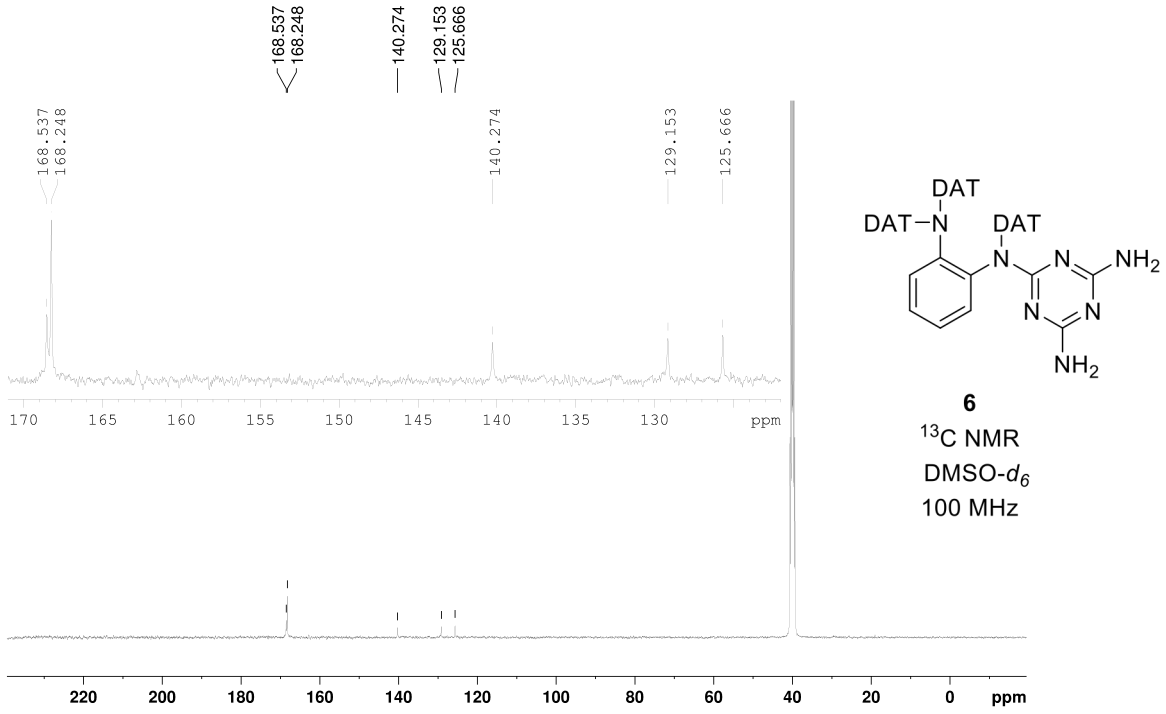
168.537
168.248
140.274
129.153
125.666
170
165
160
155
150
145
140
135
130
ppm
220
200
180
160
140
120
100
80
60
40
20
0
ppm
DAT
DAT–N
DAT
N
N
N
N
N
NH2
NH2
6
13C NMR
DMSO-d6
100 MHz

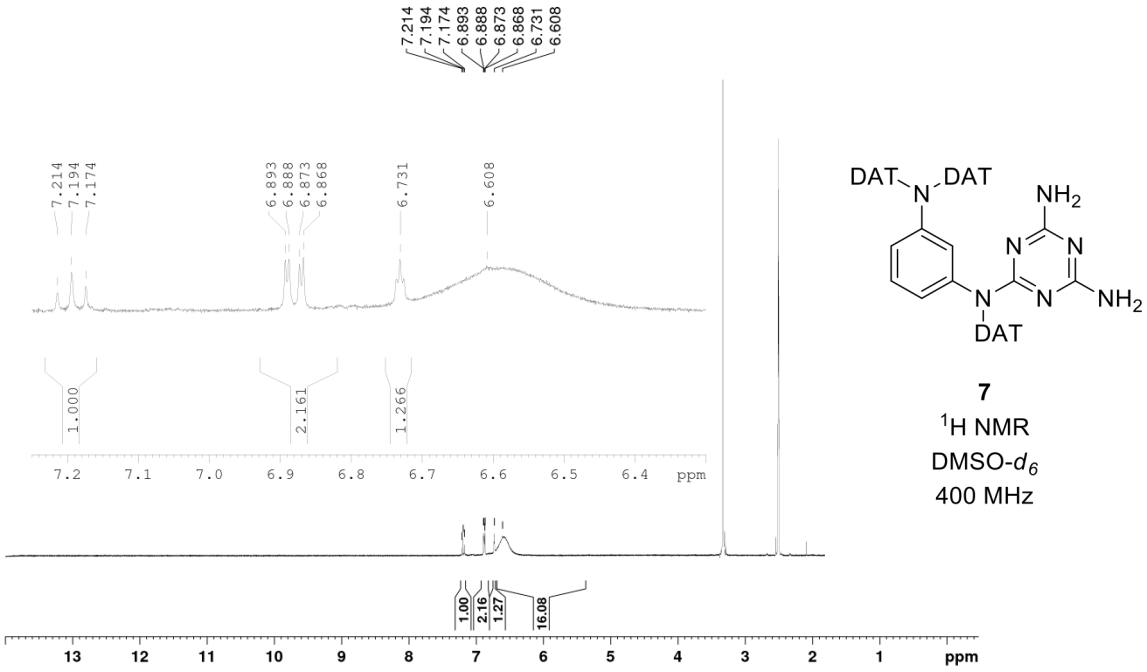

7
^{1}H NMR
DMSO-d_6
400 MHz

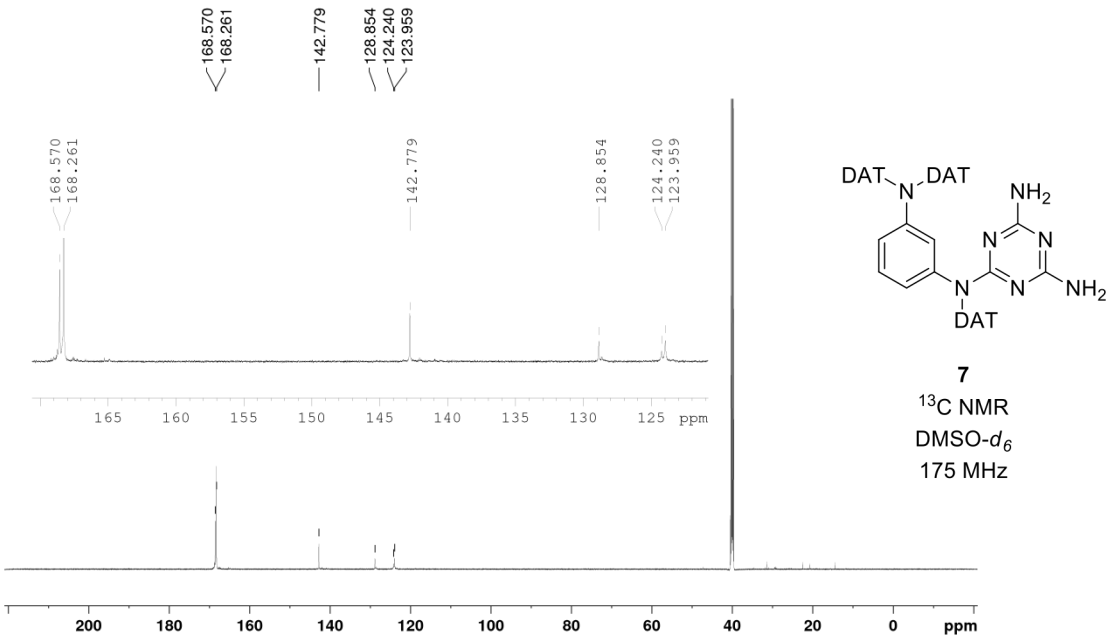

7
^{13}C NMR
DMSO-d_6
175 MHz

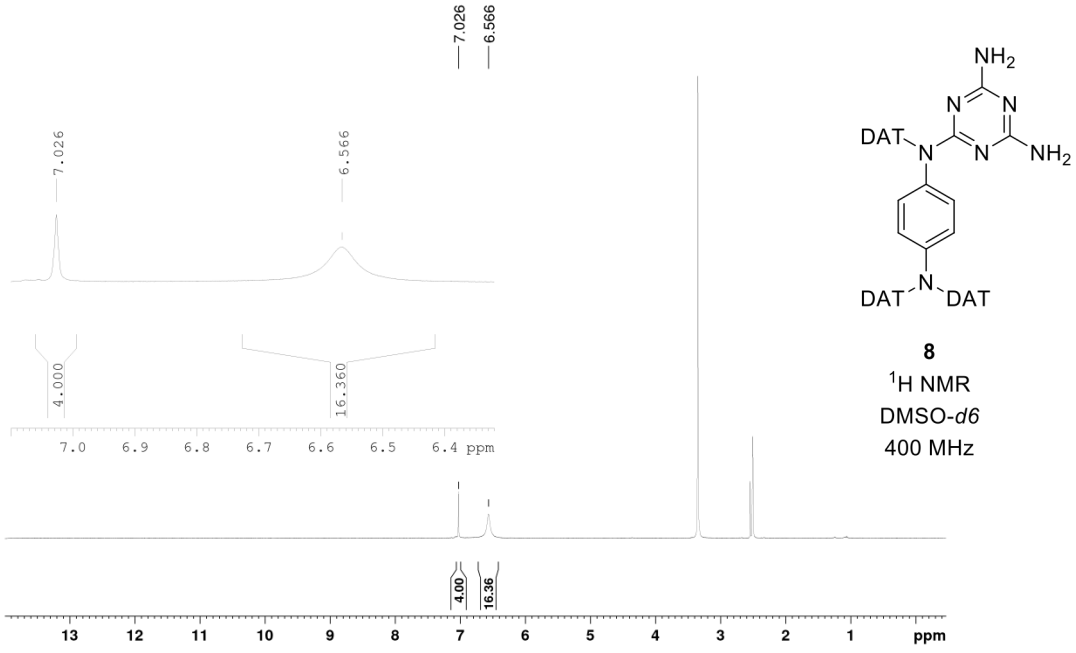

8
^{1}H NMR
DMSO-*d6*
400 MHz

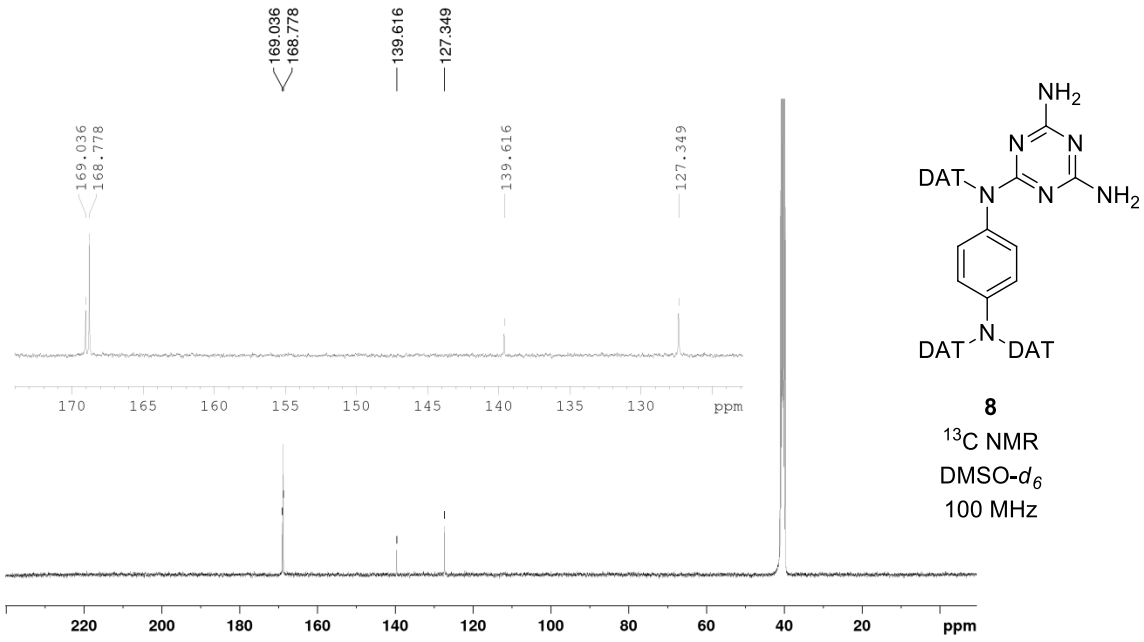
169.036
168.778
139.616
127.349
170
165
160
155
150
145
140
135
130
ppm
220
200
180
160
140
120
100
80
60
40
20
ppm
NH2
N
N
DAT
N
N
NH2
N
DAT
DAT
8
13C NMR
DMSO-d6
100 MHz

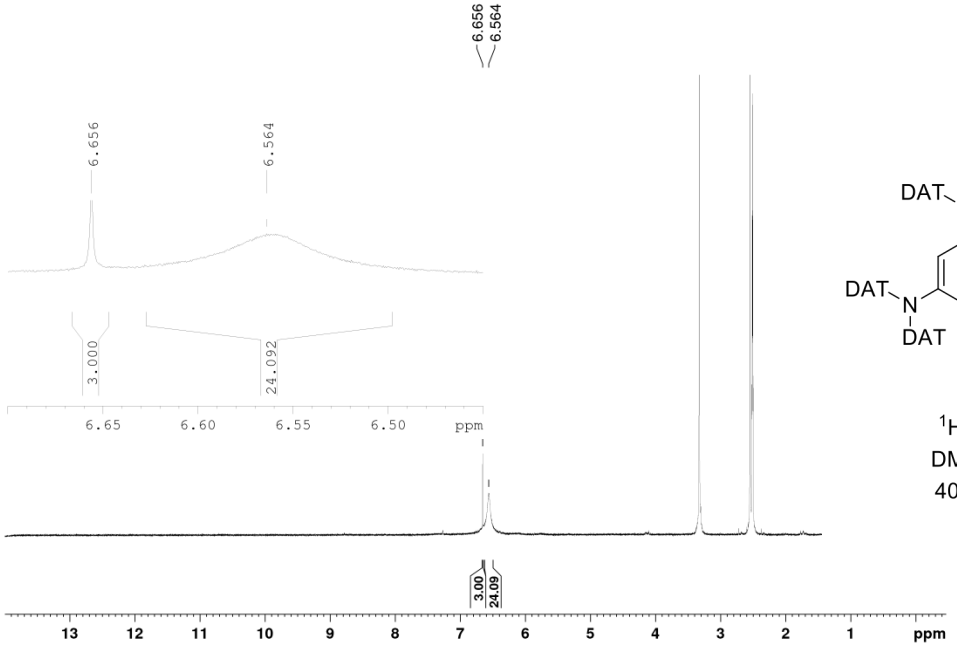

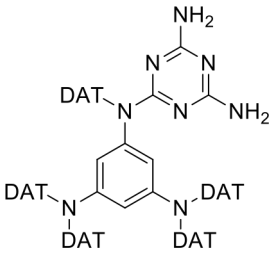

9
^{1}H NMR
DMSO-d_6
400 MHz

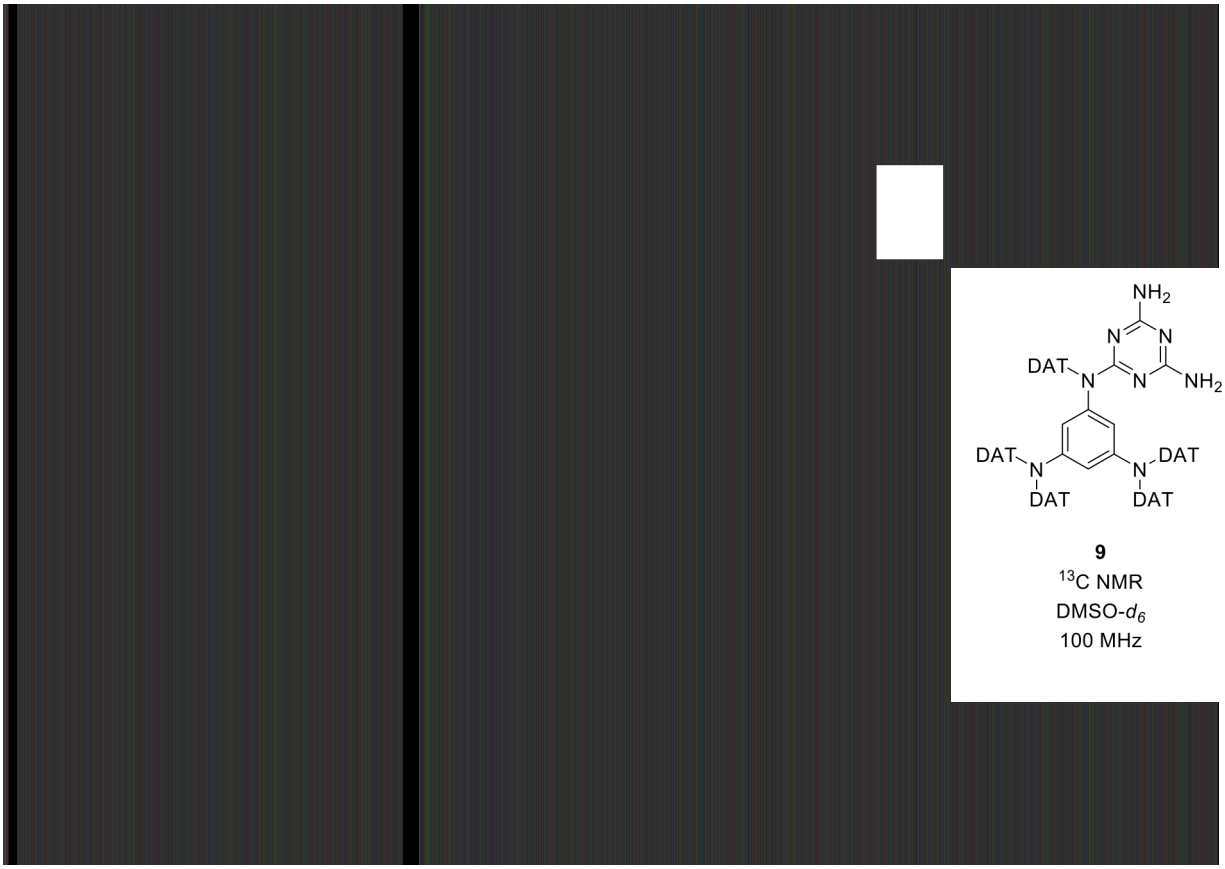

9
^{13}C NMR
DMSO-d_6
100 MHz

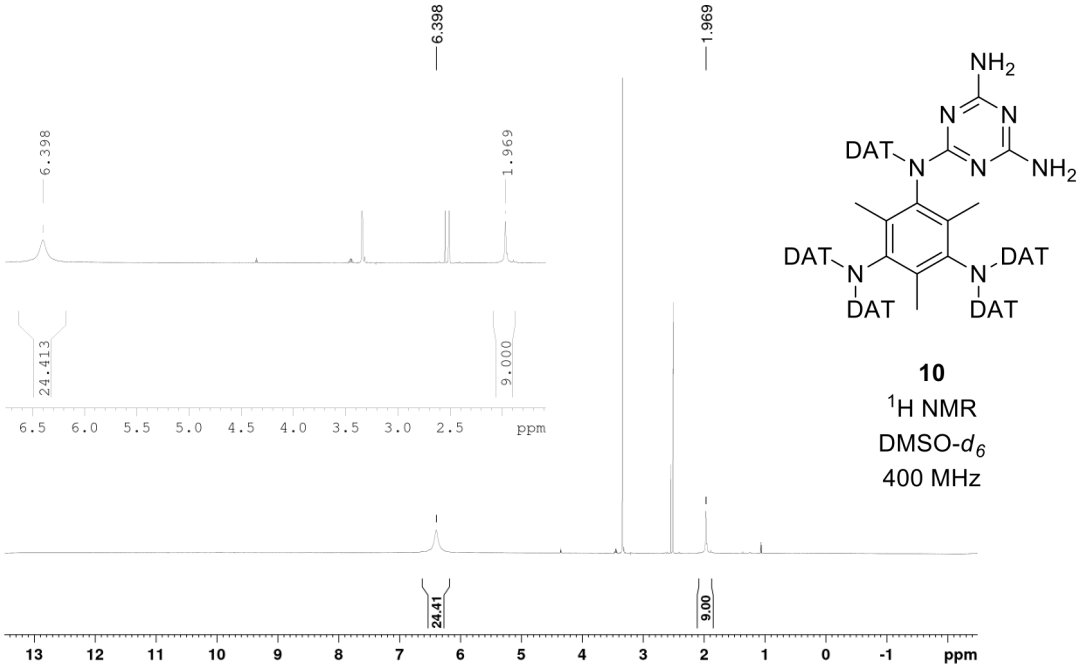

10
^{1}H NMR
DMSO-d_6
400 MHz

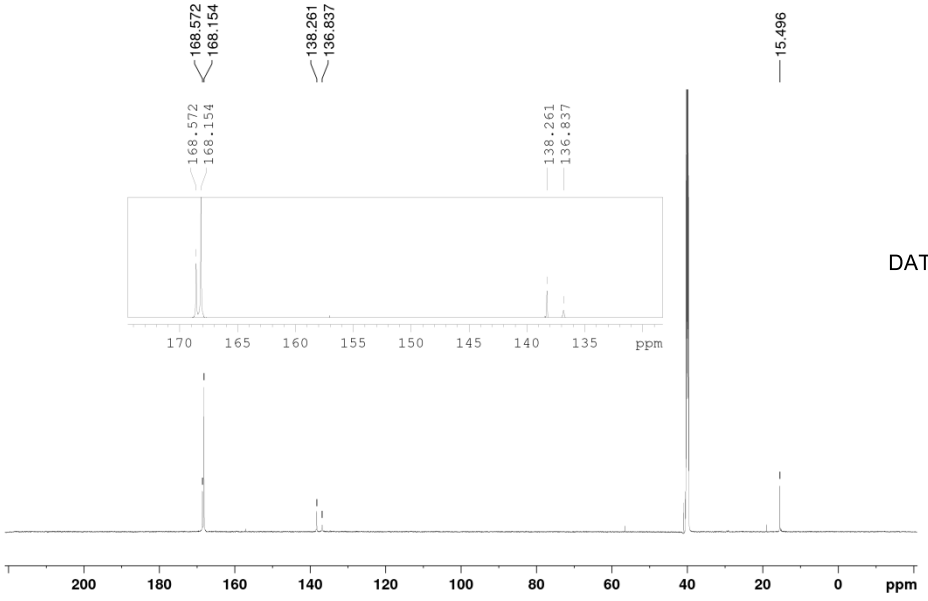

10
^{13}C NMR
DMSO-d_6
175 MHz

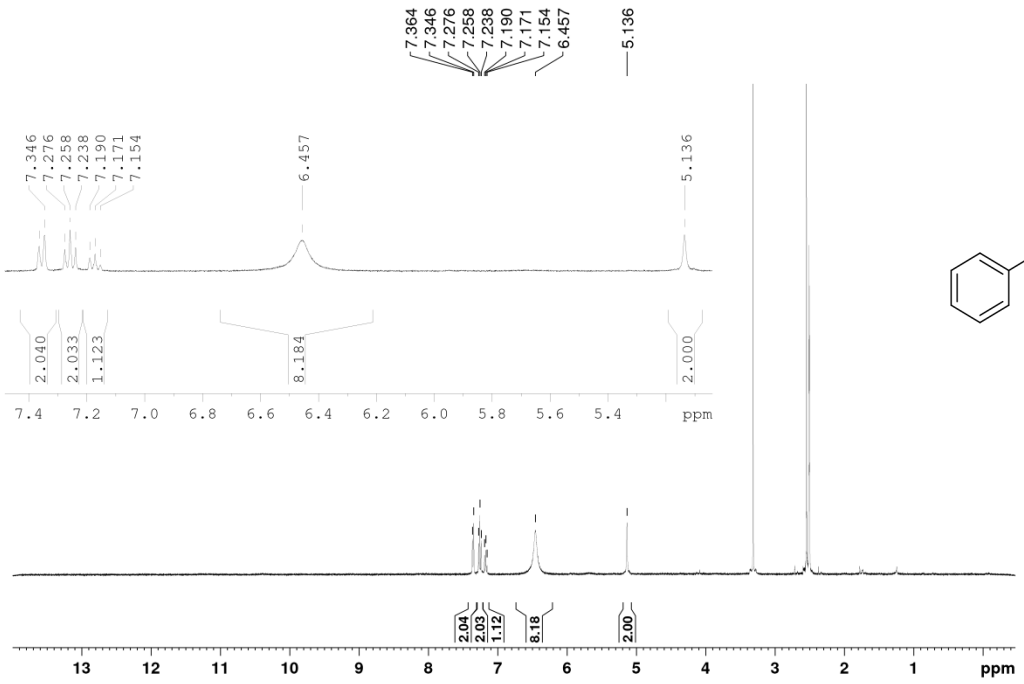

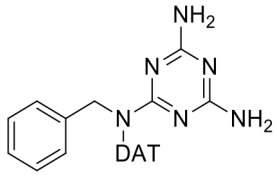

11
^{1}H NMR
DMSO-d_6
400 MHz

VI. References

(1) Bruker (2017). *APEX3* and *SAINT*, Bruker AXS Inc., Madison, Wisconsin, USA.

(2) Krause, L.; Herbst-Irmer, R.; Sheldrick, G. M.; Stalke, D. Comparison of Silver and Molybdenum Microfocus X-Ray Sources for Single-Crystal Structure Determination. *J. Appl. Cryst.* **2015**, *48*, 3–10.

(3) Sheldrick, G. M. *SHELXT* – Integrated Space-Group and Crystal-Structure Determination. *Acta Crystallogr.* **2015**, *A71*, 3–8.

(4) Sheldrick, G. M. Crystal Structure Refinement with *SHELXL*. *Acta Crystallogr*. **2015**, *C71*, 3–8.

(5) Spek, A. L. *PLATON* SQUEEZE : A Tool for the Calculation of the Disordered Solvent Contribution to the Calculated Structure Factors. *Acta Crystallogr*. **2015**, *C71*, 9–18.

(6) Dolomanov, O. V.; Bourhis, L. J.; Gildea, R. J.; Howard, J. A. K.; Puschmann, H. *OLEX2*: A Complete Structure Solution, Refinement and Analysis Program. *J. Appl. Crystallogr*. **2009**, *42*, 339–341.

(7) Baburin I. A.; Blatov V. A.; Carlucci L.; Ciani, G.; Proserpio D. M. Interpenetrated Three-Dimensional Networks of Hydrogen-Bonded Organic Species: A Systematic Analysis of the Cambridge Structural Database. *Cryst. Growth Des*. **2008**, *8*, 519–539.